

N 70-30076

NASA CONTRACTOR
REPORT

NASA CR-61327

ANALYSIS OF LOWER ATMOSPHERIC DATA
FOR DIFFUSION STUDIES

By F. A. Record, R. N. Swanson, H. E. Cramer,
and R. K. Dumbauld

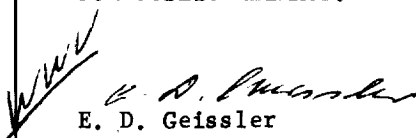
GCA Corporation
GCA Technology Division
Bedford, Massachusetts

April 1970

**CASE FILE
COPY**

Prepared for

NASA-GEORGE C. MARSHALL SPACE FLIGHT CENTER
Marshall Space Flight Center, Alabama 35812

1. REPORT NO. CR-61327	2. GOVERNMENT ACCESSION NO.	3. RECIPIENT'S CATALOG NO.	
4. TITLE AND SUBTITLE ANALYSIS OF LOWER ATMOSPHERIC DATA FOR DIFFUSION STUDIES		5. REPORT DATE April 1970	
		6. PERFORMING ORGANIZATION CODE	
7. AUTHOR(S) F. A. Record, R. N. Swanson, H. E. Cramer and R. K. Dumbauld		8. PERFORMING ORGANIZATION REPORT #	
9. PERFORMING ORGANIZATION NAME AND ADDRESS GCA Corporation GCA Technology Division Bedford, Massachusetts		10. WORK UNIT NO.	
		11. CONTRACT OR GRANT NO. NAS8-30503	
12. SPONSORING AGENCY NAME AND ADDRESS Aero-Astroynamics Laboratory George C. Marshall Space Flight Center Marshall Space Flight Center, Alabama 35812		13. TYPE OF REPORT & PERIOD COVERED Local Contractor Report	
		14. SPONSORING AGENCY CODE	
15. SUPPLEMENTARY NOTES			
16. ABSTRACT <p>The principal technical objectives under this contract were to recommend mathematical diffusion models for use in estimating toxic fuel hazards at Kennedy Space Center, and to develop requisite meteorological inputs for these models from analyses of measurements made previously at Kennedy Space Center and other locations.</p> <p>Mr. John W. Kaufman, the Contracting Officer's Representative, and Mr. Charles K. Hill of the Atmospheric Dynamics Branch of the Aero-Astroynamics Laboratory at Marshall Space Flight Center supplied the meteorological data used in the development of model inputs and arranged for the computer programming and data processing carried out at the Computational Laboratory at Marshall Space Flight Center. Mr. William W. Vaughan, Chief of the Aerospace Environment Division, Marshall Space Flight Center, provided guidance throughout the program.</p> <p>The following professional staff members of the GCA Technology Division Environmental Sciences Laboratory contributed importantly to this report: Dr. J. E. Faulkner, Mr. R. H. Huerta, and Mr. I. Kim.</p>			
17. KEY WORDS		18. DISTRIBUTION STATEMENT FOR PUBLIC RELEASE:	
		 E. D. Geissler Director, Aero-Astroynamics Laboratory	
19. SECURITY CLASSIF. (of this report) UNCLASSIFIED	20. SECURITY CLASSIF. (of this page) UNCLASSIFIED	21. NO. OF PAGES 136	22. PRICE

SUMMARY

This report describes generalized diffusion models selected for use in estimating toxic fuel hazards at Kennedy Space Center and the development of requisite meteorological inputs for these models through an intensive analysis of measurements from the NASA 150-meter Meteorological Tower Facility, Jimsphere and radiosonde flights at KSC.

The generalized diffusion models selected for use at KSC are adjustable for initial cloud dimensions near the source and source emission time and are in principle applicable to all source types. The basic model format is similar to the conventional Gaussian plume equation. Additional terms have been added to account for the effects on cloud growth of the depth of the mixing layer and vertical wind shear, and for cloud depletion by decay, precipitation scavenging and gravitational settling. Subsets of equations have been developed for calculating buoyant plume rise caused by the liberation of thermal energy at the source. Although the models are of the steady-state type, provision is also made to accommodate simple step changes in atmospheric structure at arbitrary travel distances or travel times downwind from the source.

Because of the 5-kilometer depth of the atmosphere that must be considered in the KSC toxic fuel problem, the above models have been incorporated in a multi-layer construct which has been programmed for computer calculations of concentration fields under Contract NAS8-21453.

In the development of requisite meteorological inputs for the multi-layer diffusion model, a detailed study was made of data from NASA's 150-meter Meteorological Tower Facility at Kennedy Space Center. Attention was centered on defining the properties of representative vertical profiles of wind speed, temperature, and the lateral intensity of turbulence and establishing the dependence

of these profile properties on mean wind speed, wind direction, and time of day. For general application at Kennedy Space Center, curves were prepared for estimating 10-minute values of σ_A and σ_E at a height of 18 meters under various wind speed and stability conditions. Similar sets of curves, using wind speed and stability as predictors, were prepared for use in estimating the power-law dependence of wind speed and σ_A on height. Under near-neutral conditions, σ_A and σ_E are approximately 9 and 5 degrees respectively for all wind speeds, and the wind speed profile power-law exponent p is approximately 0.30. During unstable conditions, σ_A decreases from about 20 degrees when the wind speed is 1 to 2 meters per second to about 10 degrees when the wind speed is 7 to 11 meters per second; during stable conditions, σ_A increases from about 6 degrees when the wind speed is 1 to 4 meters per second to about 7.5 degrees when the wind speed is 4 to 7 meters per second. For the corresponding wind speed ranges, σ_E decreases from about 12 degrees to 6 degrees during unstable conditions and has a constant value of about 3 degrees during stable conditions. During unstable conditions, p increases from about 0.08 when the wind speed is 1 to 2 meters per second to about 0.17 when the wind speed is 7 to 11 meters per second; during stable conditions, p decreases from about 0.45 when the wind speed is 1 to 2 meters per second to about 0.35 when the wind speed is 4 to 7 meters per second. Under all stability conditions, the power-law exponent q defining the height dependence of σ_A decreases with increasing wind speed. The exponent q also decreases with decreasing instability during unstable conditions and decreases slightly with increasing stability during stable conditions. Under moderately unstable conditions, q is about -0.05 when the wind speed is 1 to 2 meters per second and -0.35 when the wind speed is 7 to 11 meters per second. For the same range of wind speed under near-neutral conditions, q decreases from about -0.15 to -0.45. Under stable conditions, q is about -0.25 when the wind speed is 1 to 2 meters per second and -0.55 when the wind speed is 4 to 7 meters per second.

Other KSC meteorological data studied include 12 tetron flights. The average value of σ_E obtained from four over-water flights was 6.5 degrees; the

average value of σ_E obtained for eight overland flights was 10.6 degrees. Also, a study was made of the structure of land- and sea-breeze circulations at Cape Kennedy using 150-meter tower and Jimsphere data for the summer seasons of 1966 and 1967. Average profiles of wind speed and direction were prepared from these data for eight selected sea-breeze cases and five land-breeze cases. The sea-breeze profiles showed an onshore component up to a height of about 1000 meters with the maximum speed of about 8 meters per second occurring over the 200 to 300 meter height interval. The land-breeze profiles showed an off-shore component up to a height of about 600 meters with a low-level jet-type maximum of 8 meters per second at about 200 meters.

To illustrate the selection of meteorological inputs for the multi-layer diffusion models, four representative meteorological situations were selected from each of the two major seasons of the year. Layer boundaries and gross meteorological model inputs were assigned for each of the eight cases on the bases of Cape Kennedy radiosonde data. Turbulence parameters were assigned to an 18-meter reference level using the σ_A and σ_E curves developed from the analysis of the climatological data from NASA's 150-meter Meteorological Tower. Interim procedures based principally on the wind-speed profile are given to obtain σ_A and σ_E values at other heights.

For many reasons, including uncertainties in source definition as well as uncertainties contributed by atmospheric factors, the development and validation of procedures for the estimation of toxicity hazards arising from the use of rocket engine fuels must be a continuing process. Recommendations directed toward improving the accuracy of hazard predictions are offered at the end of the report.

TABLE OF CONTENTS

<u>Section</u>	<u>Title</u>	<u>Page No.</u>
1	GENERALIZED DIFFUSION MODELS FOR ESTIMATING TOXICITY HAZARDS AT KENNEDY SPACE CENTER	1
1.1	Background	1
1.2	Requirements for Atmospheric Diffusion Modeling at KSC and the Current State-of- the-Art	2
1.3	Generalized Concentration and Dosage Models Selected for use at Kennedy Space Center	5
1.4	The KSC Multi-Layer Diffusion Model	17
1.5	Specification of Meteorological and Source Inputs Required for Estimating Toxic Fuel Hazards at KSC	19
2	ANALYSIS OF KSC METEOROLOGICAL DATA	24
2.1	NASA's 150-Meter Tower Data	24
2.2	Tetron Flights	64
2.3	Land- and Sea-Breeze Circulations at KSC	67
3	METEOROLOGICAL MODEL INPUTS FOR SELECTED KSC WEATHER REGIMES	80
3.1	Selection of Layers and the Assignment of Gross Meteorological Input Parameters	81
3.2	Assignment of Turbulence Parameters	83
3.3	Meteorological Model Inputs for Selected Winter Regimes	86
3.4	Meteorological Model Inputs for Selected Summer Regimes	102
3.5	Extension to Other Launch Sites	119
4	CONCLUSIONS AND RECOMMENDATIONS	121

LIST OF FIGURES

<u>Figure No.</u>	<u>Title</u>	<u>Page No.</u>
1-1	Predicted cloud rise as a function of energy released and potential temperature change	16
2-1	Location of NASA's 150-meter Meteorological Tower Facility at Kennedy Space Center	25
2-2	NASA's 150-meter Meteorological Tower Facility at Kennedy Space Center.	27
2-3	Stratification of NASA's 150-meter Tower data	29
2-4	Sample page of computer printout provided in the analysis of Tower data	30
2-5	Ratios of the wind speeds at 60, 90, 120 and 150 meters to the wind speed at 18 meters during the winter season	32
2-6	Ratios of the wind speeds at 60, 90, 120 and 150 meters to the wind speed at 18 meters during the summer season	33
2-7	Winter nighttime values of p as a function of wind direction and wind speed	35
2-8	Summer nighttime values of p as a function of wind direction and wind speed	36
2-9	Annual daytime values of p as a function of wind direction and wind speed	38
2-10	Dependence of p on stability and the wind speed at 18 meters	39
2-11	Annual daytime wind direction range at 18 meters as a function of wind direction and wind speed	41

LIST OF FIGURES (Cont.)

<u>Figure No.</u>	<u>Title</u>	<u>Page No.</u>
2-12	Annual nighttime wind direction range at 18 meters as a function of wind direction and wind speed	42
2-13	Dependence of σ_A at 18 meters on stability and wind speed	44
2-14	Median 10-minute wind direction range at 18 meters as a function of stability	45
2-15	Annual daytime values for q as a function of wind direction and wind speed	46
2-16	Annual nighttime values for q as a function of wind direction and wind speed	47
2-17	Dependence of q on stability and wind speed	49
2-18	Dependence of σ_E at 18 meters on stability and wind speed	52
2-19	Relationships between stability and wind direction in winter	55
2-20	Relationships between stability and wind direction in summer	56
2-21	Cumulative frequency distributions of wind direction by wind speed category during winter	58
2-22	Cumulative frequency distributions of wind direction by wind speed category during summer	61
2-23	Cumulative frequency distributions of the 18-meter wind speed for two seasons	65
2-24	Time variations in vertical profiles of wind direction and speed for 13 and 14 July 1967	68

LIST OF FIGURES (Cont.)

<u>Figure No.</u>	<u>Title</u>	<u>Page No.</u>
2-25	Time variations in vertical profiles of wind speed for 21 July 1967	70
2-26	Time variations in vertical profiles of azimuth wind direction for 21 July 1967	71
2-27	Time variations in vertical profiles of wind speed for 4 and 5 July 1966	72
2-28	Time variations in vertical profiles of azimuth wind direction for 4 and 5 July 1966	73
2-29	Vertical profiles of wind speed and wind direction for the land-breeze circulation at KSC	75
2-30	Vertical profiles of wind speed and wind direction for the sea-breeze circulation at KSC	77
2-31	Hsu's (1969) synthesized model of land- and sea-breeze systems on the Texas coast	79
3-1	Seasonal variations in the time of transition from lapse to inversion and from inversion to lapse	84
3-2	Surface map for 0000 GMT, 28 November 1966	87
3-3	700-mb map for 0000 GMT, 28 November 1966	87
3-4	Vertical profiles for 27 November 1966, 2315 GMT, and assignment of layers for diffusion model	88
3-5	Surface map for 0000 GMT, 29 November 1966	92
3-6	700-mb map for 0000 GMT, 29 November 1966	92
3-7	Vertical profiles for 28 November 1966, 2315 GMT, and assignment of layers for diffusion model	93
3-8	Surface map for 0000 GMT, 10 February 1966	96

LIST OF FIGURES (Cont.)

<u>Figure No.</u>	<u>Title</u>	<u>Page No.</u>
3-9	700-mb map for 0000 GMT, 10 February 1966	96
3-10	Vertical profiles for 10 February 1966, 0255 GMT, and assignment of layers for diffusion model	97
3-11	Surface map for 1200 GMT, 8 December 1966	100
3-12	700-mb map for 1200 GMT, 8 December 1966	100
3-13	Vertical profiles for 8 December 1966, 1115 GMT, and assignment of layers for diffusion model	101
3-14	Surface map for 0600 GMT, 16 May 1967	105
3-15	700-mb map for 0000 GMT, 16 May 1967	105
3-16	Vertical profiles for 16 May 1967, 0515 GMT, and assignment of layers for diffusion model	106
3-17	Surface map for 0000 GMT, 23 July 1966	108
3-18	700-mb map for 0000 GMT, 23 July 1966	108
3-19	Vertical profiles for 22 July 1966, 2320 GMT, and assignment of layers for diffusion model	110
3-20	Surface map for 0600 GMT, 12 May 1967	112
3-21	700-mb map for 0000 GMT, 12 May 1967	112
3-22	Vertical profiles for 12 May 1967, 0515 GMT, and assignment of layers for diffusion model	113
3-23	Surface map for 1200 GMT, 1 July 1966	116
3-24	700-mb map for 1200 GMT, 1 July 1966	116
3-25	Vertical profiles for 1 July 1966, 1148 GMT, and assignment of layers for diffusion model	117

LIST OF TABLES

<u>Table No.</u>	<u>Title</u>	<u>Page No.</u>
1-1	Source Input Requirements for Generalized Prediction Models	20
1-2	Meteorological Input Requirements for Generalized Prediction Models	22
2-1	Ratios of the Annual Daytime and Nighttime Wind Speed Power-Law Exponents, p , and Wind Direction Range Power-Law Exponents, q	50
2-2	Round Hill α_w Values Measured at a Height of 16 Meters	53
2-3	Estimates of σ_w as a function of Averaging Time for Selected Portions of Tetron Flights	66
3-1	Meteorological Model Inputs for 2315 GMT, 27 November 1966	91
3-2	Meteorological Model Inputs for 2315 GMT, 28 November 1966	95
3-3	Meteorological Model Inputs for 0255 GMT, 10 February 1966	99
3-4	Meteorological Model Inputs for 1115 GMT, 8 December 1966	103
3-5	Meteorological Model Inputs for 0575 GMT, 16 May 1967	107
3-6	Meteorological Model Inputs for 2320 GMT, 22 July 1966	111
3-7	Meteorological Model Inputs for 0515 GMT, 12 May 1967	115
3-8	Meteorological Model Inputs for 1148 GMT, 1 July 1966	118

SECTION 1

GENERALIZED DIFFUSION MODELS FOR ESTIMATING TOXICITY HAZARDS AT KENNEDY SPACE CENTER

1.1 BACKGROUND

Some of the rocket engine fuels currently used at Kennedy Space Center (KSC) and many of the new candidate fuels for future use contain materials that, if released to the atmosphere, are potentially harmful to health, property, vegetation, and the ecology of the area. The release of toxic fuels to the atmosphere may occur in a variety of ways, such as from:

- Inadvertent fuel spillage during storage, transport or vehicle fueling operations
- Combustion products from normal vehicle launch
- Vehicle fallback on pad
- Vehicle destruct on pad
- Vehicle destruct after lift off and normal launch

Except for a cold fuel spill, all the above release modes are accompanied by combustion and the production of heat. Combustion processes affect the chemical and physical composition of the material released to the atmosphere and the heat produced during combustion results in a buoyant cloud or plume that may rise to great heights. Reliable quantitative estimates of the toxicity hazard posed by rocket motor fuels are thus important for current and future operations at Kennedy Space Center as well as for planning and research purposes.

Development of quantitative procedures for estimating the toxic fuel hazard at KSC has been undertaken by the GCA Technology Division under two concurrent contracts (Contracts Nos. NAS8-21453 and NAS8-30503) with the George C. Marshall Space Flight Center of the National Aeronautics and Space Administration. This report contains a description of the portion of the work completed under Contract No. NAS8-30503. Principal attention is focused on the selection of diffusion models and the development of the requisite meteorological model inputs for toxicity hazard estimation at KSC from an intensive analysis of meteorological observations made previously at Kennedy Space Center and other locations. The KSC observations include measurements made at the NASA 150-meter Meteorological Tower Facility, Jimsphere flights, and rawinsonde data. The final report under Contract No. NAS8-21453 (Dumbauld, et al., 1970) is in the form of a handbook containing a detailed description of the diffusion-prediction methodology recommended for use in toxicity hazard estimation at KSC, together with completely-worked example calculations, computer program listings and user instructions, and various graphs and nomograms for rapid manual estimation of concentrations and dosages.

The remainder of this section of the report contains a discussion of the overall problem of estimating toxic fuel hazards at KSC; a review of the state-of-the-art of atmospheric diffusion modeling; a description of the generalized diffusion models developed by the GCA Technology Division for use in hazard estimation at KSC; and specifications of the source and meteorological parameters required by these models.

1.2 REQUIREMENTS FOR ATMOSPHERIC DIFFUSION MODELING AT KSC AND THE CURRENT STATE-OF-THE-ART

The principal source types that are likely to be involved in atmospheric emissions of toxic fuel materials at Kennedy Space Center have been mentioned in

Section 1.1 above. It is evident from a consideration of these source types that, with the exception of cold fuel spills on the ground, toxic materials may be emitted anywhere between ground level and some point on the flight trajectory of vehicles launched from KSC. By direction of the NASA Contracting Officer's Representative, the upper limit of the atmosphere to be considered under the two GCA Technology Division contracts was set at 5 kilometers. Any diffusion models employed in toxic-fuel hazard estimation at KSC must therefore provide:

- An accurate description of the atmospheric transport, dispersal and decay of all airborne toxic material released as the result of normal launch operations, fuel spillage, vehicle abort or vehicle destruct between ground level and a maximum height of 5 kilometers
- Satisfactory quantitative estimates of the concentration and dosages of toxic material thus released at all down-wind distances at which these concentrations and dosages exceed established thresholds
- Satisfactory quantitative estimates of the surface deposition of toxic materials caused by gravitational settling, precipitation and other removal mechanisms

It is important to note the space and time scales implicit in the above requirements. The maximum dimensions of the volume of air that must be considered extend vertically a distance of 5 kilometers from the ground or sea surface, and extend horizontally for distances of 100 kilometers or more, depending on the circumstances. The time required for clouds of toxic material to traverse an air volume of this size is approximately 5 hours. Also, the source dimensions and other source properties are not easily reconciled with ideal point or line concepts conventionally used in diffusion models. Hilst (1967) has discussed in detail the

problem of source definition in a previous study of toxic-fuel hazards at Kennedy Space Center.

The current state-of-the-art of atmospheric diffusion modeling as revealed by Pasquill (1962) and Slade (1968), from the point of view of obtaining reliable engineering estimates of the hazard associated with the KSC toxic fuel problems outlined above, clearly leaves much to be desired. The simple truth of the matter is that the validation of diffusion-prediction techniques, even for the simplest practical problems involving continuous point-source emission over relatively short times and distances, is very incomplete. Slade describes the state-of-the-art in the Preface to *Meteorology and Atomic Energy* (1968) in these words:

"The large number of authors who have contributed to this volume guarantees that there will be some diversity of views and orientation. This diversity constitutes an accurate picture of an expanding technical field in which coincidence of approach and opinion is not always found and, indeed, may not as a general rule be possible.

The reader should not expect to find hard and fast rules for the evaluation of a specific problem. The treatment of a practical situation usually involves the use of specific quantitative techniques along with a broad variety of assumptions engendered by the imperfect knowledge of the atmosphere and the pollutant-producing device. Although these assumptions may be justified on scientific grounds, their selection can be rationally made only by someone with a broader range of experience and knowledge than can be garnered from even a careful reading of the following pages."

It is therefore not possible to apply universally-accepted and adequately-validated prediction techniques to the KSC hazard prediction problem. As a purely practical matter, comprehensive validation for most of the emission modes cited above will probably never be possible because of the vast level of effort that would be required and the infrequent occurrence of vehicle abort and destruct situations.

On the other hand, the requirements for toxic-fuel hazard estimation exist and something must be done by way of estimating at least order-of-magnitude effects, using the best available techniques and knowledge. Available information with respect to atmospheric transport and diffusion processes in the lower troposphere, for distances of the order of 100 kilometers, is fragmentary (Pasquill, 1962; Tyldesley and Wallington, 1965; and Slade, 1968, pp. 143-188). Knowledge of the mesoscale atmospheric circulations that control these processes is largely qualitative. Partial documentation of mesoscale circulations in the area surrounding Kennedy Space Center has already been accomplished. Hill (1967) has reviewed the sea-breeze circulation at KSC and described the characteristics of sea-breeze fronts. Endlich, et al., (1964) have used Jimsphere soundings made at KSC to analyze the features of vertical wind profiles in the layer extending from 200 meters above the surface to a height of 15 kilometers. Smaller scale studies of the characteristic features of the wind structure at KSC in the layer between the surface and a height of 150 meters have been made by Fichtl (1968), Fichtl and McVehil (1969), McVehil and Camnitz (1964) and Blackadar, Dutton, Panofsky, and Chaplin (1969).

It should be pointed out that atmospheric processes contribute only part of the total uncertainty involved in toxicity hazard estimations at KSC. Uncertainties as to the chemical and physical properties of the sources, source strength, source dimensions, and the amount of heat released probably contribute as much to the total uncertainty as the uncertainties contributed by atmospheric factors. Finally, the uncertainties associated with toxicity threshold levels and receptor effects may well be larger than either the source or meteorological uncertainties.

1.3 GENERALIZED CONCENTRATION AND DOSAGE MODELS SELECTED FOR USE AT KENNEDY SPACE CENTER

During the past several years, the GCA Technology Division has developed generalized concentration and dosage models that are in principle applicable to all source types, all environmental regimes, and to both microscale and mesoscale

atmospheric processes. This work has been sponsored by the U. S. Army (Cramer, et al., 1964; Cramer, et al., 1967; Cramer and Dumbauld, 1968) and the Pacific Missile Range (Cramer, Hamilton and DeSanto, 1965). Attention has been focused principally on transport and dispersal processes within the air layer between the ground and a height of 1 kilometer. In our opinion, these generalized models are ideally suited for application to the toxic-fuel hazard problem at Kennedy Space Center and provide comprehensive guidelines indicating the types of meteorological and source information required for improvements in the accuracy of hazard predictions at KSC. The basic format of the generalized models is similar to that of the Gaussian plume models described by Pasquill (1962, p. 190). Additional terms have been added to account for the effects of mesoscale factors, such as the depth of the surface mixing layer and wind shear in the mixing layer, that control vertical and lateral diffusion. The models are also fully adjustable for source dimensions and for the time duration of emission. Subsets of equations have been developed for use with the models that provide for calculations of the effective height of the source; surface deposition due to gravitational settling and precipitation-removal mechanisms; and for various meteorological predictors that are used to adapt the models to changes in atmospheric structure and surface structure. Although the models are of the steady-state type, simple step changes in atmospheric structure that occur at an arbitrary travel distance or travel time downwind from the source can be accommodated.

The generalized concentration and dosage models selected for use at Kennedy Space Center and the extension of these models to the multi-layer structure required for KSC applications are described below.

1.3.1 Generalized Concentration Model

The generalized concentration model is expressed as the product of five modular terms:

$$\text{Concentration} = \{\text{Peak Concentration Term}\} \times \{\text{Alongwind Term}\} \times \{\text{Lateral Term}\} \times \{\text{Vertical Term}\} \times \{\text{Depletion Term}\}$$

The mathematical formulas given below for the various terms are written according to conventional usage. Specifically, the concentration model is referred to a Cartesian coordinate system with the origin at $x = 0$, $y = 0$ and $z = H$, where H is the effective height of the source. The direction of x is along the mean azimuth wind direction, y is normal to the mean wind direction in the plane of the horizon, and z is directed vertically with $z = 0$ at ground level. The distribution of concentration along each of the three coordinate axes is assumed to be Gaussian. None of the above assumptions is required. The model equations are easily transformed to a polar coordinate system or other systems, and other distribution functions may be substituted for the Gaussian function.

The Peak Concentration Term refers to the concentration at the point $x = 0$, $y = 0$, $z = H$ and is defined by the expression

$$\frac{Q}{(2\pi)^{3/2} \sigma_x \sigma_y \sigma_z} \quad (1-1)$$

where

Q = source strength

σ_x = standard deviation of the alongwind concentration distribution

σ_y = standard deviation of the crosswind concentration distribution

σ_z = standard deviation of the vertical concentration distribution

The Alongwind Term is defined by the expression

$$\exp \left[- \frac{1}{2} \left(\frac{x - \bar{u}t}{\sigma_x} \right)^2 \right] \quad (1-2)$$

where

\bar{u} = mean wind speed

t = time of cloud travel

The Lateral Term is defined by the expression

$$\exp \left[-\frac{1}{2} \left(\frac{y}{\sigma_y} \right)^2 \right] \quad (1-3)$$

The Vertical Term is given by the expression

$$\begin{aligned} & \exp \left[-\frac{1}{2} \left(\frac{H-z}{\sigma_z} \right)^2 \right] + \exp \left[-\frac{1}{2} \left(\frac{H+z}{\sigma_z} \right)^2 \right] + \sum_{i=1}^{\infty} \left\{ \exp \left[-\frac{1}{2} \left(\frac{2iH_m - H - z}{\sigma_z} \right)^2 \right] \right. \\ & + \exp \left[-\frac{1}{2} \left(\frac{2iH_m - H + z}{\sigma_z} \right)^2 \right] + \exp \left[-\frac{1}{2} \left(\frac{2iH_m + H - z}{\sigma_z} \right)^2 \right] \\ & \left. + \exp \left[-\frac{1}{2} \left(\frac{2iH_m + H + z}{\sigma_z} \right)^2 \right] \right\} \quad (1-4) \end{aligned}$$

where

H = effective source height

H_m = height of the top of the mixing layer

The multiple reflection terms following the summation sign stop the vertical cloud growth at the top of the mixing layer and change the form of the vertical concentration distribution from Gaussian to rectangular.

The Depletion Term refers to the loss of material by simple decay processes, precipitation scavenging, or gravitational settling. The form of the Depletion Term for each of these processes is:

$$\text{(Decay)} \quad \exp [-kt] \quad (1-5)$$

$$\text{(Precipitation Scavenging)} \quad \exp [-\Lambda t] \quad (1-6)$$

(Gravitational Settling)

$$\exp \left[-\frac{1}{2} \left(\frac{H - (V_s x / \bar{u})}{\sigma_z} \right)^2 \right] + \exp \left[-\frac{1}{2} \left(\frac{H - 2H_m - (V_s x / \bar{u})}{\sigma_z} \right)^2 \right] \quad (1-7)$$

where

k = decay coefficient or fraction of material lost per unit time

t = time

Λ = washout coefficient or fraction of material removed by scavenging per unit time

V_s = settling velocity

When Equation (1-7) is used for the Depletion Term, the Vertical Term given by Equation (1-4) is set equal to unity. This causes the cloud axis to be inclined downward at the angle $\tan^{-1}(V_s / \bar{u})$ with respect to the horizon, following W. Schmidt's sedimentation hypothesis (see Pasquill, 1962, p. 226); material that deposits on the ground surface is retained and not reflected. The vertical growth of the cloud is stopped at the top of the mixing layer and reflected toward the ground by the second exponential term in Equation (1-7). The depletion by gravitational settling, of material containing a size distribution is calculated by partitioning the distribution into various settling-velocity categories, solving Equation (1-7) for each settling velocity, and superposing the solutions.

1.3.2 Generalized Dosage Model

The generalized dosage model is similar in form to the generalized concentration model and is defined by the product of four modular terms:

$$\text{Dosage} = \{\text{Peak Dosage Term}\} \times \{\text{Lateral Term}\} \\ \times \{\text{Vertical Term}\} \times \{\text{Depletion Term}\}$$

The Peak Dosage Term is given by the expression

$$\frac{Q}{2\pi \bar{u} \sigma_y \sigma_z} \quad (1-8)$$

where

Q = source strength

\bar{u} = mean wind speed

σ_y = standard deviation of the crosswind dosage distribution

σ_z = standard deviation of the vertical dosage distribution

The remaining terms in the generalized dosage model are defined in the same manner as the corresponding terms for the generalized concentration model which are given by Equations (1-3), (1-4), (1-5), (1-6) and (1-7).

1.3.3 Subset of Equations for σ_y , σ_z , and σ_x

The following subset of equations is used to define the distance dependence of the standard deviations of the crosswind, vertical and alongwind distributions in the generalized concentration and dosage models described above:

$$\sigma_y\{x\} = \left[\sigma_A'^2\{\tau\} x_r^2 \left(\frac{x+x_y}{x_r} \right)^{2\alpha} + \left(\frac{\Delta\theta'x}{4.3} \right)^2 \right]^{1/2} \quad (1-9)$$

where

$\sigma_A'\{\tau\}$ = standard deviation of the azimuth wind angle in radians at height H for the release time τ

x_r = unit reference distance

x_y = virtual distance

$$= x_r \left(\frac{\sigma_{yo}}{\sigma'_A \{\tau\} x_r} \right)^{1/\alpha}$$

σ_{yo} = standard deviation of the crosswind distribution at the source

α = lateral diffusion coefficient of the order of unity

$\Delta\theta'$ = azimuth wind direction shear in radians within the layer containing the cloud

$$\sigma_z \{x\} = \sigma'_E x_r \left(\frac{x+x_z}{x_r} \right)^\beta \quad (1-10)$$

where

σ'_E = standard deviation of the wind elevation angle in radians at height H

x_z = virtual distance

$$= x_r \left(\frac{\sigma_{zo}}{\sigma'_E x_r} \right)^{1/\beta}$$

σ_{zo} = standard deviation of the vertical distribution at the source

β = vertical diffusion coefficient of the order of unity

$$\sigma_x \{x\} = \left[\left(\frac{L \{x\}}{4.3} \right)^2 + \sigma_{xo}^2 \right]^{1/2} \quad (1-11)$$

where

$L \{x\}$ = alongwind cloud length when the center of the cloud is at distance x from the source

$$= \frac{0.28 (\Delta u) (x)}{\bar{u}}$$

Δu = wind speed shear within the layer containing the cloud

σ_{xo} = standard deviation of the alongwind distribution at the source

In Equation (1-9) above, σ'_A is expressed as a function of the release time τ . Values of σ'_A for nearly instantaneous releases are difficult to measure directly, but can be calculated from the following semi-empirical relationship (Cramer, et al., 1964):

$$\sigma'_A\{\tau\} = \sigma'_A\{\tau_0\} \left(\frac{\tau}{\tau_0} \right)^{1/5} \quad (1-12)$$

where τ_0 is ≤ 10 minutes. The standard deviation of the wind elevation angle σ'_E is assumed independent of the release time τ because of the relatively narrow frequency range in the power spectrum of the vertical wind velocity component that contains significant amounts of turbulent energy. This assumption is generally valid at heights ≤ 100 meters above the ground surface. In the presence of large convective cells and at heights of the order of 1 kilometer, the assumption that σ'_E is independent of τ likely does not hold. However, the effect on the accuracy of ground-level concentration and dosage estimates is thought to be slight.

The source dimensions σ_{x_0} , σ_{y_0} , and σ_{z_0} in the above subset refer to a stabilized cloud or plume that has just reached equilibrium with ambient atmospheric conditions following the completion of the emission phase. These source dimensions are best estimated from direct measurements or observations. The virtual distances x_y and x_z are used to adjust the lateral and vertical terms of the generalized models for the initial source dimensions σ_{y_0} and σ_{z_0} . Two virtual distances are employed to facilitate the treatment of asymmetrical sources where $\sigma_{y_0} \neq \sigma_{z_0}$. The height of the stabilized cloud above ground level, when the emission mode is accompanied by the release of significant amounts of thermal energy, must be estimated from observations or by means of a mathematical formula for buoyant plume rise such as that given in Section 1.3.6 below.

1.3.4 Model Formulas for Ground Deposition Caused by Precipitation Scavenging and Gravitational Settling

The total amount of material deposited on the ground surface by precipitation scavenging, at some distance x , is given by the expression

$$\frac{\Lambda Q}{\sqrt{2\pi} \sigma_y \bar{u}} \left\{ \exp \left[-\frac{1}{2} \left(\frac{y}{\sigma_y} \right)^2 \right] \right\} \left\{ \exp \left[-\Lambda \left(\frac{x}{\bar{u}} - t \right) \right] \right\} \quad (1-13)$$

where t is the time at which the precipitation begins. The principal assumptions made in deriving the above expression are:

- The rate of precipitation is steady over an area that is large compared to the horizontal dimension of the cloud of toxic material
- The precipitation originates at a level above the top of the toxic cloud so that hydrometeors pass vertically through the entire cloud
- The time duration of the precipitation is sufficiently long so that the entire alongwind length of the toxic cloud passes over the point x

Engelmann (see Slade, 1968, pp. 208-221) discusses the general problem of calculating the amount of material removed by precipitation scavenging and recommends values of the coefficient Λ that may be combined with precipitation rates to obtain estimates of total surface deposition.

The total deposition due to the gravitational settling of heavy particles or droplets, with settling velocity V_s , at a downwind distance x from the

source and on the projection of the alongwind cloud axis on the ground plane, is given by the expression

$$\frac{Q}{\sqrt{2\pi} \sigma_y} \frac{d}{dx} \left\{ \frac{1}{\sqrt{2\pi} \sigma_z} \int_{-\infty}^0 \exp \left[-\frac{1}{2} \left(\frac{H - (V_s x/\bar{u})}{\sigma_z} \right)^2 \right] \right. \\ \left. + \exp \left[-\frac{1}{2} \left(\frac{H - 2H_m - (V_s x/\bar{u})}{\sigma_z} \right)^2 \right] \right\} dz \quad (1-14)$$

After the integration and differentiation are performed, the above expression becomes

$$\frac{Q}{2\pi \sigma_y} \left\{ \left[\frac{\beta H + \left(1 - \left(\frac{\beta x}{x+x_z} \right) \right) V_s (x+x_z)/\bar{u}}{\sigma_z (x+x_z)} \right] \exp \left[-\frac{1}{2} \left(\frac{H - (V_s x/\bar{u})}{\sigma_z} \right)^2 \right] \right. \\ \left. + \left[\frac{\beta (2H_m - H) - \left(1 - \left(\frac{\beta x}{x+x_z} \right) \right) V_s (x+x_z)/\bar{u}}{\sigma_z (x+x_z)} \right] \exp \left[-\frac{1}{2} \left(\frac{2H_m - H + (V_s x/\bar{u})}{\sigma_z} \right)^2 \right] \right\} \quad (1-15)$$

1.3.5 Calculations of Buoyant Plume Rise

Because of the large amounts of thermal energy that may be released during normal launch, vehicle destruct, or other malfunctions, it is essential to have a satisfactory method of estimating the buoyant rise of material thus released. Although much work has been done on the rise of hot plumes from industrial stacks, relatively little information is available for instantaneous

sources. The best available plume rise formula for instantaneous sources is probably that of Morton, Taylor and Turner (1956). According to Briggs (see Slade, 1968, p. 199), the expression for buoyant rise Δh given by these three authors can be written as

$$\Delta h = 2.66 \left(\frac{Q'}{C_p \rho \frac{\partial \Theta}{\partial z}} \right)^{1/4} \quad (1-16)$$

where

Δh = cloud rise (meters)

Q' = energy released (kilocalories)

C_p = specific heat of air

ρ = air density (kg m^{-3})

$\frac{\partial \Theta}{\partial z}$ = potential temperature gradient

If $\Delta \Theta$ is defined as the change in potential temperature over Δh , the above equation can be written as

$$\Delta h = (2.66)^{4/3} \left(\frac{Q'}{C_p \rho \Delta \Theta} \right)^{1/3} \quad (1-17)$$

Assuming $C_p = 0.24 \text{ kcal/kg } ^\circ\text{C}$ and $\rho = 1.18 \text{ kg m}^{-3}$, Equation (1-17) can be restated as

$$\Delta h = 5.61 \left(\frac{Q'}{\Delta \Theta} \right)^{1/3} \quad (1-18)$$

Briggs concluded that the observed cloud rises from nuclear tests were about 30 percent higher than those predicted by the Morton, Taylor and Turner model. However, the slope of the power curve given by Equation (1-18) appears to fit the data quite well. A more satisfactory fit to the data is achieved when the value of the constant is increased to 8.0. Figure 1-1 shows the buoyant cloud

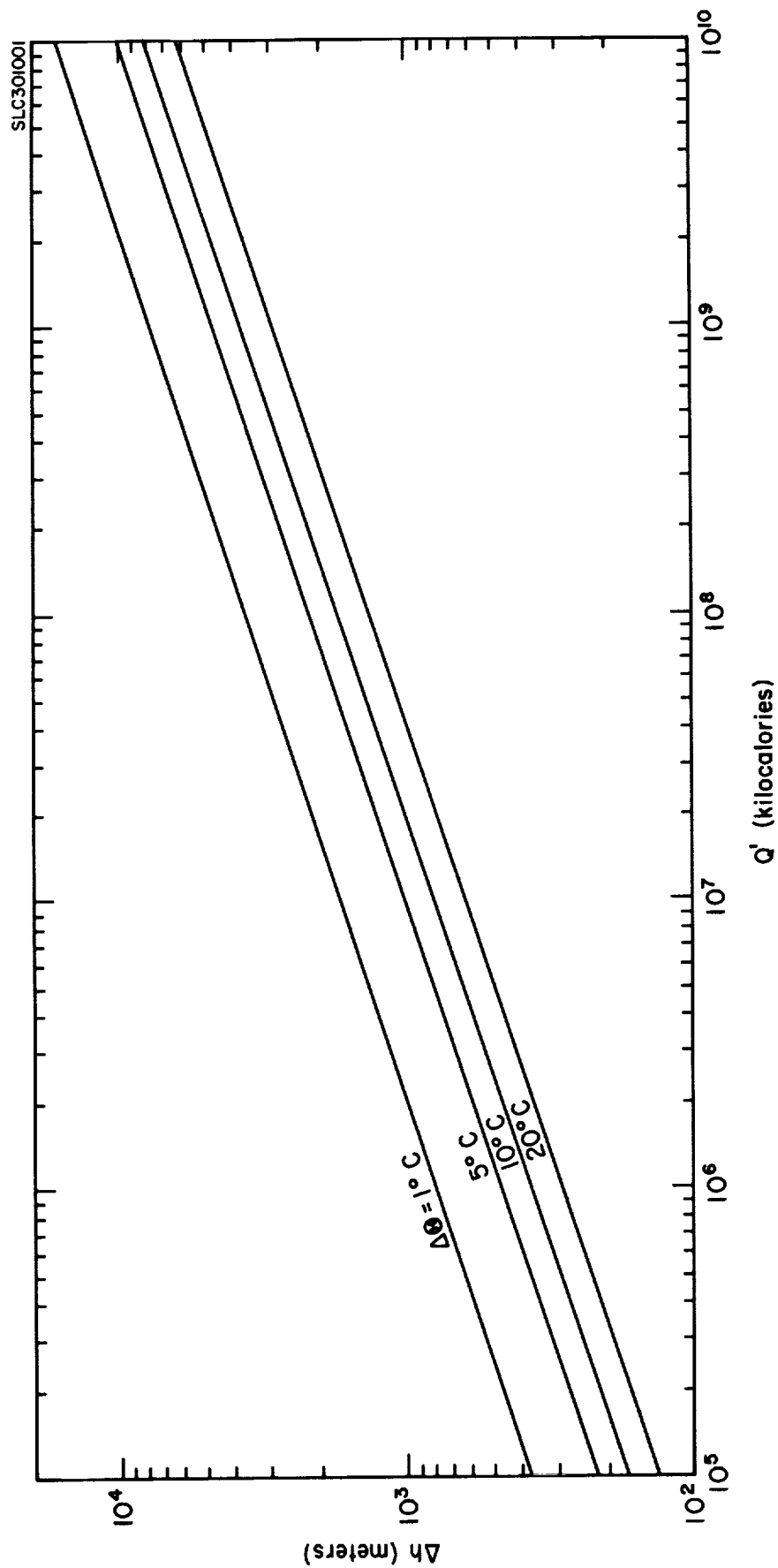


FIGURE 1-1. Predicted cloud rise as a function of energy released Q' and potential temperature change $\Delta\Theta$ over height Δh .

rise for selected values of $\Delta\Theta$ obtained from

$$\Delta h = 8.0 \left(\frac{Q'}{\Delta\Theta} \right)^{1/3} \quad (1-19)$$

If the gradient of potential temperature with height is used instead of $\Delta\Theta$, the above expression for Δh becomes

$$\Delta h = 4.76 \left(\frac{Q'}{\partial\Theta/\partial z} \right)^{1/4} \quad (1-20)$$

Equation (1-20) fits cloud rise data from high-explosive detonations recently published by Church (1969). Susko, Kaufman, and Hill (1968) have shown that the plume rise formula given by Morton, Taylor, and Turner (1956) provides satisfactory estimates of the buoyant rise of exhaust plumes from statically fired rocket engines.

1.4 THE KSC MULTI-LAYER DIFFUSION MODEL

As shown in Section 3 of this report, the meteorological structure at Kennedy Space Center between ground level and the top of the reference air volume for hazard estimation at a height of 5 kilometers often comprises several layers with very distinctive wind, temperature and humidity fields. A typical vertical profile at KSC shows an easterly sea-breeze circulation in the surface layer, separated by a transition zone, from a regime of westerly winds at the top of the reference volume. Large horizontal spatial variations in wind regimes also occur in the lower levels of the reference volume, usually as a consequence of the land-water interface.

These large spatial variations in wind regimes must somehow be dealt with, if only in an approximate fashion, if the generalized diffusion models described above are to be of practical use in hazard estimation at KSC. The vertical stratification problem is handled by applying the generalized models to individual layers, in which the meteorological structure is reasonably homogeneous. Layer boundaries are placed arbitrarily at the points of major discontinuities in the vertical profiles of wind, temperature and humidity. For simplicity, it is assumed that there is no flux

of toxic material across layer boundaries due to turbulent mixing. Provision is made for the flux of material across layer boundaries only as the result of gravitational settling or precipitation scavenging.

Step changes in meteorological structure of layers, at some arbitrary time or downwind distance from the point of release, are accommodated by stopping the transport and diffusion processes in the layers affected by the change in structure, calculating new sets of initial source and meteorological model input parameters, and re-starting the transport and diffusion process with the new inputs.

Two geometries are involved in the multi-layer concepts outlined above. The first is a layer geometry used with the Cartesian coordinate system of the generalized models in which the x-axis is along the mean wind direction in the layer. The second geometry refers to a basic reference grid for the area surrounding KSC that is referred to fixed spatial coordinates. Transformation equations that relate the two geometries are easily written.

The above concepts of a multi-layer diffusion model have been incorporated in a computer program written in FORTRAN V. The mathematical specification for this program including a complete description of the diffusion models, user's instructions, and example calculations using meteorological inputs from the selected case studies in Section 3 of this report, are given in the Toxic Fuel Diffusion Handbook completed concurrently by the GCA Technology Division under Contract No. NAS8-21453.

The program is comprised of subroutines specifically formulated to calculate concentration and dosage fields downwind of the various release modes specified in Section 1.1 above, to satisfy the requirements for the multi-layer model construct set forth in Section 1.2, and to present the results of the calculations in a variety of useful formats. The meteorological and source input requirements of the computer program are described below.

1.5 SPECIFICATION OF METEOROLOGICAL AND SOURCE INPUTS REQUIRED FOR ESTIMATING TOXIC FUEL HAZARDS AT KSC

1.5.1 Source Inputs

The generalized prediction models described above apply to the following modes of release of potentially toxic materials:

- Cold fuel spillage
- Exhaust products from normal launch
- Vehicle fallback, vehicle destruct or motor burnout on pad
- Vehicle destruct after lift off and normal launch

For each release mode, the basic source information required consists of the amount and rate of toxic material release, the dimensions and position in space of the cloud after reaching equilibrium, and the physical and chemical properties of the material in the stabilized cloud. The source input requirements for the most general type of release are given in Table 1-1. In the case of a cold spill, the source approximates a continuous ground-level source; the source strength is expressed in kilograms per second, and the alongwind cloud dimensions σ_{x0} , σ_x are not required. In the case of a normal launch, the vertical dimension of the stabilized cloud is given by the depth of the layer.

1.5.2 Meteorological Inputs

The meteorological inputs for the generalized prediction models are in principle determined from a detailed knowledge of the wind,

TABLE 1-1
SOURCE INPUT REQUIREMENTS FOR GENERALIZED
PREDICTION MODELS

Model Input	Symbol	Units
Source Strength - Total weight of each toxic product released to the atmosphere	Q	kg
Time duration of release	τ	sec
Effective height of release of cloud after reaching equilibrium	H	m
Initial cloud dimensions after reaching equilibrium		
• Standard deviation of the alongwind distribution of material within the cloud	σ_{x0}	m
• Standard deviation of the crosswind distribution of material within the cloud	σ_{y0}	m
• Standard deviation of the vertical distribution of material within the cloud	σ_{z0}	m
Total quantity of heat generated during release	Q'	kcal
Physical and chemical properties of material in the stabilized cloud including:		
• Decay coefficient or fraction of material	k	sec ⁻¹
• Settling velocity of particles or droplets	V _s	m sec ⁻¹

temperature and humidity fields within the reference air volume mentioned previously. For the normal launch, vehicle fallback, and destruct release modes this reference volume may extend vertically to a height of 5 kilometers, and radially from the point of release to maximum horizontal distances of the order of 100 kilometers. For these release modes, the assignment of layer boundaries and the selection of gross meteorological inputs must, at the present time, be made from a very limited number of radiosonde soundings, supplemented by Jimsphere data. Guidelines for the assignment of layer boundaries and gross inputs are given in Section 3.1, with examples based on Cape Kennedy radiosonde data. Suggested procedures for specifying model turbulence parameters are given in Section 3.2. For a reference height of 18 meters, these parameters are based on an analysis of 2 years' climatological data from the NASA 150-meter Meteorological Tower Facility (Section 2.1). To obtain values at other heights within the surface layer, interim procedures are based on the wind speed profile. Minimal values of turbulence are assumed in layers which are decoupled from the surface layer or in layers above the surface layer where no convection is occurring.

For the cold spill, the reference volume required may be only a few hundred meters in depth and extend to maximum horizontal distances of the order of 10 kilometers. In this case, the emphasis in specifying the meteorological inputs is placed on surface and tower observations. In the absence of observational data, the wind profile within the surface layer may be estimated from the surface wind speed and stability using curves presented in Figure 2-13.

Table 1-2 gives the meteorological model inputs which are required at a reference level within the surface layer and at each of the layer boundaries used in the multi-layer model. From the inputs in Table 1-2, values of \bar{u} , θ , σ_A and σ_E are calculated at the required heights, and values of wind shear $\Delta\bar{u}$, direction shear $\Delta\theta$, and the vertical gradient of potential temperature $\frac{d\theta}{dz}$

TABLE 1-2
METEOROLOGICAL INPUT REQUIREMENTS FOR
GENERALIZED PREDICTION MODELS

Model Input	Symbol	Units
Mean wind speed	\bar{u}	m sec ⁻¹
Mean wind direction	θ	deg
Potential temperature	θ	deg K
Standard deviation of the azimuth wind angle	σ'_A	radians
Standard deviation of the elevation wind angle	σ'_E	radians

are calculated for each layer containing the cloud. The value of σ_A is adjusted to the release time τ by means of the one-fifth power law (Equation 1-12). Other required inputs are the height of the top of the surface mixing layer H_m and the washout coefficient Λ .

Potential temperature, used in the calculation of buoyant plume rise, is not required for cold spill calculations.

SECTION 2

ANALYSIS OF KSC METEOROLOGICAL DATA

2.1 NASA'S 150-METER TOWER DATA

Two years of data collected at NASA's 150-meter tower have been analyzed to provide the basis for the development of a model input climatology for use in estimating downwind concentration fields from low-level releases at Cape Kennedy. In the analysis, emphasis has been placed on defining characteristic vertical profiles of wind speed, temperature, and the standard deviation of azimuth wind direction for the winter and summer seasons and establishing the dependence of these profiles on wind speed, wind direction, and time of day. In addition, the frequency of occurrence of wind direction as a function of time of day and season has been calculated for selected wind-speed classes.

2.1.1 Description of NASA's 150-meter Meteorological Tower Facility

NASA's 150-meter Meteorological Tower Facility is located within the Launch Complex 39 area, about 5 kilometers inland from the Atlantic Ocean, on Merritt Island at Kennedy Space Center, Florida. As shown in Figure 2-1, the Tower Facility, indicated by a solid triangle, is about 5 kilometers north of the Vehicle Assembly Building (VAB) and slightly more than 5 kilometers northwest of Launch Complex 39A. Banana Creek is south of the Tower Facility and a small inlet (Happy Creek) is located within 100 meters of the base of the tower. The ground surface near the tower consists of sandy soil covered by scrub palmetto about 1 meter in height. The base of the tower is at an elevation of 2 meters. Natural air flow to the tower is largely unrestricted with the exception of trees, about 10 meters high, located with respect to the tower as follows:

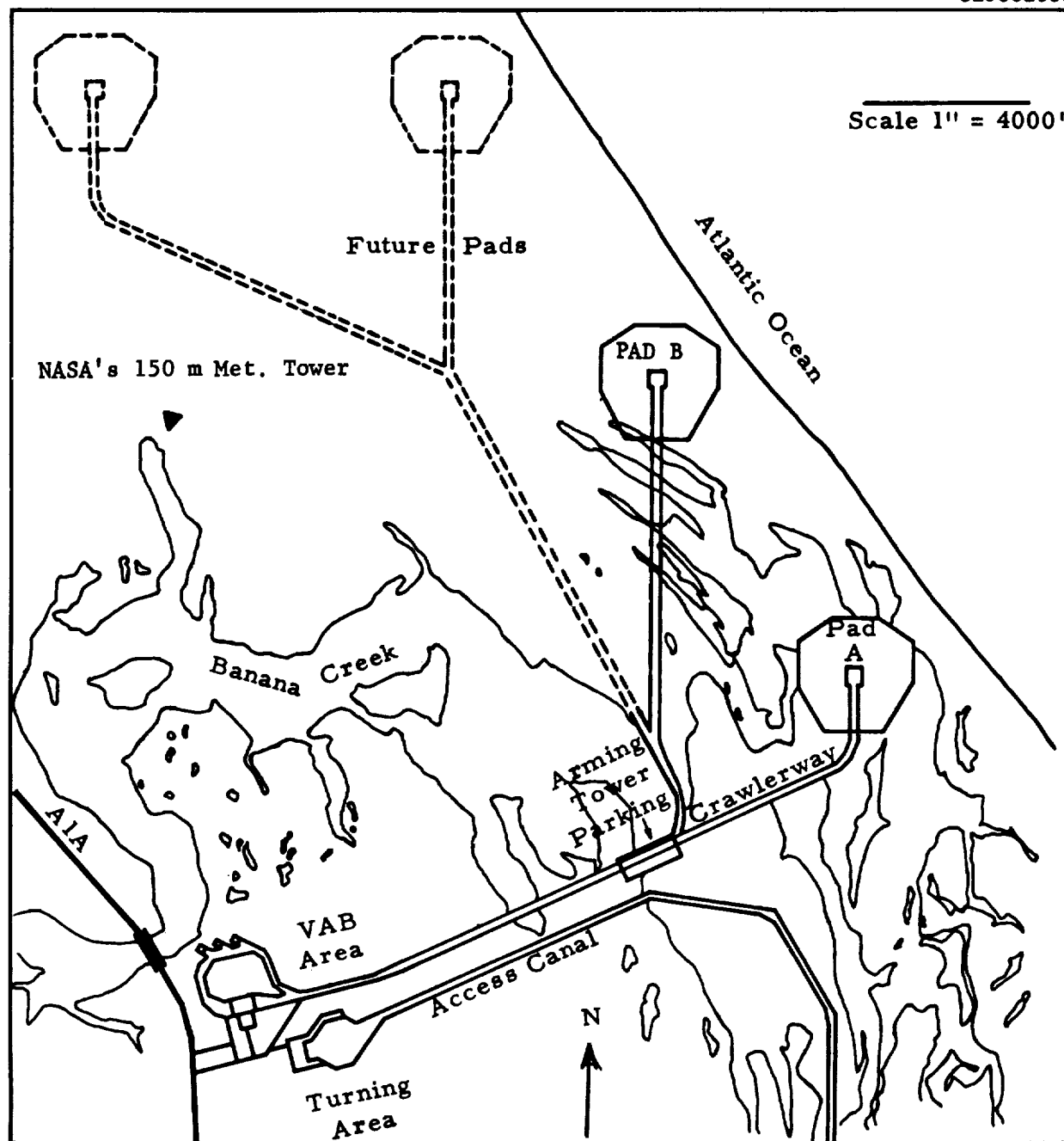


FIGURE 2-1. Location of NASA's 150-meter Meteorological Tower Facility in Launch Complex 39 at Kennedy Space Center (after Kaufman and Keene, 1968).

<u>Sector</u> (deg)	<u>Distance from Tower</u> (m)
90 to 135	450
160 to 180	200
230 to 300	200

The Tower Facility is comprised of the two towers shown in Figure 2-2. The small 18-meter tower is located 18 meters to the northeast of the main 150-meter tower. Climet Model C1-14 wind speed and direction sensors are positioned at the 3-, 10- and 18-meter levels on the small tower and at the 18-, 30-, 60-, 90-, 120- and 150-meter levels of the main tower. To minimize tower shadow effects, the 150-meter tower has a dual wind-measuring array with one boom facing toward the northeast and the other facing southwest. The selection of the array from which data are to be recorded may be made either manually or automatically by means of a wind direction selector.

Temperature gradient measurements are made with shielded and aspirated thermocouples located at the 3- and 18-meter levels on the small tower and at the 30-, 60-, 120- and 150-meter levels on the main tower, with the reference thermojunction at the 3-meter level of the small tower. The 3-meter level ambient temperature is recorded separately.

Data recording capabilities include strip chart recorders for all sensor outputs in addition to an analog tape recorder for the wind speed and direction data. A detailed description of the Tower Facility and instrumentation is given by Kaufman and Keene (1968).

2.1.2 Processing of the Data

Strip chart records have been collected routinely at the NASA Meteorological Tower Facility since 1966 and reduced by the National Weather

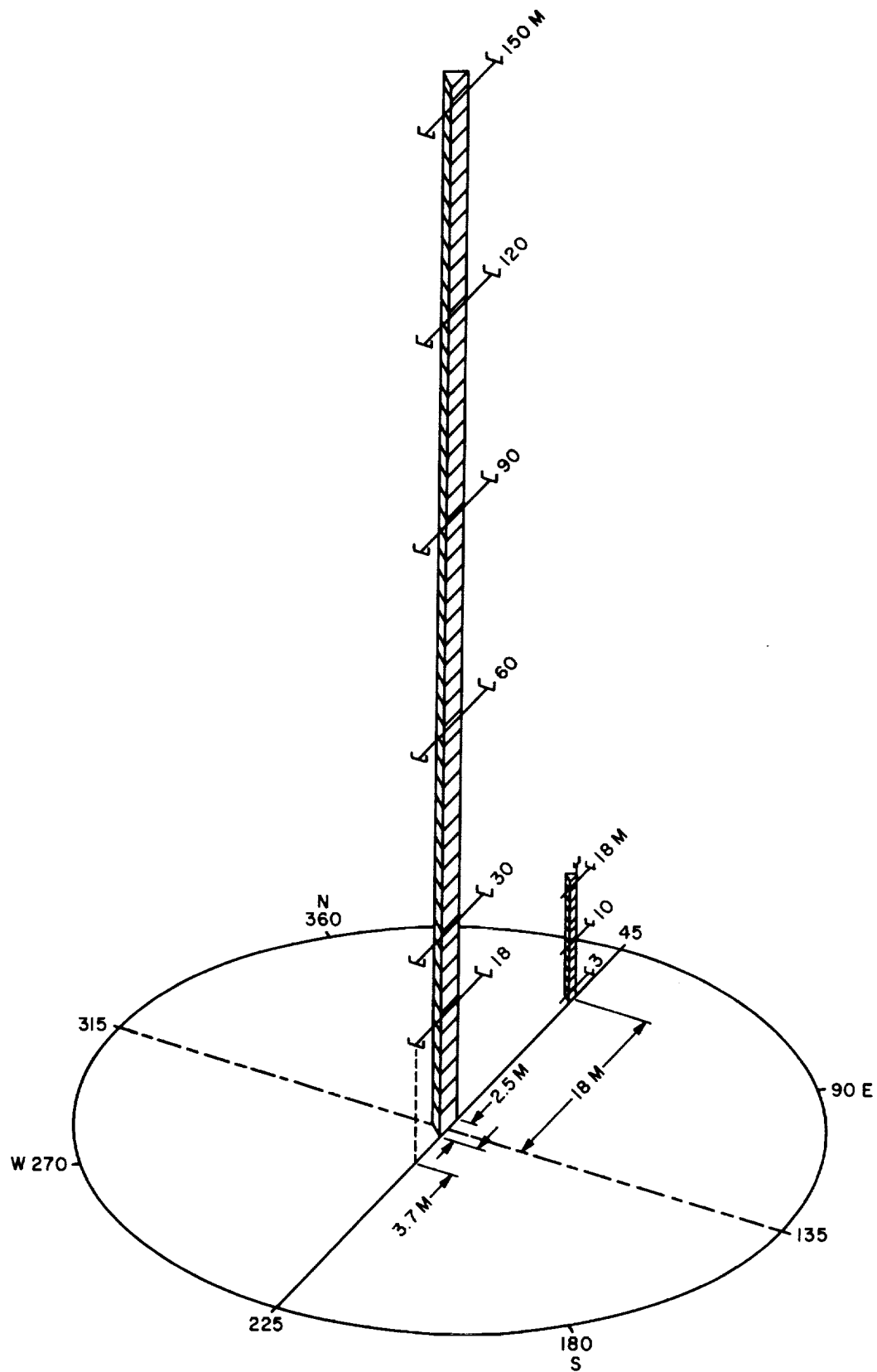


FIGURE 2-2. NASA's 150-meter Meteorological Tower Facility at Kennedy Space Center.

Records Center at Asheville, North Carolina. The reduced data comprise mean, minimum and maximum values of wind speed and wind direction at each tower level for the first 10 minutes of each hour; and temperature gradient data at the start of each 10-minute period. Reduced tower data for the two years 1966 and 1967 were made available for analysis under this contract.

Analysis procedures were designed to determine relationships between profile characteristics and turbulence parameters and other meteorological variables that could be used to predict the meteorological inputs required by the diffusion models described in Section 1.2. In carrying out the analysis, the 2-year data set was first separated into subsets according to season, time of day, wind direction and wind speed. Since it was not known a priori what data classes would prove most suitable, the division into subsets for this initial analysis was made in considerable detail. Figure 2-3 outlines the breakdown of the 2-year data set into the 1152 basic subsets used in the analysis. The division into time subsets separates the 24-hour day into daytime, nighttime and transition periods. Wind speeds and directions used in the data stratification are those observed at the 18-meter level of the 150-meter tower.

The Computational Laboratory at Marshall Space Flight Center provided statistical estimates of the desired parameters for each of the subsets listed in Figure 2-3. An example of the output of the computer program is shown in Figure 2-4 where the parameters are identified as:

DR = Wind direction range over a 10-minute period

U = Mean wind speed

UR = Wind speed range over a 10-minute period

T = Temperature in degrees centigrade. Differences are the temperature at the upper level minus the temperature at the 3-meter level

3, 18, ... 150 = Tower level in meters above the ground

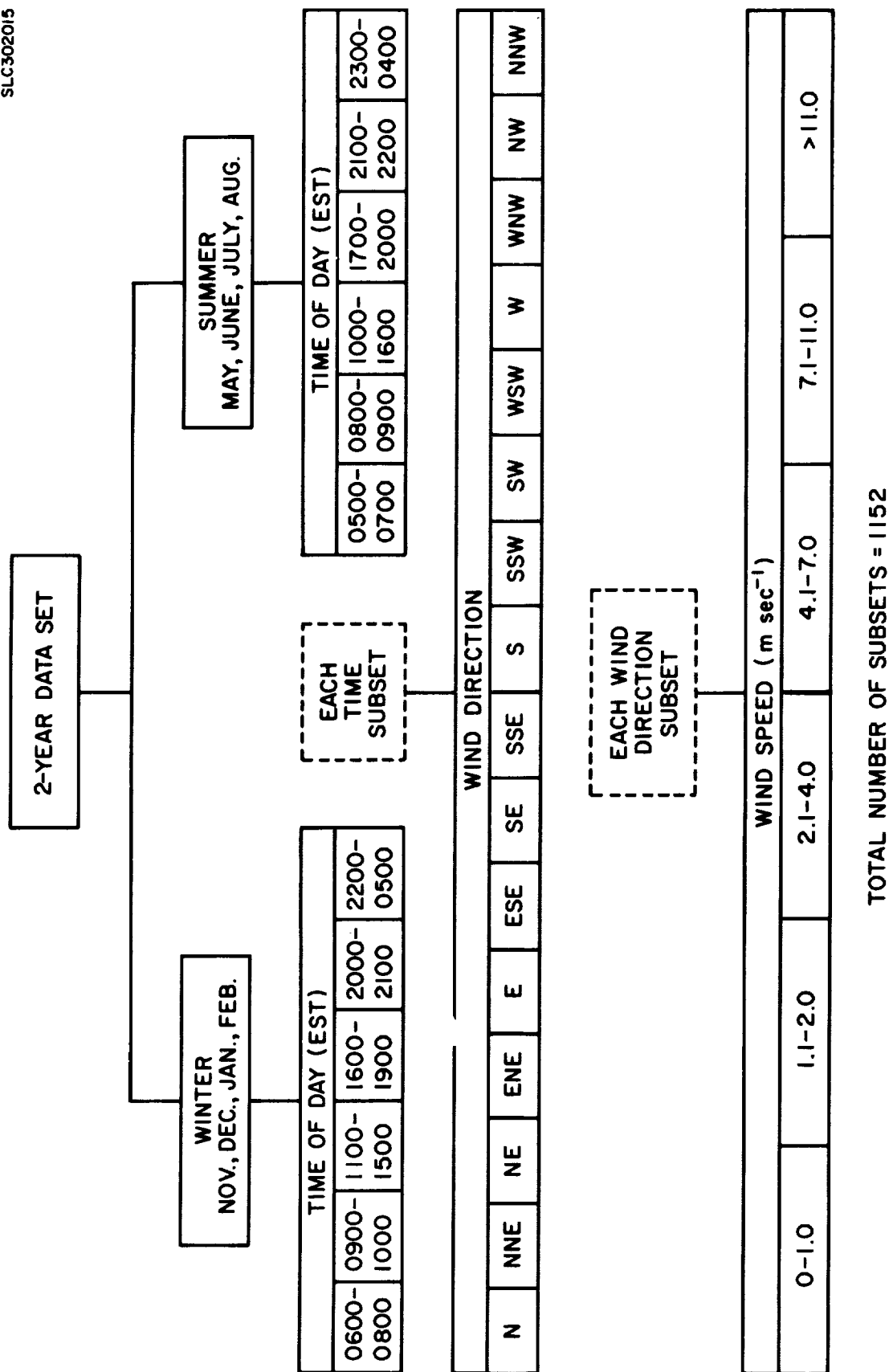


FIGURE 2-3. Stratification of NASA's 150-meter Tower data by season, time of day, wind direction and wind speed.

KMT 150M TOWER DIFFUSION STUDY DATA ANALYSIS

SEASON - SUMMER

TIME OF OBSERVATIONS (EST) - 2300.0000,0100,0200,0300,0400

WIND DIRECTION GROUP
169 - 191 DEGREES

PARAMETER	CASES	0.0 - 1.0				1.1 - 2.0				WIND SPEED GROUPS (M/SEC)				4.1 - 7.0				7.1 - 11.0				> 11.0							
		MEAN		MEDIAN		CASES		MEAN		MEDIAN		CASES		MEAN		MEDIAN		CASES		MEAN		MEDIAN		CASES		MEAN		MEDIAN	
DR10	7	47.	43.	29	40.	36.	71	43.	42.	24	56.	53.	8	39.	40.	0	0.	0.	0.	0.	0.	0.	0.	0.	0.	0.	0.	0.	
UR30/UR18	7	1.2	.8	25	.9	.8	64	.9	.9	20	.9	.9	6	.8	.7	0	0.	0.	0.	0.	0.	0.	0.	0.	0.	0.	0.	0.	
UR60/UR18	6	1.1	.4	29	.7	.6	63	.7	.6	17	.6	.6	8	.7	.7	0	0.	0.	0.	0.	0.	0.	0.	0.	0.	0.	0.	0.	
UR90/UR18	6	.8	.3	23	.6	.4	55	.5	.5	11	.5	.4	6	.5	.5	0	0.	0.	0.	0.	0.	0.	0.	0.	0.	0.	0.	0.	
UR120/UR18	7	1.1	.2	27	.6	.4	62	.5	.4	18	.4	.3	6	.5	.4	0	0.	0.	0.	0.	0.	0.	0.	0.	0.	0.	0.	0.	
UR150/UR18	6	.7	.2	25	.5	.4	64	.4	.3	14	.3	.3	6	.8	.5	0	0.	0.	0.	0.	0.	0.	0.	0.	0.	0.	0.	0.	
U18	7	.8	.9	29	1.6	1.5	71	2.9	2.8	24	4.9	4.7	8	8.0	7.7	0	0.	0.	0.	0.	0.	0.	0.	0.	0.	0.	0.	0.	
U30/U18	7	1.84	1.33	28	1.22	1.17	69	1.12	1.13	24	1.10	1.14	8	1.08	1.07	0	0.	0.	0.	0.	0.	0.	0.	0.	0.	0.	0.	0.	
U60/U18	6	3.57	2.81	29	1.96	1.73	65	1.60	1.60	18	1.46	1.40	8	1.53	1.59	0	0.	0.	0.	0.	0.	0.	0.	0.	0.	0.	0.	0.	
U90/U18	6	4.78	3.73	24	2.50	2.34	58	1.94	1.88	14	1.62	1.55	6	1.83	1.83	0	0.	0.	0.	0.	0.	0.	0.	0.	0.	0.	0.	0.	
U120/U18	7	5.60	4.13	27	2.84	2.64	67	2.09	2.02	18	1.70	1.71	6	1.83	1.81	0	0.	0.	0.	0.	0.	0.	0.	0.	0.	0.	0.	0.	
U150/U18	5	4.25	4.00	24	2.56	2.54	59	2.10	2.00	17	1.91	1.85	6	1.90	1.90	0	0.	0.	0.	0.	0.	0.	0.	0.	0.	0.	0.	0.	
UR18	7	.82	.70	29	1.31	1.30	71	2.35	2.19	24	4.35	4.12	8	7.10	7.12	0	0.	0.	0.	0.	0.	0.	0.	0.	0.	0.	0.	0.	
UR30/UR18	7	1.20	1.00	29	1.09	1.10	69	1.00	.96	24	1.02	1.01	8	.91	.87	0	0.	0.	0.	0.	0.	0.	0.	0.	0.	0.	0.	0.	
UR60/UR18	6	1.56	1.26	29	1.42	1.23	65	1.13	1.09	18	1.03	.99	8	1.04	1.03	0	0.	0.	0.	0.	0.	0.	0.	0.	0.	0.	0.	0.	
UR90/UR18	6	1.35	.77	24	1.27	1.00	58	.93	.91	14	.92	.87	6	.80	.78	0	0.	0.	0.	0.	0.	0.	0.	0.	0.	0.	0.	0.	
UR120/UR18	7	1.72	1.43	27	1.03	.93	67	1.02	.98	18	.79	.82	6	.89	.90	0	0.	0.	0.	0.	0.	0.	0.	0.	0.	0.	0.	0.	
UR150/UR18	5	1.16	1.20	24	1.38	1.00	59	.99	.94	17	.88	.78	6	.86	.87	0	0.	0.	0.	0.	0.	0.	0.	0.	0.	0.	0.	0.	
T3-T18	7	1.960	2.055	23	1.171	.972	69	.529	.278	23	.227	.111	8	.021	.000	0	0.	0.	0.	0.	0.	0.	0.	0.	0.	0.	0.	0.	
T3-T20	7	2.246	2.278	28	1.480	1.167	69	.626	.333	23	.157	-.055	8	-.361	-.417	0	0.	0.	0.	0.	0.	0.	0.	0.	0.	0.	0.	0.	
T3-T120	7	2.730	2.000	22	1.616	1.278	58	.661	.500	20	-.144	-.472	6	-.935	-.944	0	0.	0.	0.	0.	0.	0.	0.	0.	0.	0.	0.	0.	
T3-T150	0	.000	.000	0	.000	.000	0	.000	.000	0	.000	.000	0	.000	.000	0	0.	0.	0.	0.	0.	0.	0.	0.	0.	0.	0.	0.	

FIGURE 2-4. Sample page of computer printout provided in the analysis of NASA's 150-meter Tower data.

The 3- to 150-meter temperature difference data were inadvertently excluded from the statistical summary supplied by the MSFC Computational Laboratory.

2.1.3 The Vertical Profile of Wind Speed

One of the input parameters to the diffusion models discussed in Section 1.2 is the mean wind speed at some specified height or integrated over a layer. It is generally accepted (Sellers, 1965) that a simple power law defined by the expression

$$\bar{u} \{z_1\} / \bar{u} \{z_2\} = (z_1/z_2)^p$$

adequately describes the wind profile for diffusion calculations near the earth's surface. In this expression, \bar{u} is the mean wind speed at height z and the subscripts 1 and 2 denote two measurement heights. The value of the exponent p is related to atmospheric stability and surface roughness. The principal advantage of the power law over some of the more complicated profile expressions lies in the ease with which it can be defined and used to extrapolate wind speed from one height to another. Estimates of the power law exponent p over a height of approximately 150 meters have been made for Cape Kennedy from the NASA Meteorological Tower data.

As a first step in estimating the exponent p , the ratios of the wind speed at 60, 90, 120 and 150 meters to the wind speed at 18 meters were plotted against the 16 wind direction sectors shown in Figure 2-3. Separate curves were prepared for daytime and nighttime periods and for wind speed categories of 2-4 and 4-7 meters per second. The curves for the winter and summer seasons are given in Figures 2-5 and 2-6, respectively. These figures show the expected pronounced diurnal variation in the ratios, with nighttime values averaging about one and one-half times the daytime values. Average values of

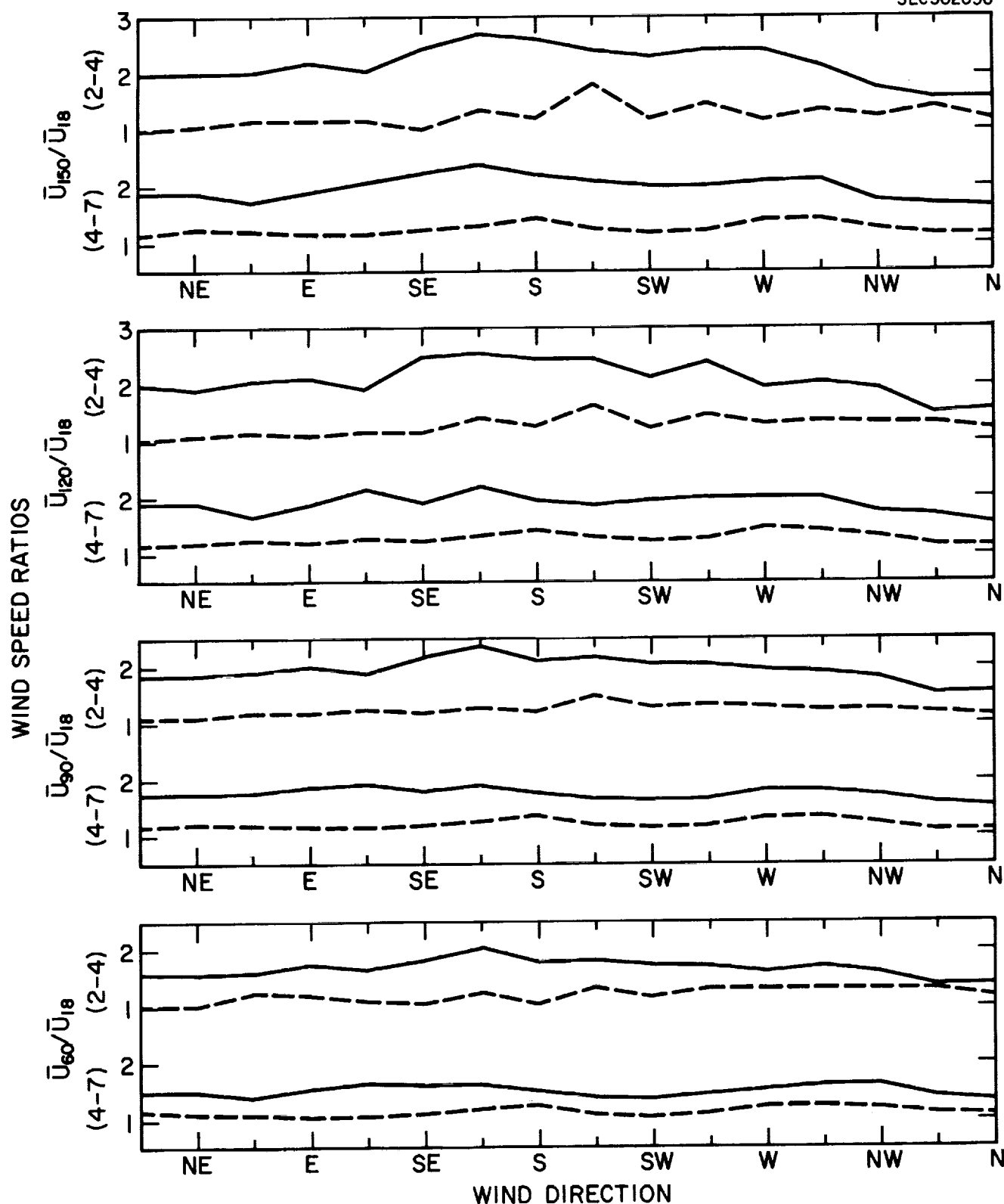


FIGURE 2-5. Ratios of the wind speeds at 60, 90, 120 and 150 meters to the wind speed at 18 meters during the winter season for two wind speed categories and two time periods. Solid curves are for 2200-0500 EST; dashed curves are for 1100-1500 EST. Wind speed categories in meters per second are shown in parentheses.

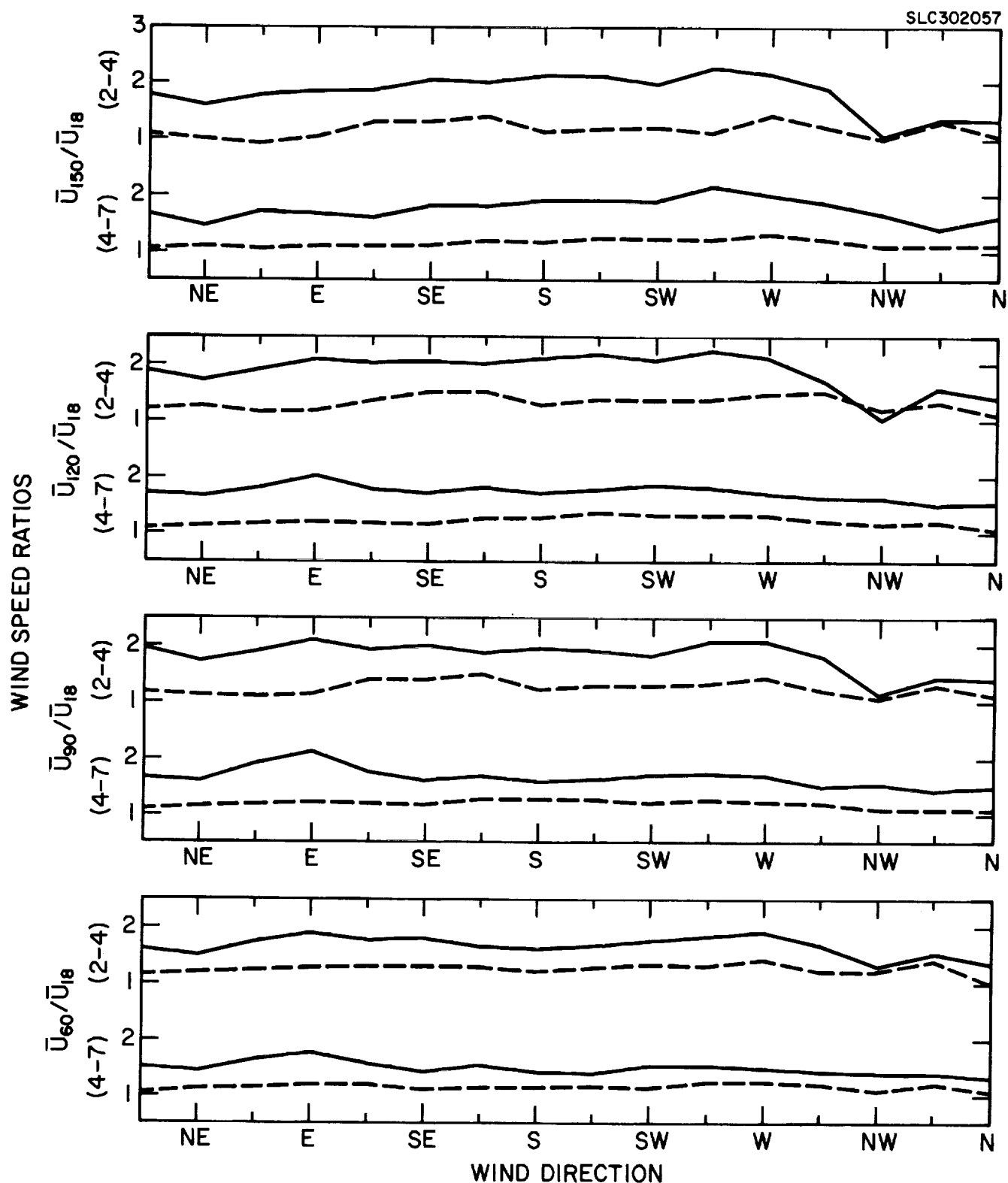


FIGURE 2-6. Ratios of the wind speeds at 60, 90, 120 and 150 meters, to the wind speed at 18 meters during the summer season for two wind speed categories and two time periods. Solid curves are for 2300-0400 EST; dashed curves are for 1000-1600 EST. Wind speed categories in meters per second are shown in parentheses.

the ratios increase with increasing height through the 90-meter level as expected, but show little increase at higher elevations. The most obvious effect of wind direction on the wind speed profile is indicated by the low values of the wind speed ratios at all levels for nighttime periods having low wind speeds and northwesterly winds. This decrease is not as pronounced for the higher wind speed category at night and is not evident in either wind speed category during the day. Minor irregularities in the curves may in part be due to differences in surface roughness, but are also a reflection of the small number of cases within some of the data subsets.

Examination of Figures 2-5 and 2-6 in conjunction with the results of a study of surface roughness in the vicinity of the tower by Fichtl (1968) indicated that the following five wind direction classes could be used in the assignment of p values to the wind profile: 34 to 101, 102 to 168, 169 to 236, 237 to 303, and 304 to 033 degrees. Plots of wind speed versus height, using the combined data, were constructed on logarithmic paper for four wind speed categories. These graphs, in addition to providing a simple check on data quality and continuity, were in a form that facilitated the estimation of the power-law exponent p for each profile. The exponent p was determined by visually fitting a straight line to the data where the speeds showed an orderly increase with height. The slope of this line, which by definition is the exponent p , was then measured. Values of wind speed profile power-law exponent p were determined principally over the height interval from 18 to 90 meters to avoid the discontinuity in the profile that frequently appears between 90 and 150 meters. The values of p calculated by the procedure described above were plotted on polar coordinate paper and smoothed curves were drawn for each wind speed category.

Figures 2-7 and 2-8 present the winter and summer nighttime values of p , respectively, as functions of mean wind speed and mean wind direction at the 18-meter level. Seasonal differences in the wind speed profiles

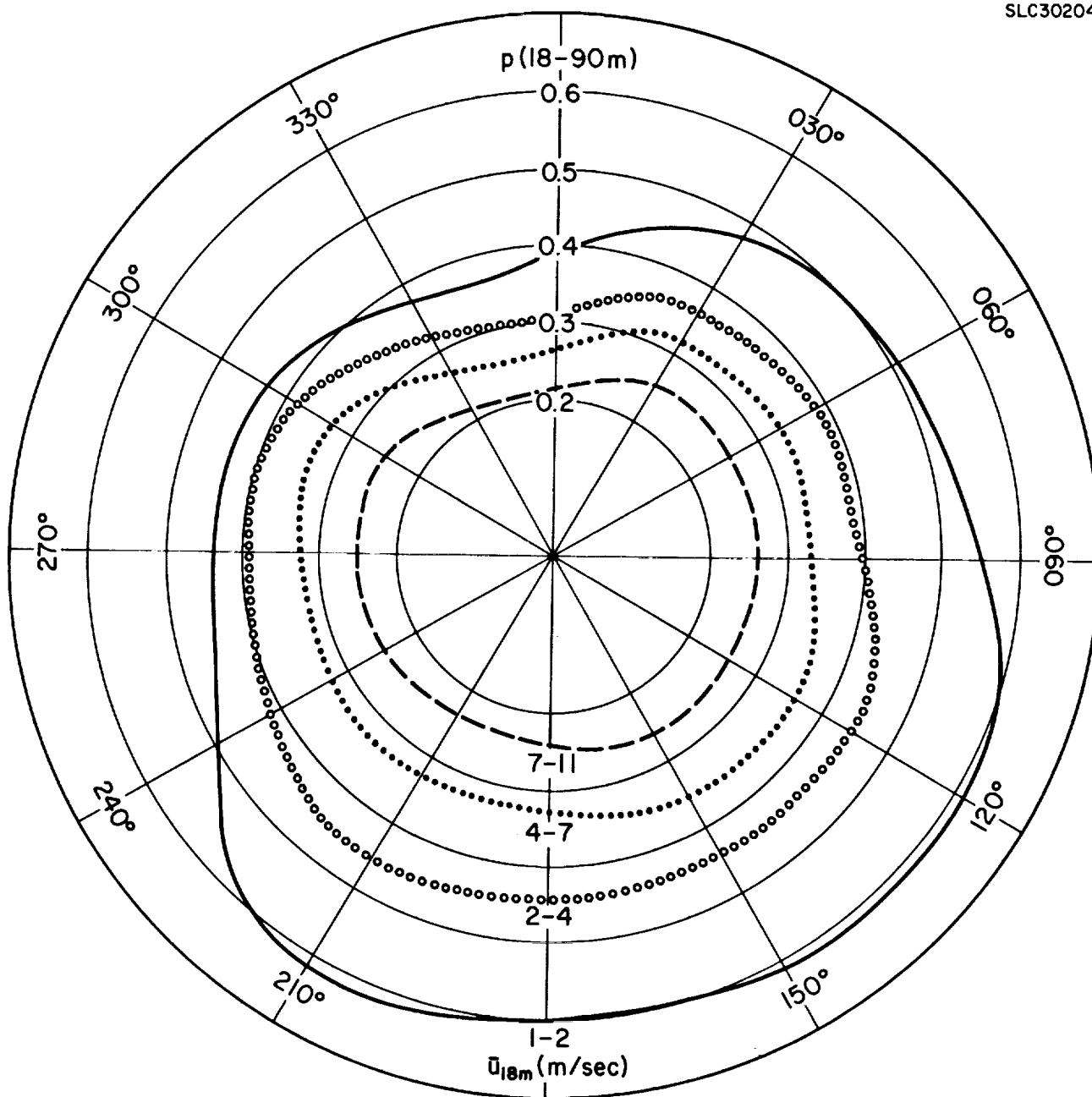


FIGURE 2-7. Winter nighttime values of p as a function of the wind direction and wind speed at 18 meters.

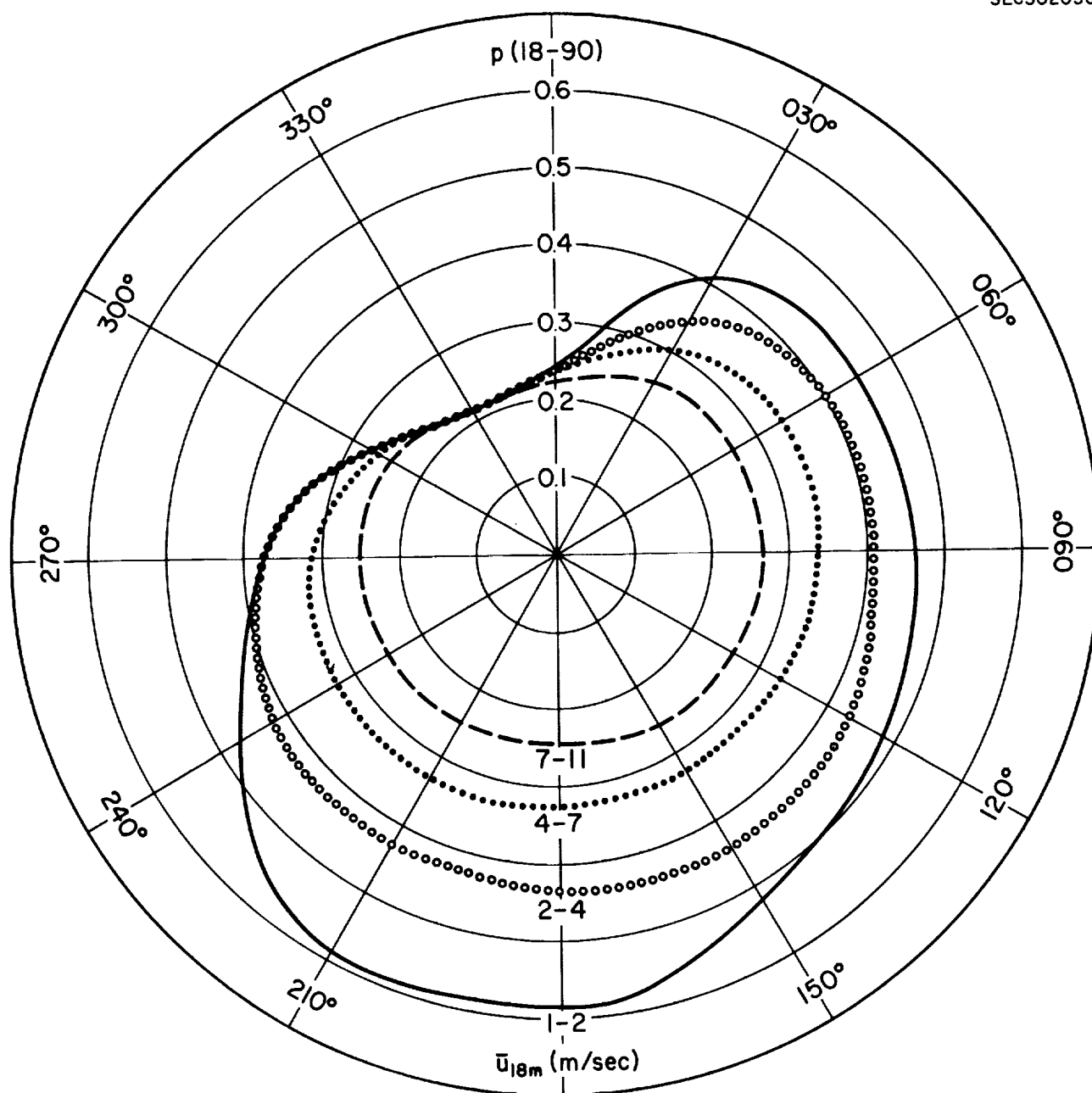


FIGURE 2-8. Summer nighttime values of p as a function of the wind direction and wind speed at 18 meters.

for the 1-2 meter per second category are likely a result of differences in atmospheric stability. For wind speeds greater than 2 meters per second, the p curves for both seasons are similar, except for wind directions from northwest through north. Estimates of p for the daytime period are given in Figure 2-9. Because no significant seasonal differences were observed in the daytime p curves, the data were combined to provide annual curves. Wind speed profiles for the daytime 1-2 meter per second category are so irregular that no evaluation of p could be made.

Figure 2-10, which shows p as a function of wind speed and stability, has been prepared as a convenient method for estimating p for general application at Kennedy Space Center. The individual curves in the figure were constructed by plotting p values, calculated from the average ratio of the wind speeds at 18 and 90 meters, against the average temperature difference between 3 and 60 meters for each wind speed-time period category. Data for all wind directions were included, and the smoothed curves were fitted by eye to the data with no distinction being made between winter and summer data points. These curves indicate a near-neutral value for p of about 0.3 which agrees closely with the near-neutral p values of 0.27 and 0.29 for Quickborn, Germany and Brookhaven, New York reported by DeMarrais (1959).

2.1.4 The 10-Minute Range of Azimuth Wind Direction

The standard deviations of the azimuth and elevation angles of wind direction are related to the lateral and vertical components of gustiness, σ_v and σ_w , through the expressions

$$\sigma_A \approx \frac{\sigma_v}{\bar{u}} \quad \text{and} \quad \sigma_E \approx \frac{\sigma_w}{\bar{u}}$$

where σ_A and σ_E are the standard deviations of the azimuth and elevation angles in radian measure, respectively, and \bar{u} is the mean wind speed. The quantities σ_A and σ_E are basic indices of diffusion in the lateral and vertical directions and are used as direct inputs to many diffusion models, including the ones recommended

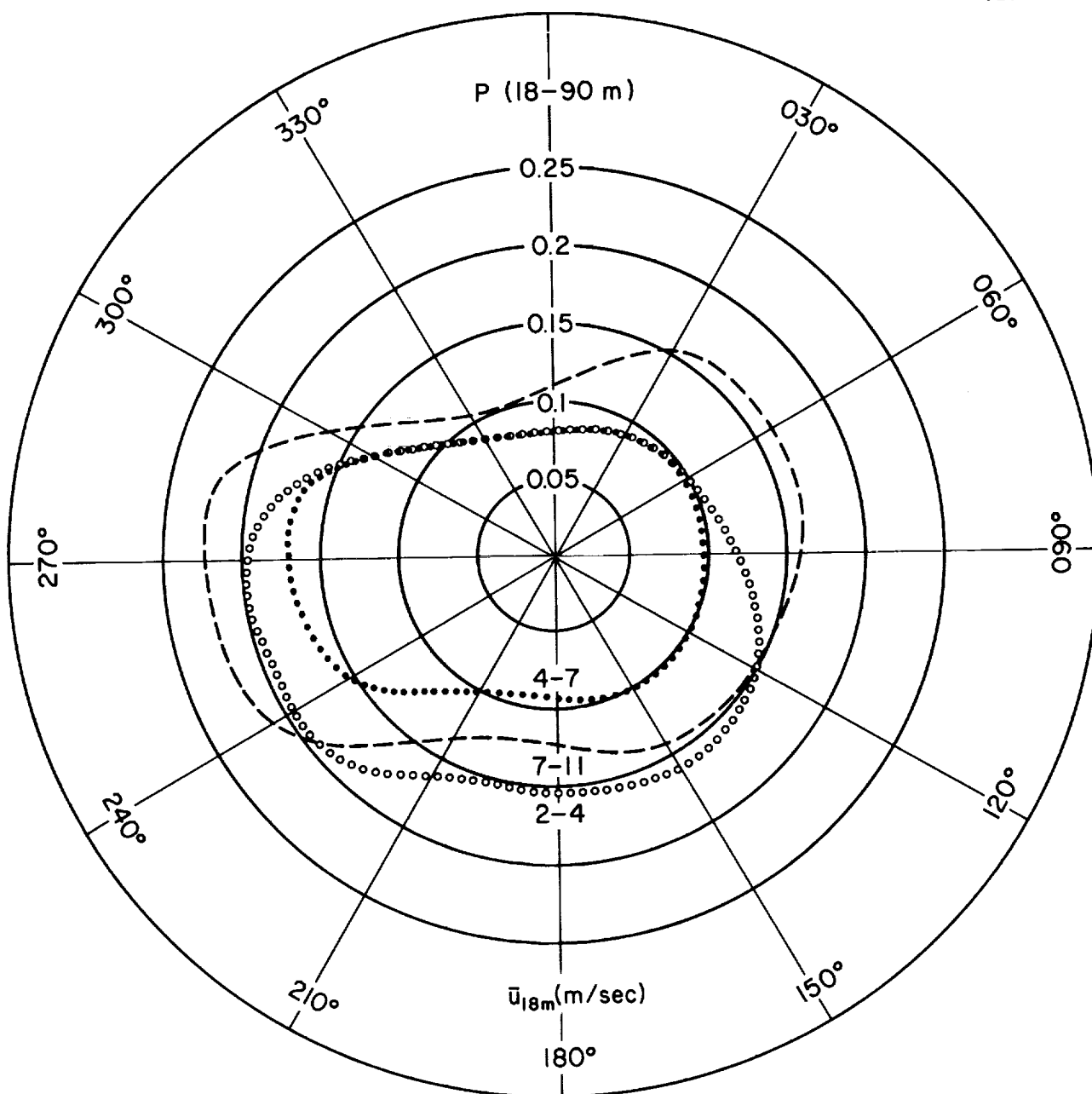


FIGURE 2-9. Annual daytime values of p as a function of the wind direction and wind speed at 18 meters.

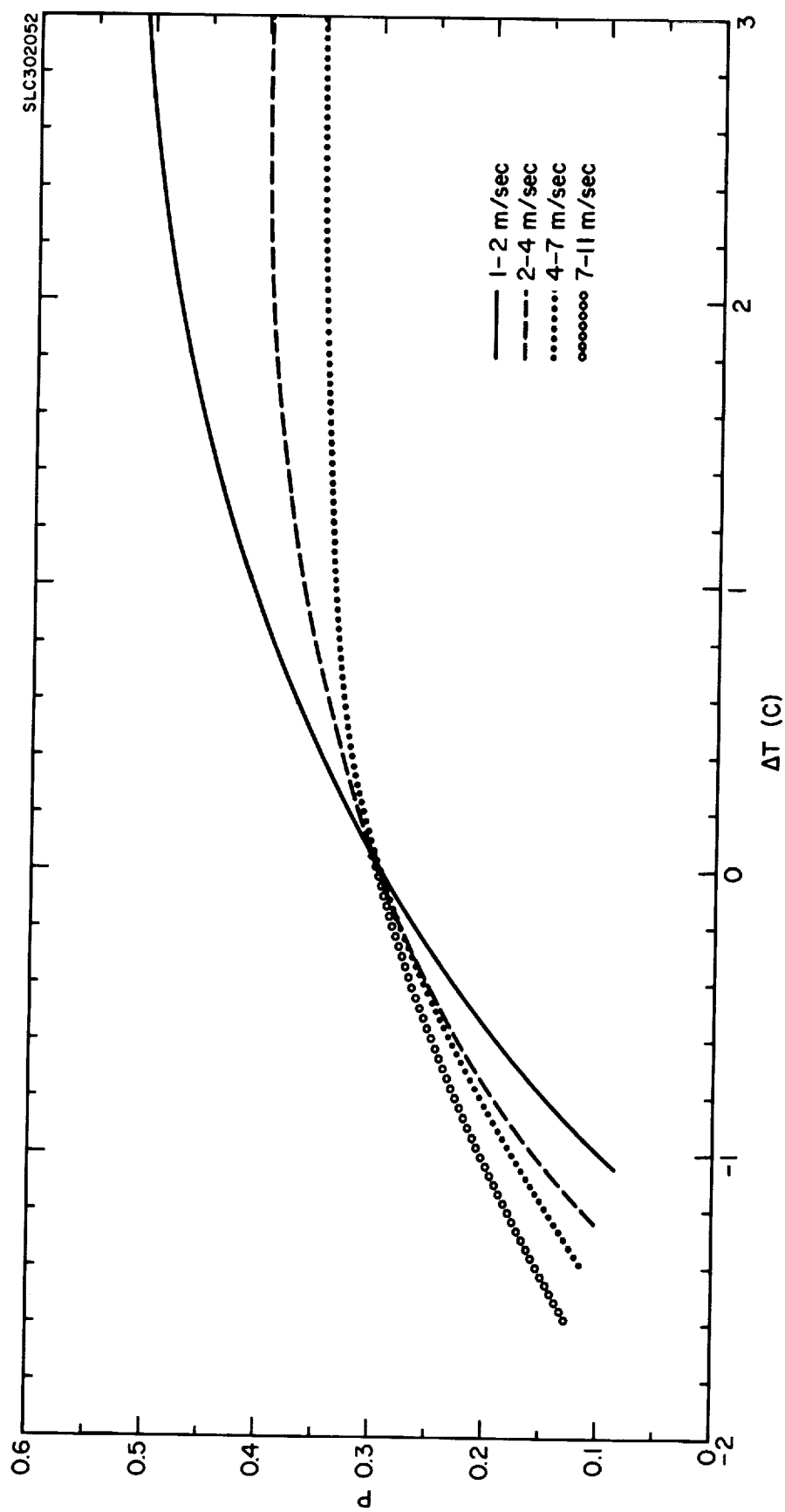


FIGURE 2-10. Dependence of p on stability and the wind speed at 18 meters. ΔT is the temperature at 60 meters minus the temperature at 3 meters.

in Section 1.3 for use at Cape Kennedy. No direct measurements of σ_A or σ_E are routinely made at the NASA 150-meter Tower Facility.* However, the maximum and minimum azimuth directions recorded for each 10-minute period provide range data that can be scaled to obtain estimates of σ_A . The requisite scaling factor for the wind-direction range data collected at the Meteorological Tower Facility is one-sixth (Slade, 1968, p. 47).

The dependence of σ_A on wind direction, wind speed, season and time of day was investigated in terms of the range data collected at a height of 18 meters on the Meteorological Tower. Since seasonal differences were found to be small, the data were combined to provide annual estimates. Summaries of the range data for daytime and nighttime periods are presented in Figures 2-11 and 2-12, respectively. A large diurnal variation in the range during light wind conditions is apparent in the figures. For example, with wind speeds from 2-4 meters per second, the direction range averages about 85 degrees during the daytime and only about 35 degrees during the nighttime. The principal dependence of the range on wind direction is the increase which occurs with westerly winds, particularly during the daytime. This increase is probably caused by the trees west of the tower site. A sharp decrease is observed in direction range when the winds are from 327 to 023 degrees. This decrease is believed to result from difficulties in determining the direction range during crossover. For this reason, the ranges for northerly winds have been excluded from the analysis. The curves of wind direction range for this sector were obtained by extrapolation of the curves for adjacent sectors.

*Five-minute σ_A values have been calculated from a limited number of high-resolution measurements made on the NASA 150-meter Tower Facility during neutral and unstable stratification by Alexander, et al., (1967). Their results for the 18-meter level are in close agreement with the curves in Figure 2-13.

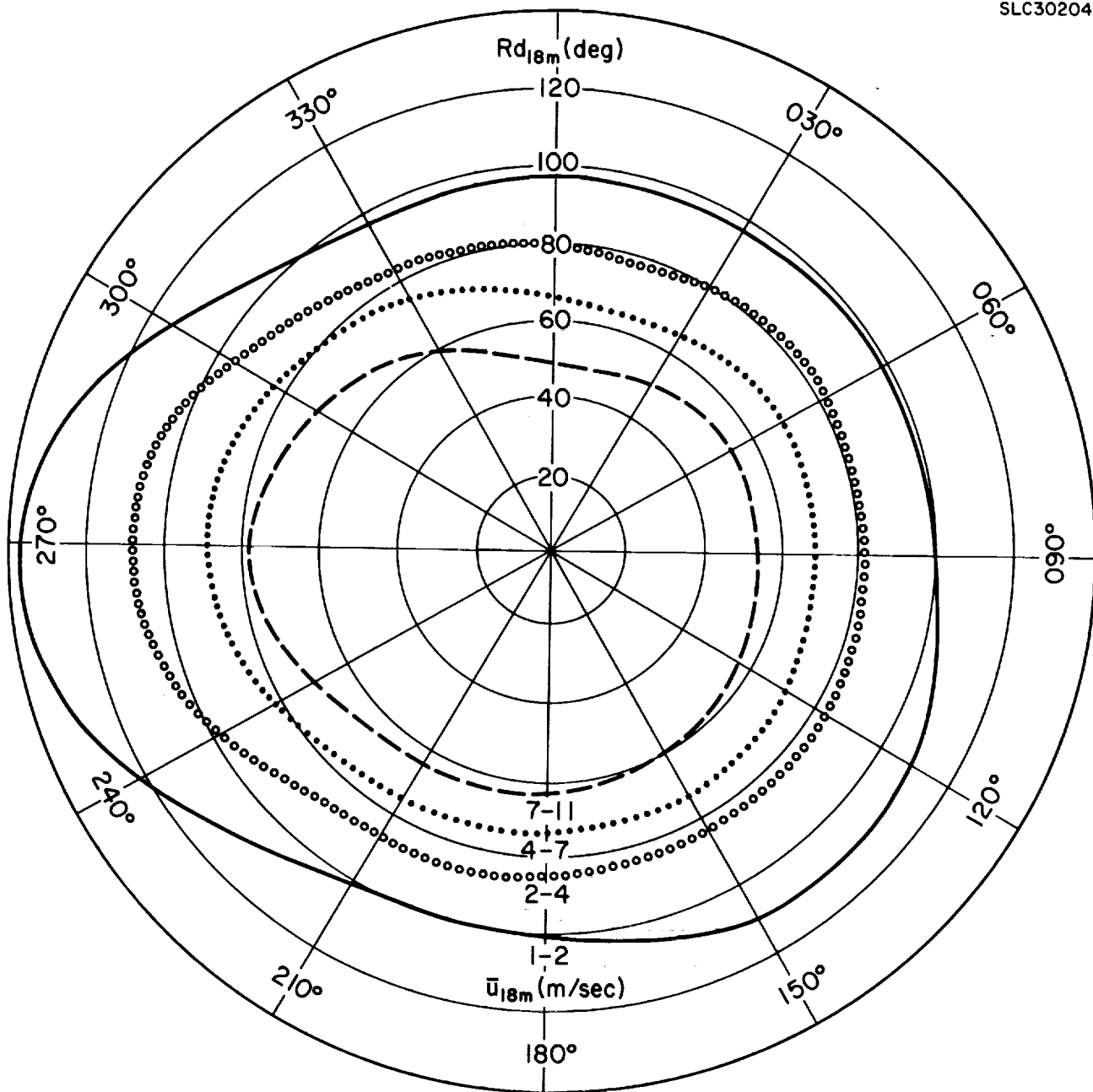


FIGURE 2-11. Annual daytime wind direction range R_d at 18 meters as a function of the wind direction and wind speed at 18 meters.

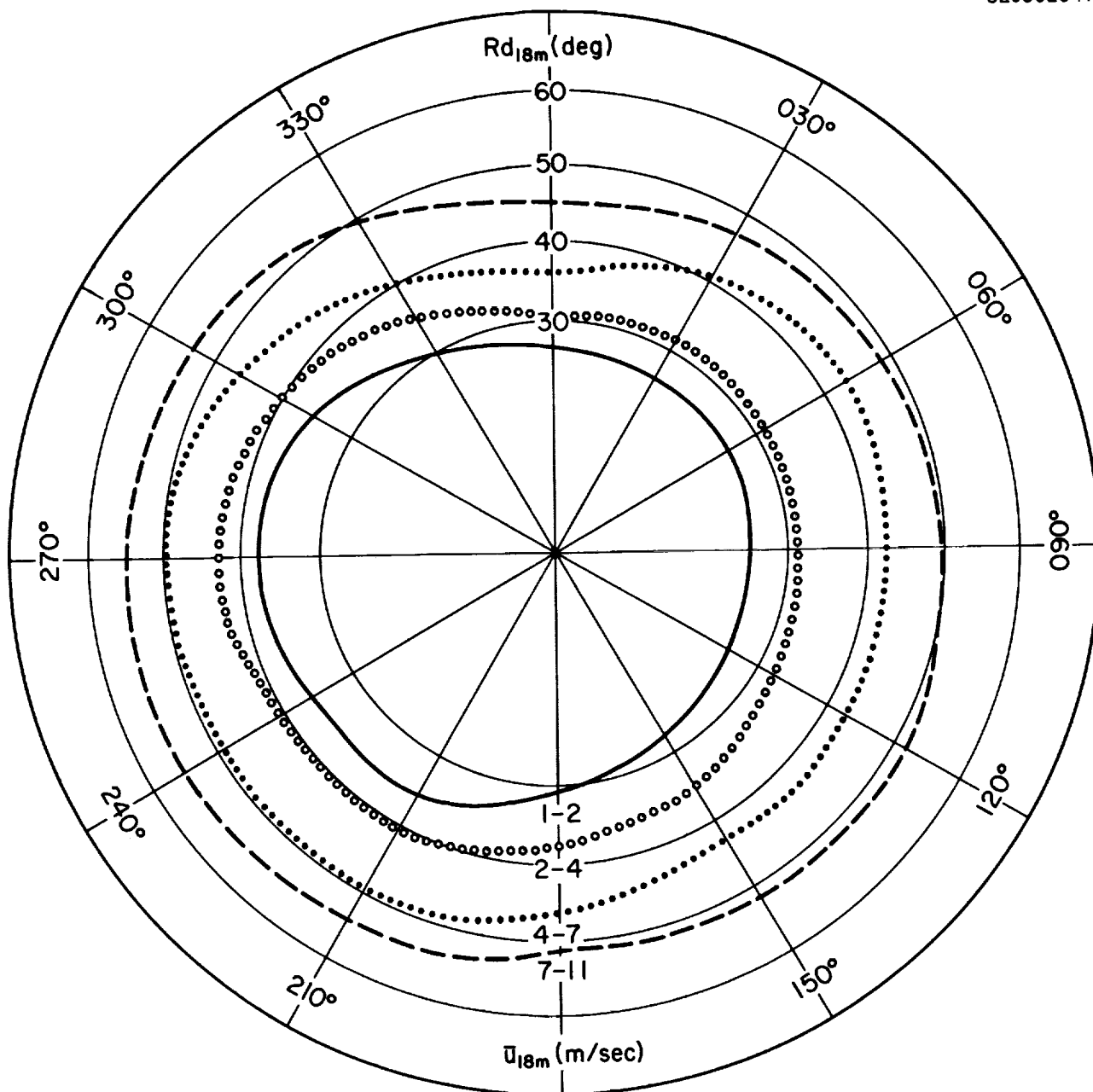


FIGURE 2-12. Annual nighttime wind direction range R_d at 18 meters as a function of the wind direction and wind speed at 18 meters.

Figure 2-13 has been prepared to provide estimates of σ_A for general application at the Kennedy Space Center under various wind speed and stability conditions. To prepare the curves, the median 18-meter direction ranges were plotted against the temperature difference between the 60- and 30-meter levels of the tower for each of four wind speed categories, using the data for all time periods, both seasons, and all wind directions except northerly. Winds from the northerly sector were excluded because of the possibility of crossover problems mentioned above. The wind direction range scales of the working plots were converted to σ_A by means of the one-sixth scaling factor. The dependence of the wind direction range on stability is strongest during light winds and decreases with increasing wind speed. Very stable conditions do not occur with strong winds at the 18-meter level, and the curve for winds of 7 to 11 meters per second extends only to conditions of slight stability. As might be expected, the range data show a large amount of scatter. An example of the plots from which the curves were prepared is shown in Figure 2-14. The curves shown in Figures 2-13 and 2-14 were drawn through median values within selected ΔT intervals.

The height dependence of the 10-minute wind direction range was expressed by the power-law relationship

$$R_d\{z_1\}/R_d\{z_2\} = (z_1/z_2)^q$$

and estimates of q as a function of mean wind speed and wind direction were determined graphically. The results, which apply principally over the height interval from 18 to 90 meters, are shown for daytime and nighttime periods in Figures 2-15 and 2-16, respectively. Because seasonal differences in the profiles appeared to be insignificant, only annual curves are presented. In the analysis, the range data were combined into the five direction categories used previously in the treatment of wind speed profiles. The curves were extrapolated through the sector from 327 to 023 degrees.

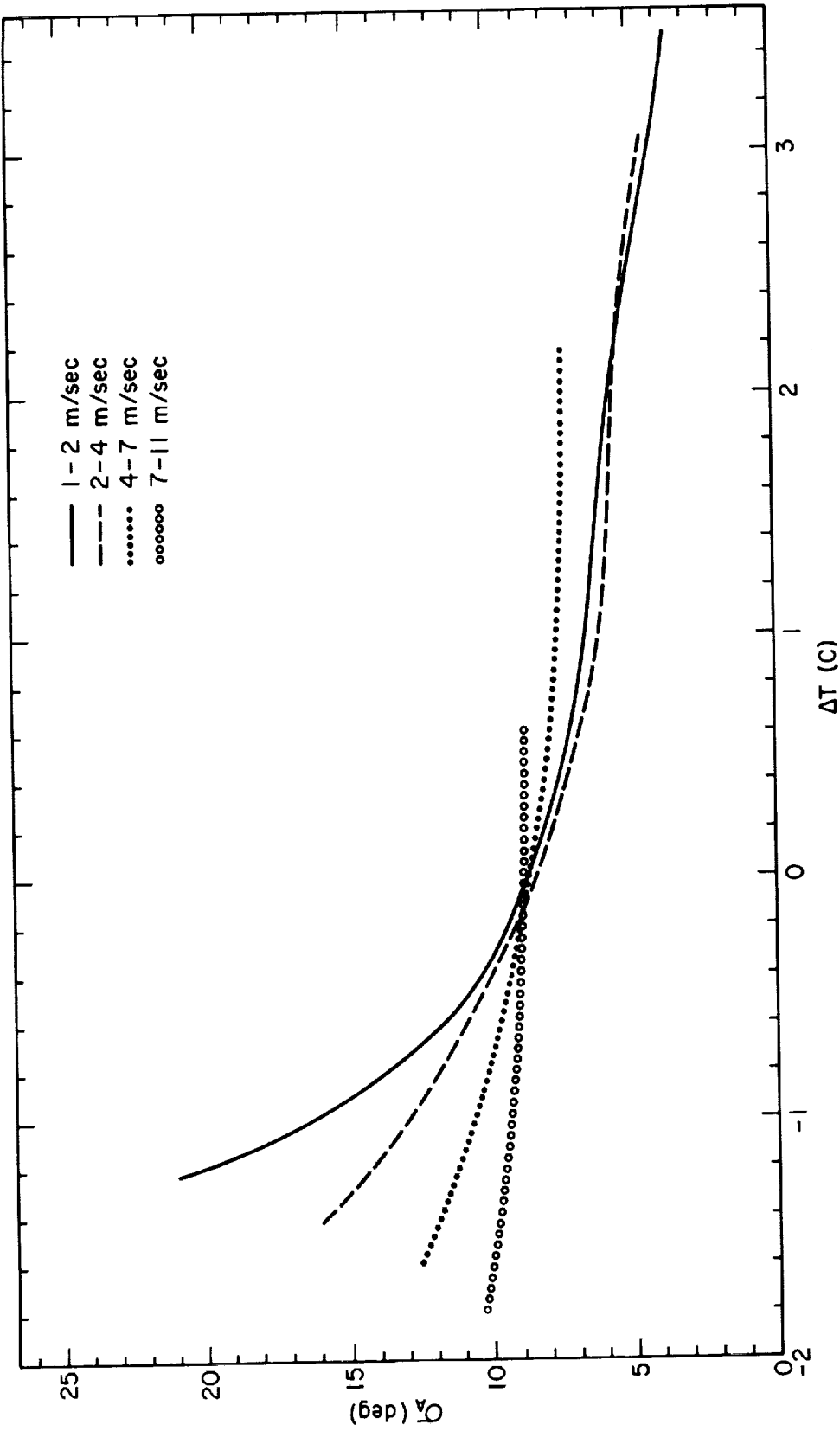


FIGURE 2-13: Dependence of σ_A at 18 meters on stability and wind speed at 18 meters. ΔT is the temperature at 60 meters minus the temperature at 3 meters.

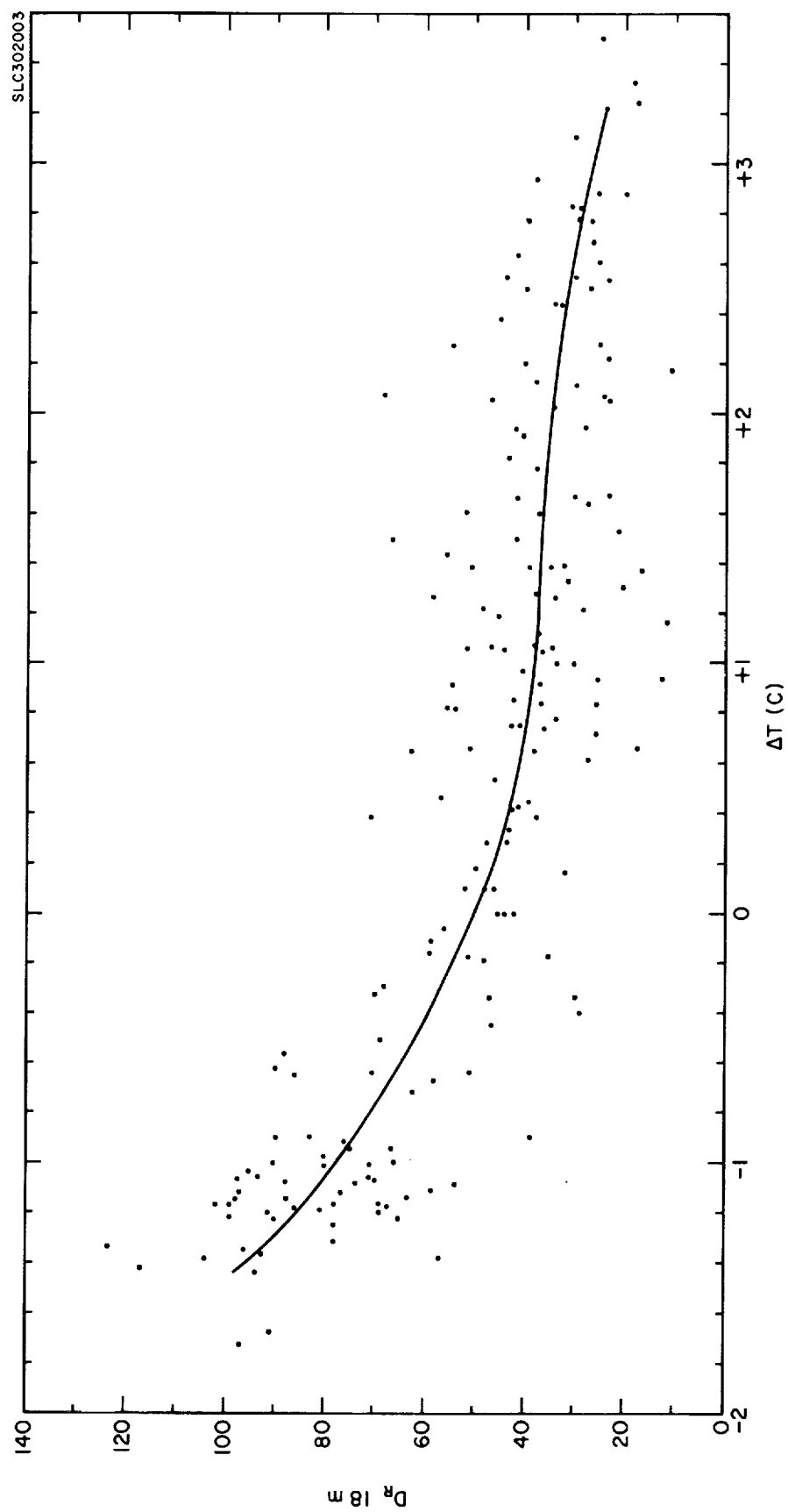


FIGURE 2-14. Median 10-minute wind direction range at 18 meters versus the temperature difference between 3 meters and 60 meters for the 2-4 meter per second wind speed category.

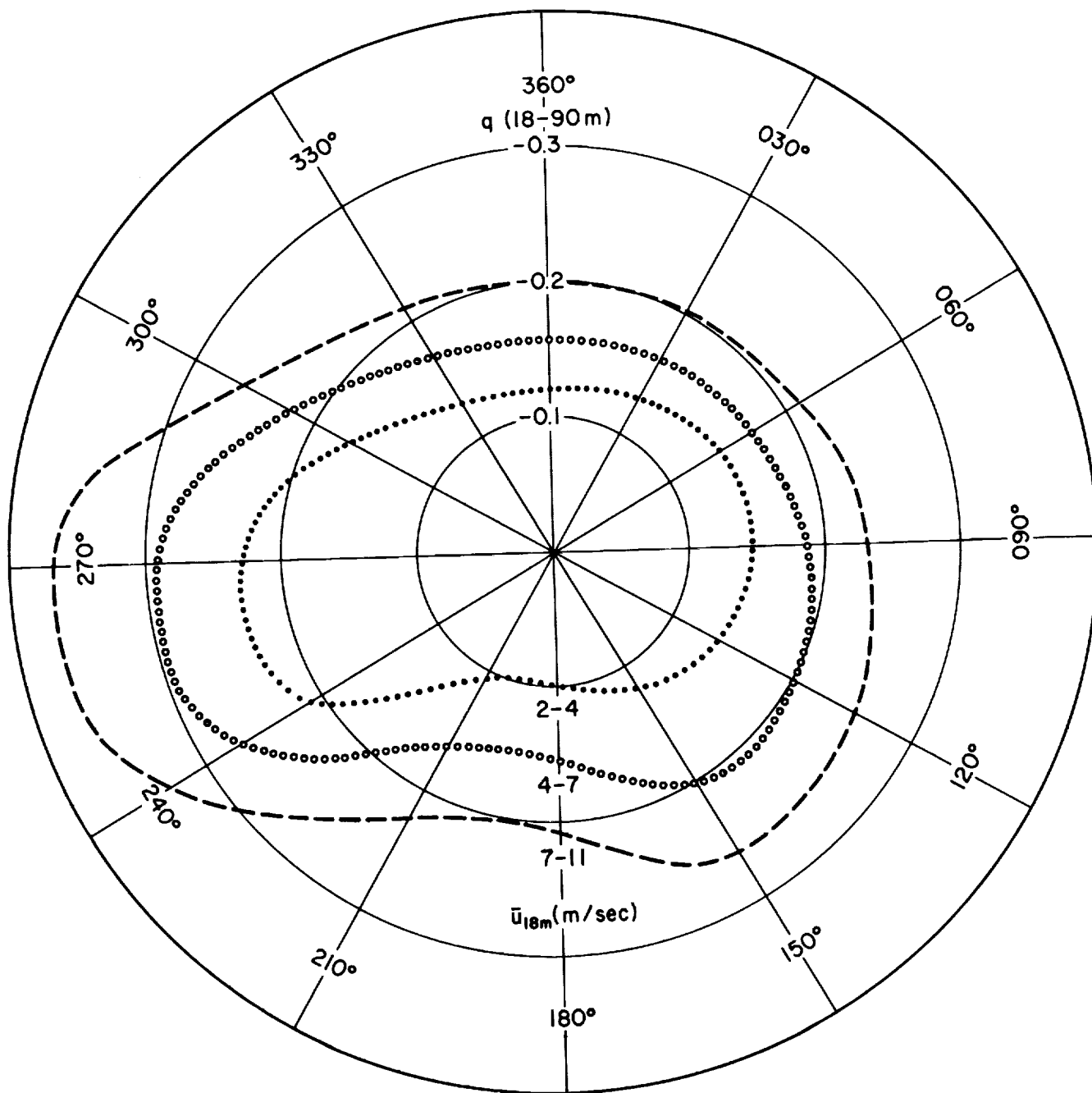


FIGURE 2-15. Annual daytime values for q as a function of wind direction and wind speed at 18 meters.

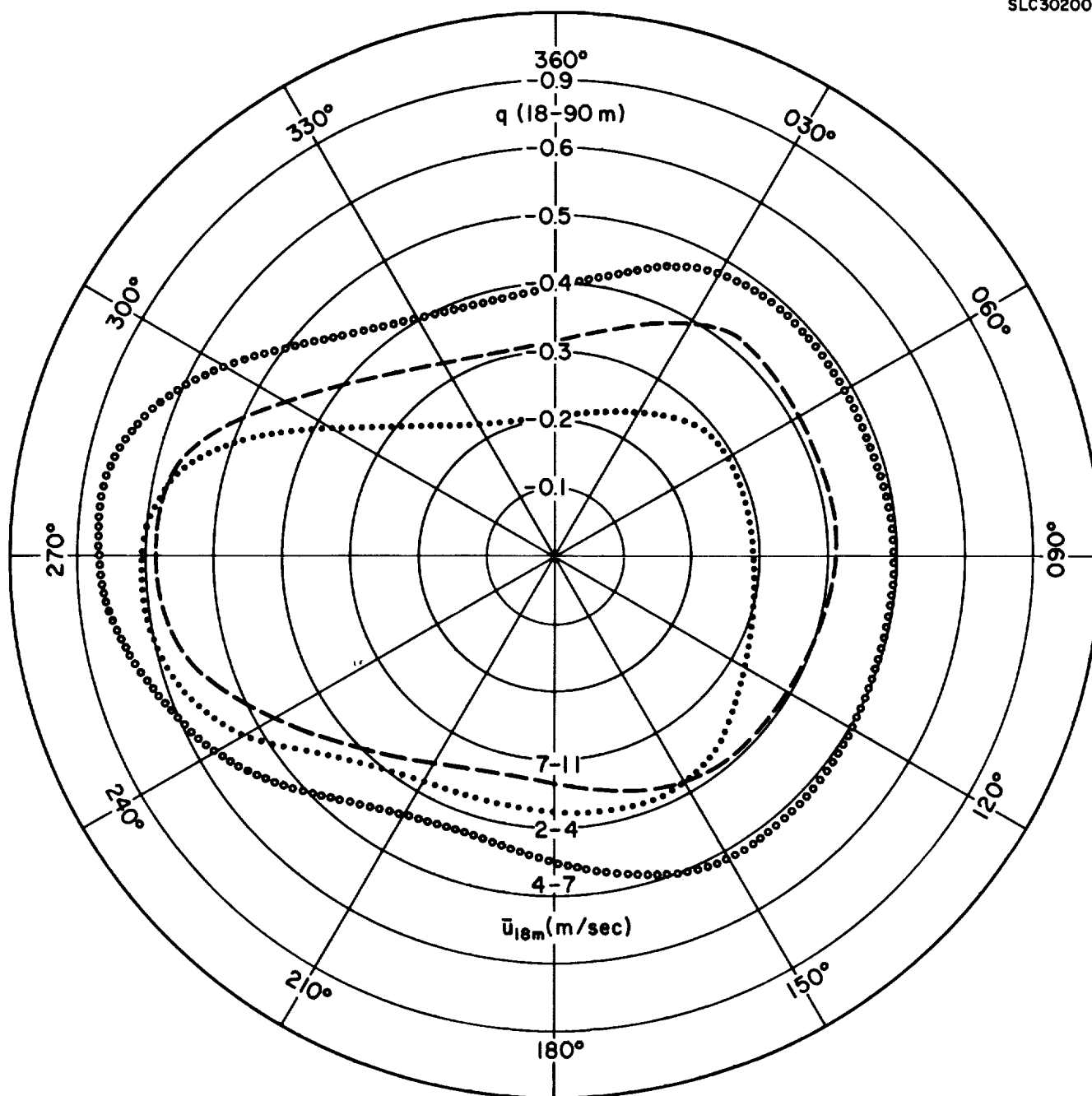


FIGURE 2-16. Annual nighttime values for q as a function of wind direction and wind speed at 18 meters.

An interesting feature of these curves which is present in both the daytime and nighttime results is the large increase in q associated with westerly winds. This is apparently a result of the increase in direction ranges at the lower tower levels noted in Figures 2-11 and 2-12 caused by the trees located west of the site.

General curves for the estimation of q over the height of the tower have been established by procedures similar to those used in preparing the curves for p shown in Figure 2-10. The curves for estimating q are presented in Figure 2-17 and show q over the height interval from 18 to 90 meters as a function of wind speed and stability. In preparing the curves, all data were used except those for wind directions between 327 and 033 degrees.

2.1.5 Variation of the Standard Deviation of the Lateral Wind Component σ_v with Height

It is generally assumed that the standard deviation of the lateral wind component σ_v is insensitive to changes in height (see, for example, Lumley and Panofsky, 1964). It can be seen from the relationship $\sigma_v = \sigma_A \bar{u}$ that this condition is met when the wind speed power-law exponent p is equal in magnitude but opposite in sign to the σ_A power-law exponent q . The assumption that $p = -q$ has been checked between heights of 18 and 90 meters at the NASA Meteorological Tower site by obtaining values of p and q from the preceding figures and calculating ratios of p/q . Values of p and the absolute value of the ratio p/q for selected wind directions and wind speed ranges are shown in Table 2-1. When the 18-meter wind speeds are greater than 4 meters per second, σ_v decreases with increasing height regardless of wind direction or time of day as indicated by $|p/q|$ values substantially less than one. Under light wind conditions (2-4 meters per second) the value of the ratio when averaged over all wind directions is 0.96 in the daytime and 1.15 in the nighttime. However, there is a wide

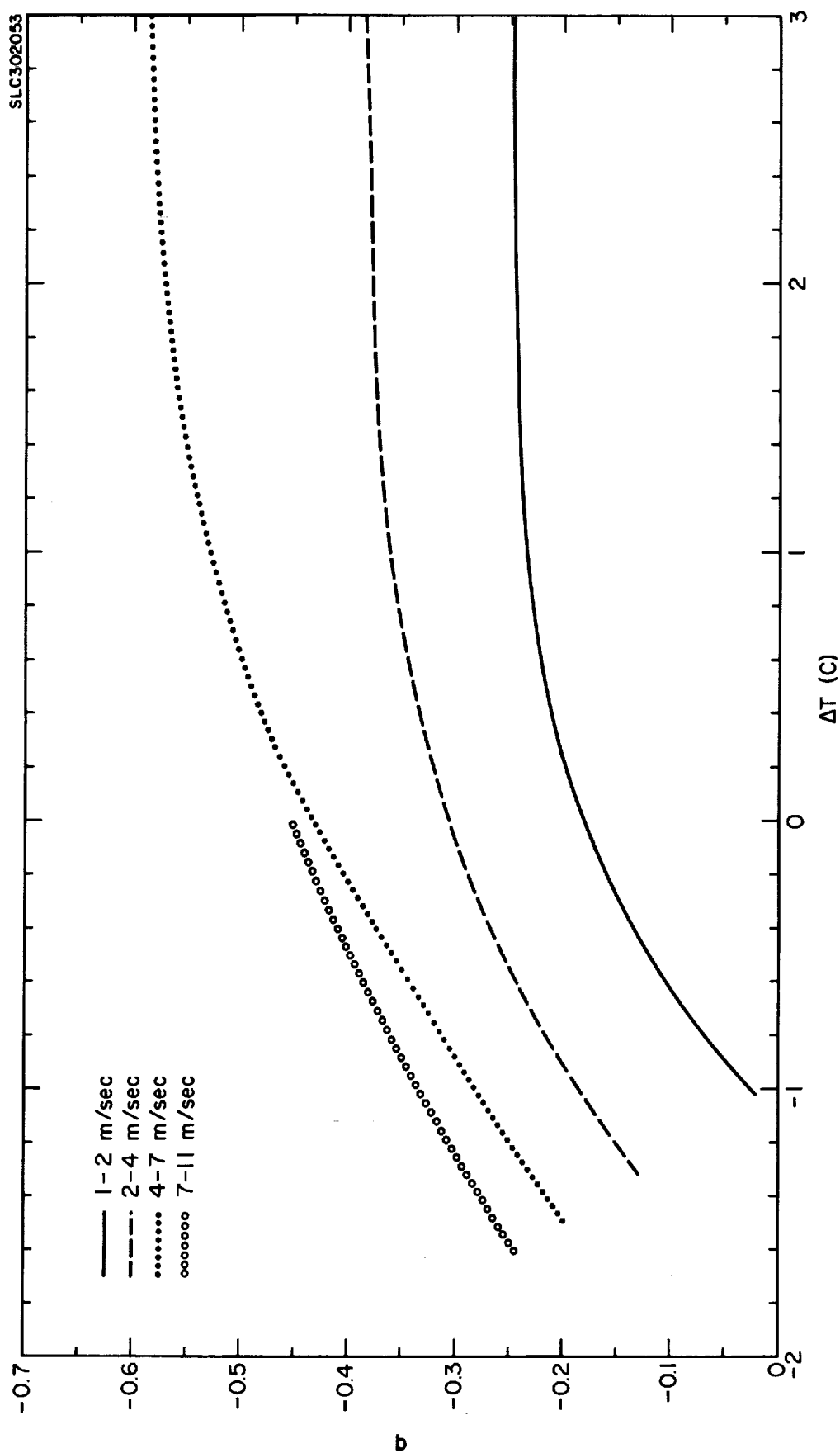


FIGURE 2-17. Dependence of q on stability and the wind speed at 18 meters. ΔT is the temperature at 60 meters minus the temperature at 3 meters.

TABLE 2-1

RATIOS OF THE ANNUAL DAYTIME AND NIGHTTIME WIND SPEED POWER-LAW EXPONENTS, p , AND WIND DIRECTION RANGE POWER-LAW EXPONENTS, q .

Midpoint of 18-Meter Wind Direction Interval (deg.)	Wind Speed (m/sec)									
	2-4		4-7		7-11		2-4		4-7	
	p		p		p		p		p	
	p/q	p/q	p/q	p/q	p/q	p/q	p/q	p/q	p/q	p/q
Annual Daytime										
Annual Nighttime										
030	0.09	0.69	0.09	0.57	0.15	0.75	0.36	1.44	0.32	0.67
060	0.10	0.71	0.10	0.59	0.17	0.78	0.39	1.34	0.34	0.69
090	0.12	0.80	0.10	0.53	0.16	0.70	0.40	1.33	0.34	0.68
120	0.15	1.07	0.10	0.50	0.15	0.60	0.44	1.33	0.35	0.70
150	0.17	1.42	0.10	0.50	0.14	0.54	0.44	1.16	0.34	0.67
180	0.16	1.60	0.09	0.60	0.12	0.57	0.44	1.16	0.34	0.76
210	0.17	1.55	0.10	0.62	0.13	0.59	0.44	1.16	0.33	0.75
240	0.19	0.90	0.15	0.56	0.21	0.64	0.42	0.79	0.33	0.58
270	0.20	0.86	0.17	0.59	0.22	0.59	0.38	0.62	0.32	0.48
300	0.13	0.76	0.13	0.59	0.17	0.65	0.33	0.87	0.30	0.54
330	0.08	0.62	0.08	0.47	0.11	0.52	0.28	1.22	0.25	0.61
360	0.07	0.58	0.07	0.44	0.12	0.60	0.28	1.33	0.25	0.62

variation with wind direction within each period. During the daytime, the sectors with midpoints of 120, 150, 180 and 210 degrees have ratios greater than one; during the nighttime all sectors except those with midpoints of 240, 270 and 300 degrees have ratios greater than one.

2.1.6 Estimates of σ_E at a Height of 18 Meters

In the absence of direct measurements, estimates of σ_E required for model inputs are best made from measurements obtained at other sites. Values of σ_E at a reference height of 18 meters suggested for use in diffusion models for Kennedy Space Center may be obtained from Figure 2-18, for various combinations of wind speed and stability. The curves in Figure 2-18 were obtained by scaling the σ_A curves in Figure 2-13 in accordance with measurements made at a height of 16 meters at the Round Hill site on the shore of Buzzards Bay in Massachusetts (Cramer, Record and Tillman, 1966). Table 2-2 shows mean Round Hill values for three stability conditions and three wind speed categories. For any wind speed category, σ_E decreases with increasing stability. In unstable conditions, σ_E decreases with increasing wind speed; under stable conditions, σ_E increases with increasing wind speed. The high values of σ_E under light winds and instability are associated with convection; the highest values under stable conditions result from mechanical turbulence and are associated with moderate wind speeds. The Round Hill values were calculated from 1-second bivariate observations over sampling periods of about 1 hour. However, these values may be used as 10-minute model inputs since there is little increase in σ_E at 18 meters for sampling times larger than 10 minutes.

2.1.7 The Vertical Temperature Gradient

Temperature gradient data for the 3- to 60-meter and the 60- to 120-meter layers for the winter and summer seasons have been related to the

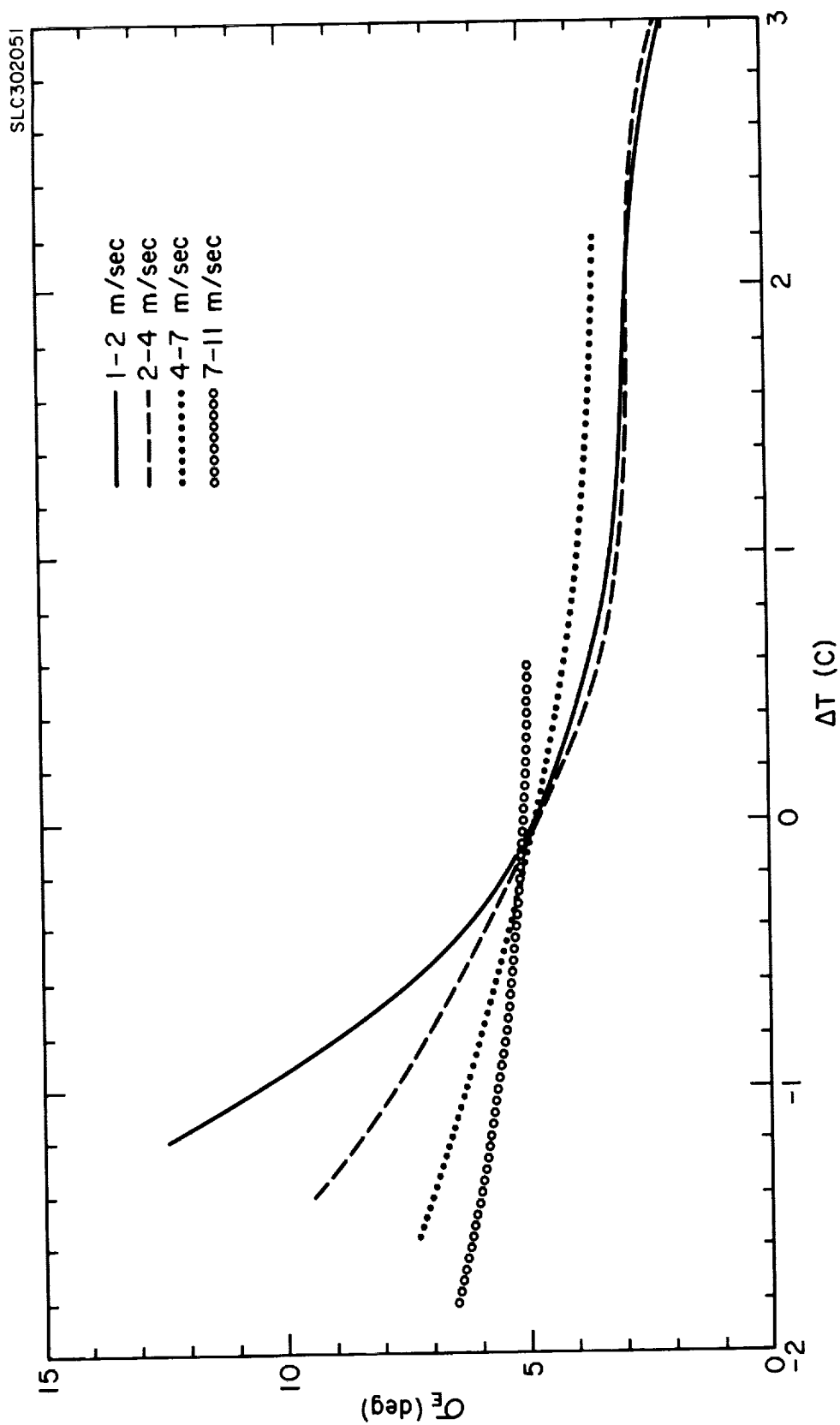


FIGURE 2-18. Dependence of σ_E at 18 meters on stability and wind speed at 18 meters.
 ΔT is the temperature at 60 meters minus the temperature at 3 meters.

TABLE 2-2
 ROUND HILL σ_E VALUES MEASURED AT A
 HEIGHT OF 16 METERS

Wind Speed (m sec ⁻¹)	σ_E (deg)		
	Unstable	Near Neutral/ Transitional	Stable
2-4	9	3.5	3
4-7	7	5.5	4
7-11	6	5.5	-

wind speed and wind direction at the 18-meter level. The results for the day-time and nighttime periods are shown in Figures 2-19 and 2-20. In these figures, the median temperature differences for the two height intervals have been plotted as a function of wind direction for two wind speed classes. The curves have been smoothed by eye to eliminate extreme values believed to have resulted from the small sample size associated with certain wind directions. A positive ΔT indicates an inversion, while a negative ΔT indicates a lapse. Daytime temperature profiles do not indicate any pronounced seasonal differences for the two wind speed classes considered. The influence of wind direction during daytime is small and is confined to the lower 60 meters. Above the 60-meter level the daytime temperature gradient is approximately dry adiabatic.

The nighttime temperature profiles for the two wind speed categories, on the other hand, vary significantly with season and wind direction. As expected, the strongest nighttime temperature inversions occur under low wind speed conditions and are more intense during winter than summer. Except for northerly and northwesterly wind directions, the magnitude of the inversion between 3 and 60 meters is nearly 3C in winter for the 2 to 4 meters per second wind speed category. During the summer when the wind speed is from 4 to 7 meters per second, the 3- to 60-meter layer is nearly isothermal when the winds have a westerly component, and shows a slight inversion when the winds have an easterly component. A pronounced minimum in the median curves for the 3- to 60-meter layer is associated with south-southwesterly winds of 4 to 7 meters per second in winter and with winds of 2 to 4 meters per second in summer. In the summer, the layer from 60 to 120 meters is nearly isothermal for all wind directions, for wind speeds of 2 to 4 meters per second. For the higher wind speed category, the gradient is negative for all wind directions. In winter, the median ΔT curves for west-southwesterly winds of less than 4 meters per second indicate a ground based inversion extending to heights in excess of 60 meters.

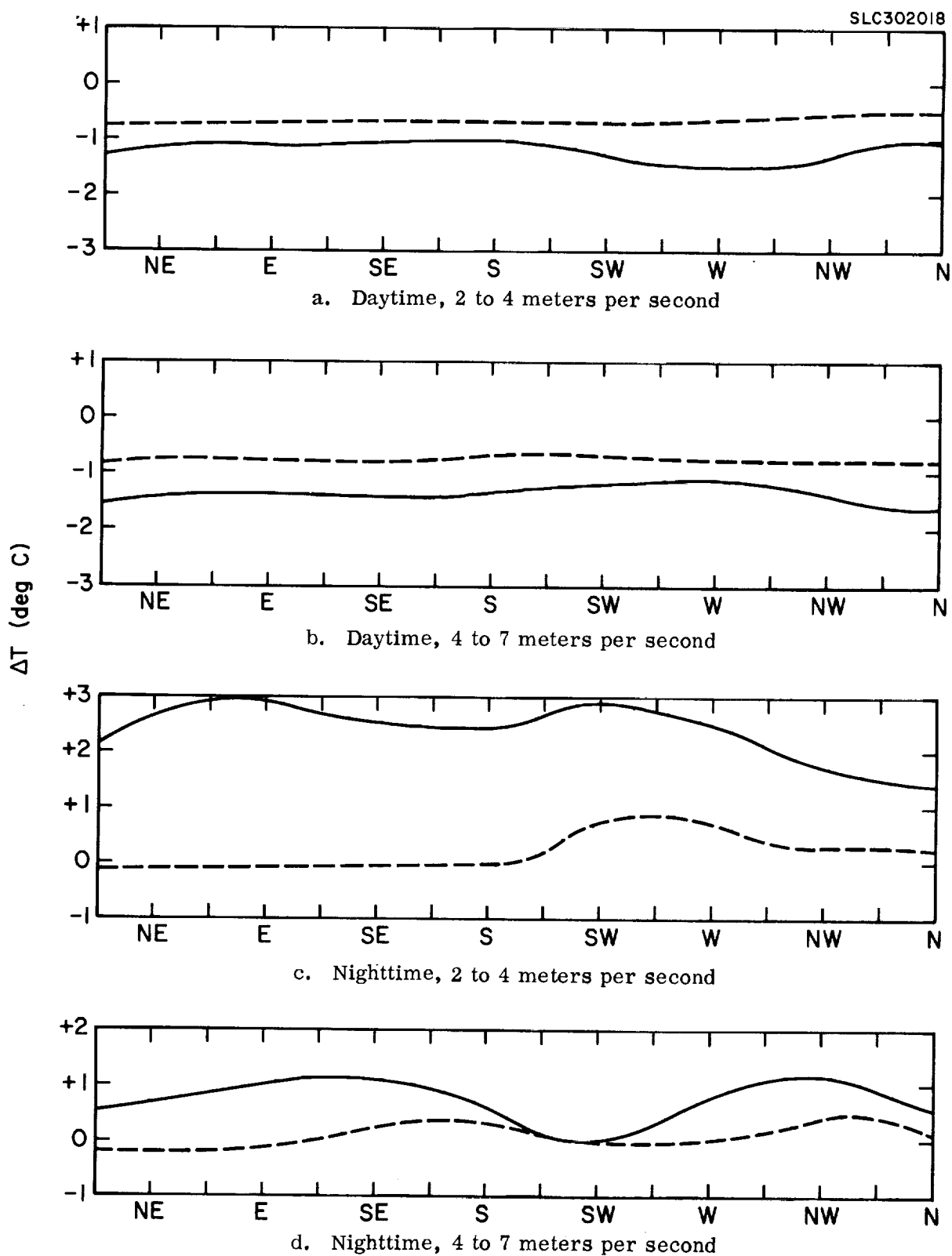
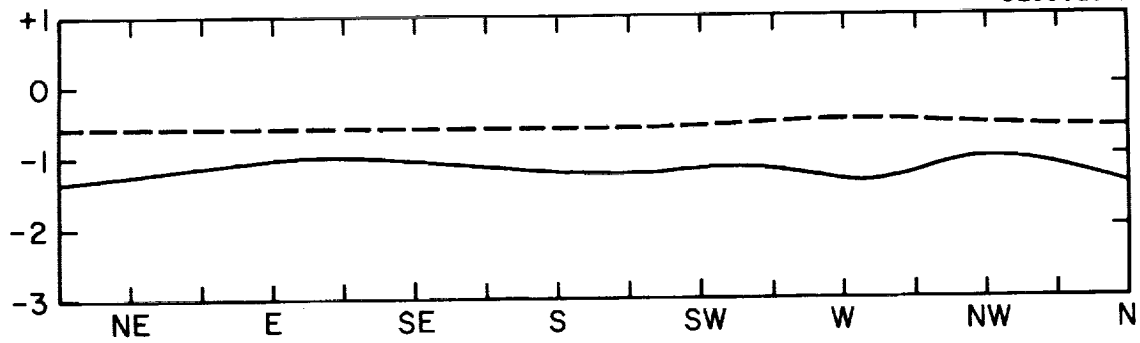
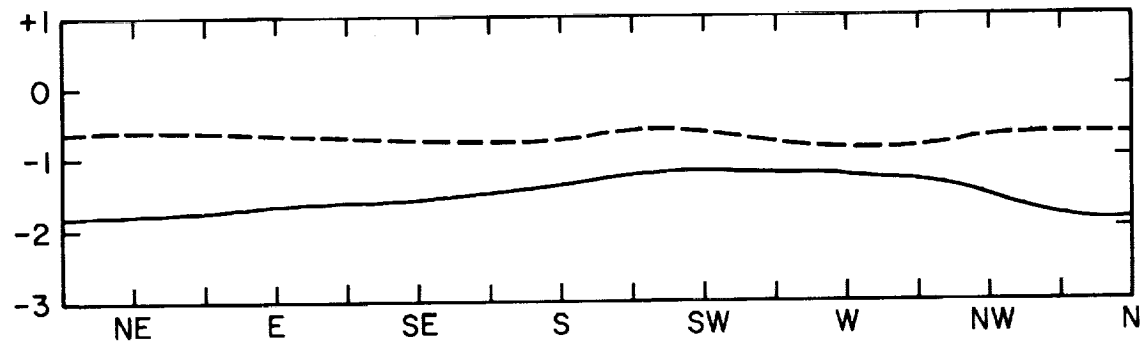


FIGURE 2-19. Relationships between stability and wind direction for two wind speed categories in winter. Solid curves are $T_{60m} - T_{30m}$; dashed curves are $T_{120m} - T_{60m}$.

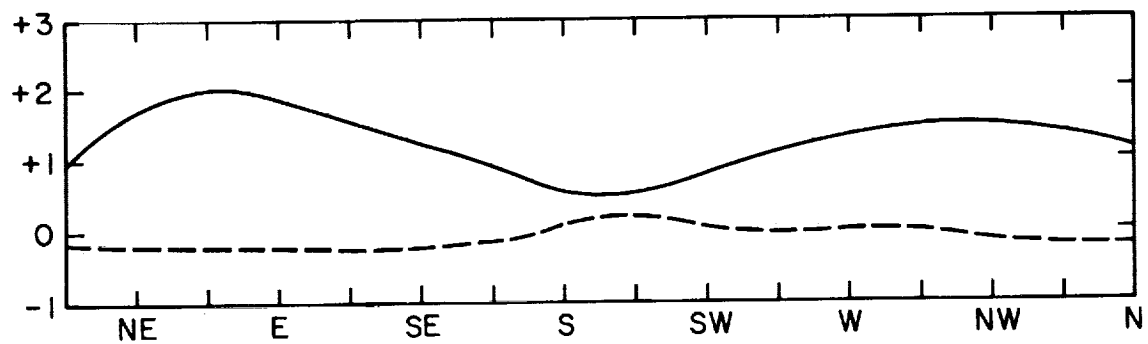


a. Daytime, 2 to 4 meters per second

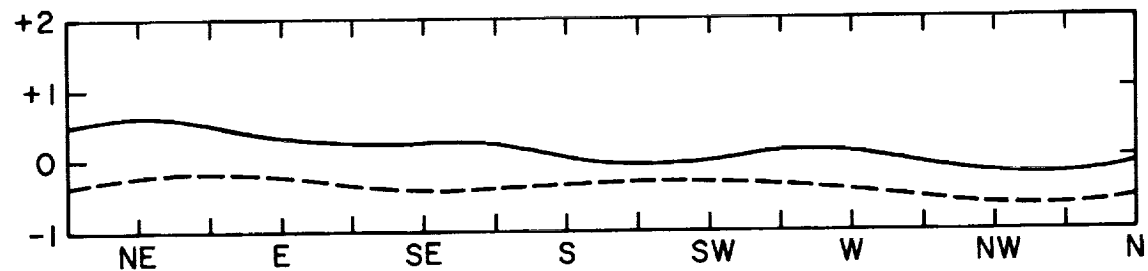


b. Daytime, 4 to 7 meters per second

ΔT (deg C)



c. Nighttime, 2 to 4 meters per second



d. Nighttime, 4 to 7 meters per second

FIGURE 2-20. Relationships between stability and wind direction for two wind speed categories in summer. Solid curves are $T_{60m} - T_{3m}$; dashed curves are $T_{120m} - T_{60m}$.

2.1.8 Frequency of Occurrence of Wind Speed and Wind Direction Classes

The transport of airborne material is directly dependent on wind speed and direction. In addition, the analysis of the tower data has shown that other meteorological inputs required for the prediction of concentration levels from ground-level releases at Cape Kennedy are related to the prevailing wind conditions. Although current synoptic meteorological data can be used to predict wind speed and direction for maximum time periods of one or two days, climatological summaries are required for longer period planning. To supplement other climatological data, the frequency of occurrence of selected wind speed and direction classes have been summarized using the wind data collected at the 18-meter level of the 150-meter tower.

Figures 2-21 and 2-22 show the cumulative frequency distributions of wind direction by wind speed category for the winter and summer seasons, respectively, for six time periods. As shown in Figure 2-21, the most frequent wind directions during the winter months are northwest through north. During the night and early morning the predominant direction is northwesterly; during the daytime and evening the predominant direction is northerly. Secondary maximums occur for north-northeasterly and southerly winds for all time periods with the exception of 1600-1900 EST when all directions with an easterly component occur with nearly the same frequency. The summer season curves show the influence of the sea breeze-land breeze circulations. During the night, the predominant wind directions are south-southeast through south-southwest, and by early morning the predominant direction is south-southwest. The affect of the sea breeze shows clearly in the shift to easterly winds and higher wind speeds during the 1000-1600 EST period. Throughout the remainder of the day and evening the wind veers and becomes south-southeasterly by 2100-2200 EST.

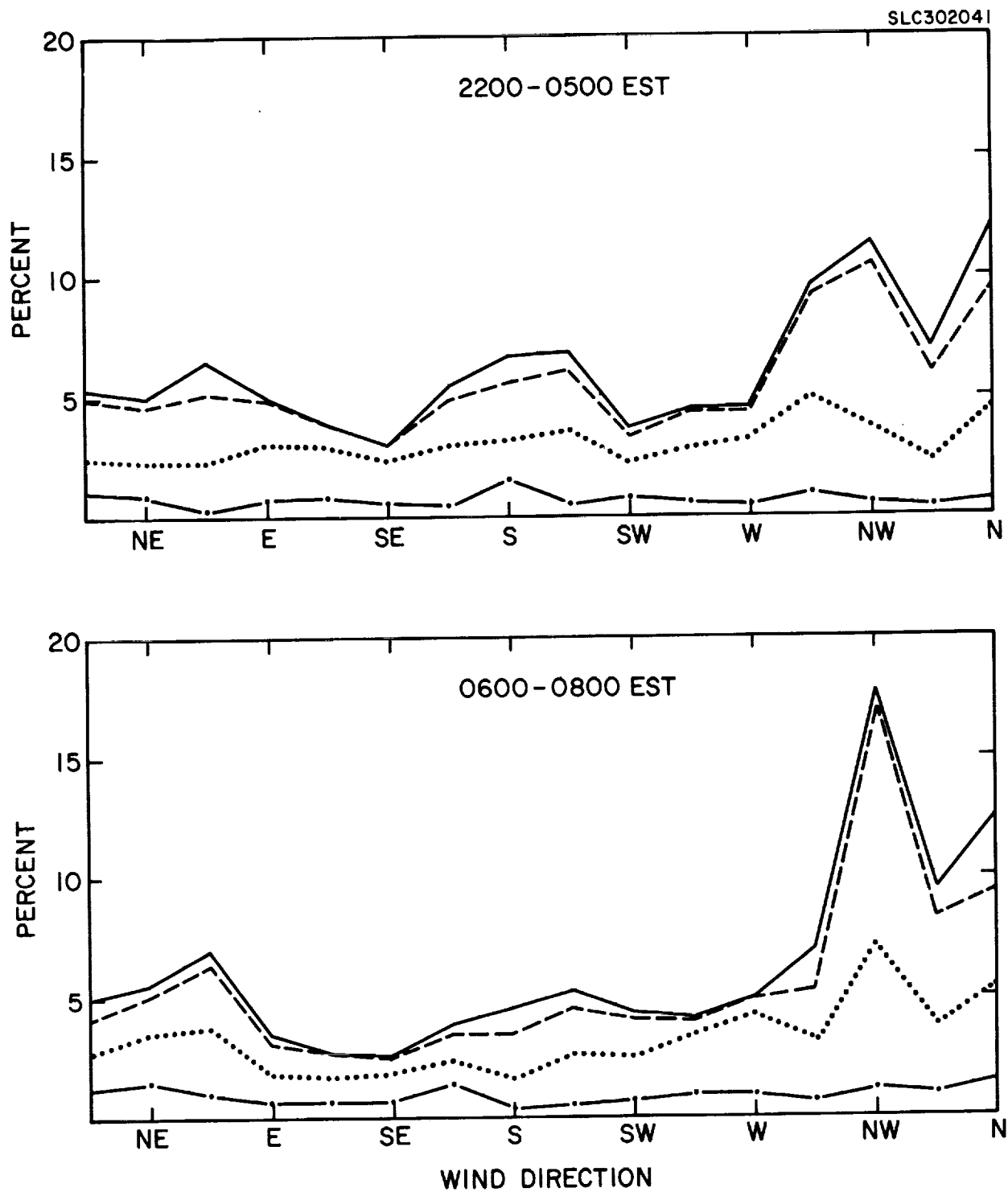


FIGURE 2-21. Cumulative frequency distributions of wind direction by wind speed category for six time periods during winter. Wind categories are: — . — <2 m/sec; <4 m/sec; ----- <7 m/sec; ————— all wind speeds.

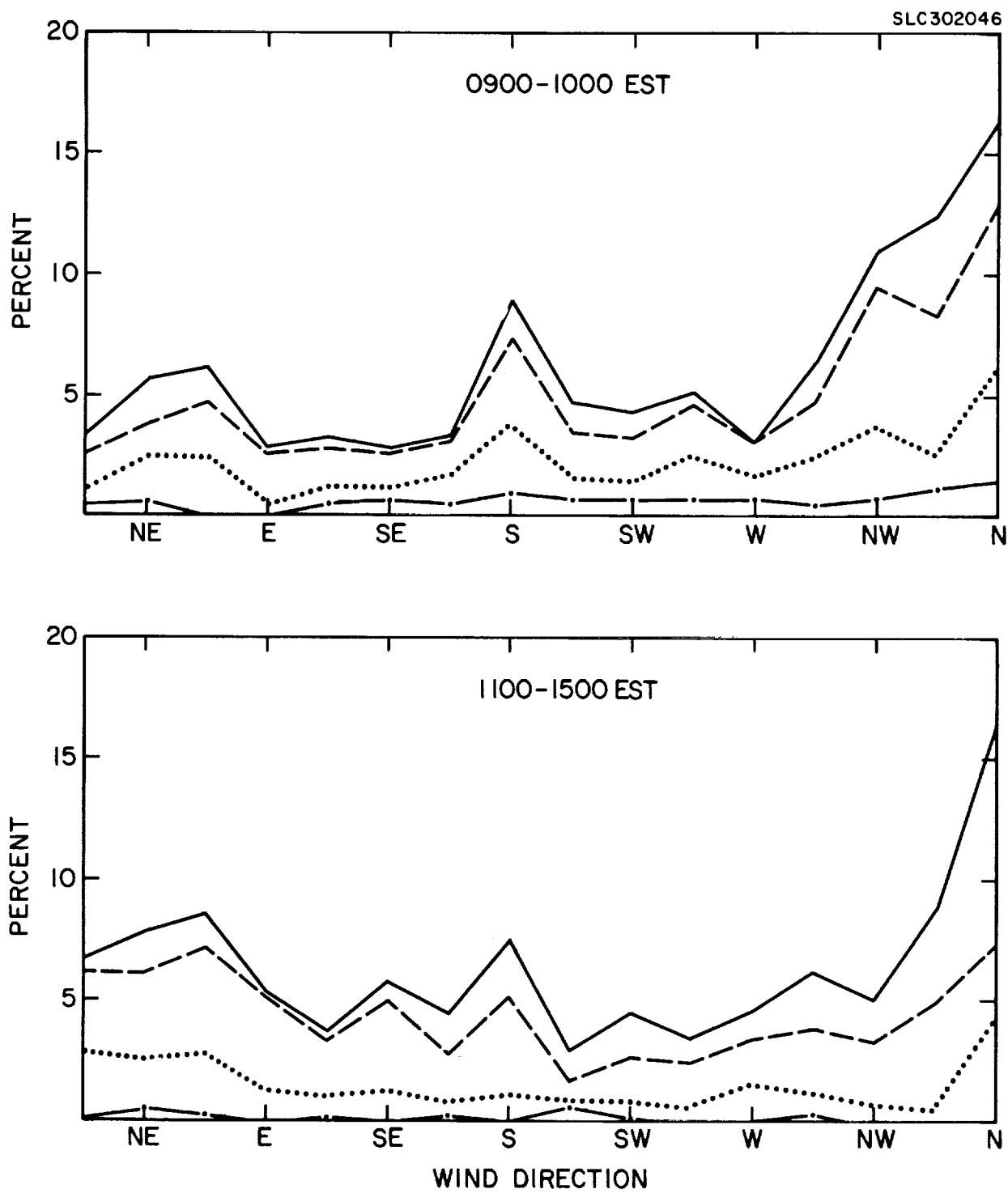


FIGURE 2-21. (Continued)

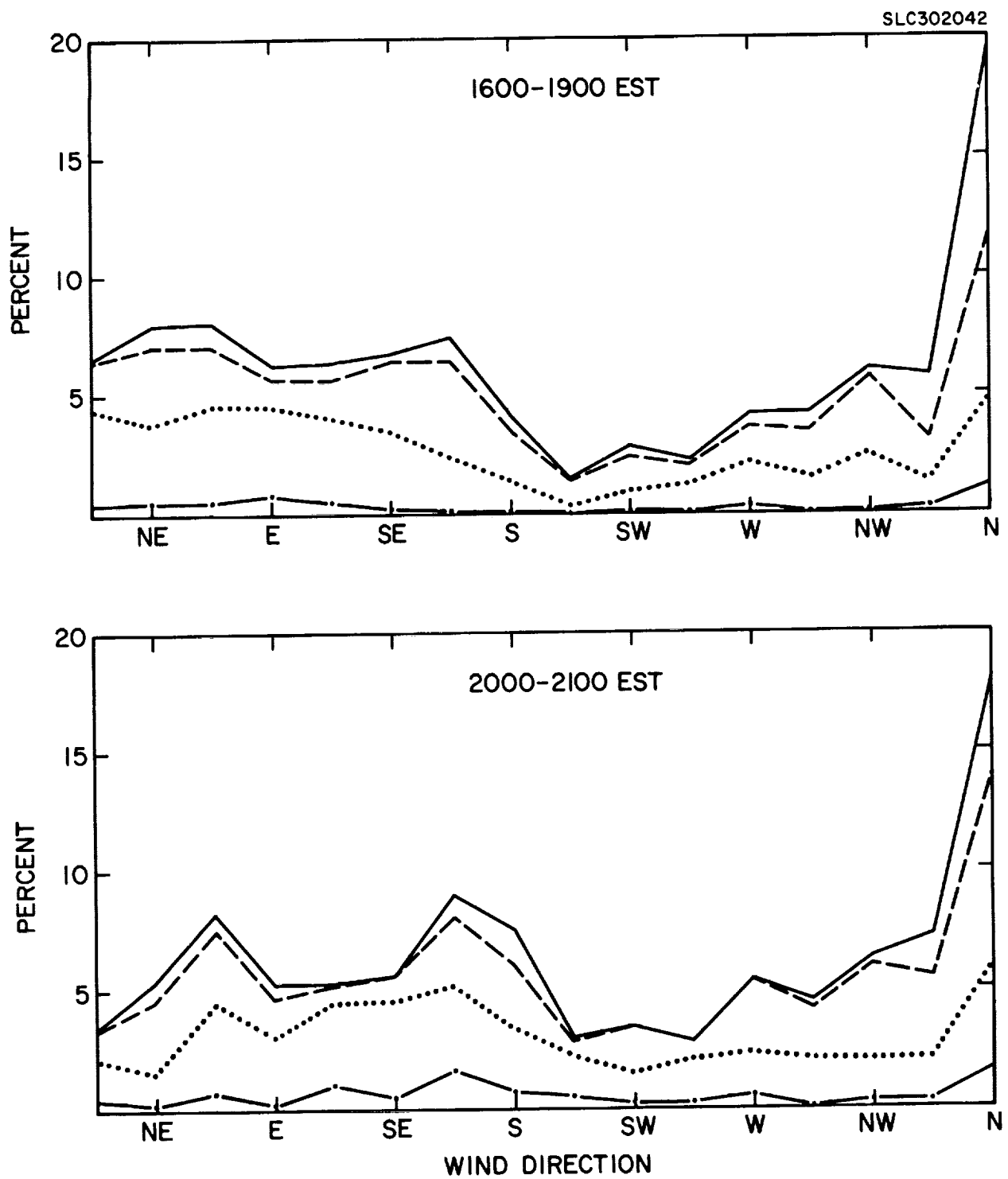


FIGURE 2-21. (Continued)

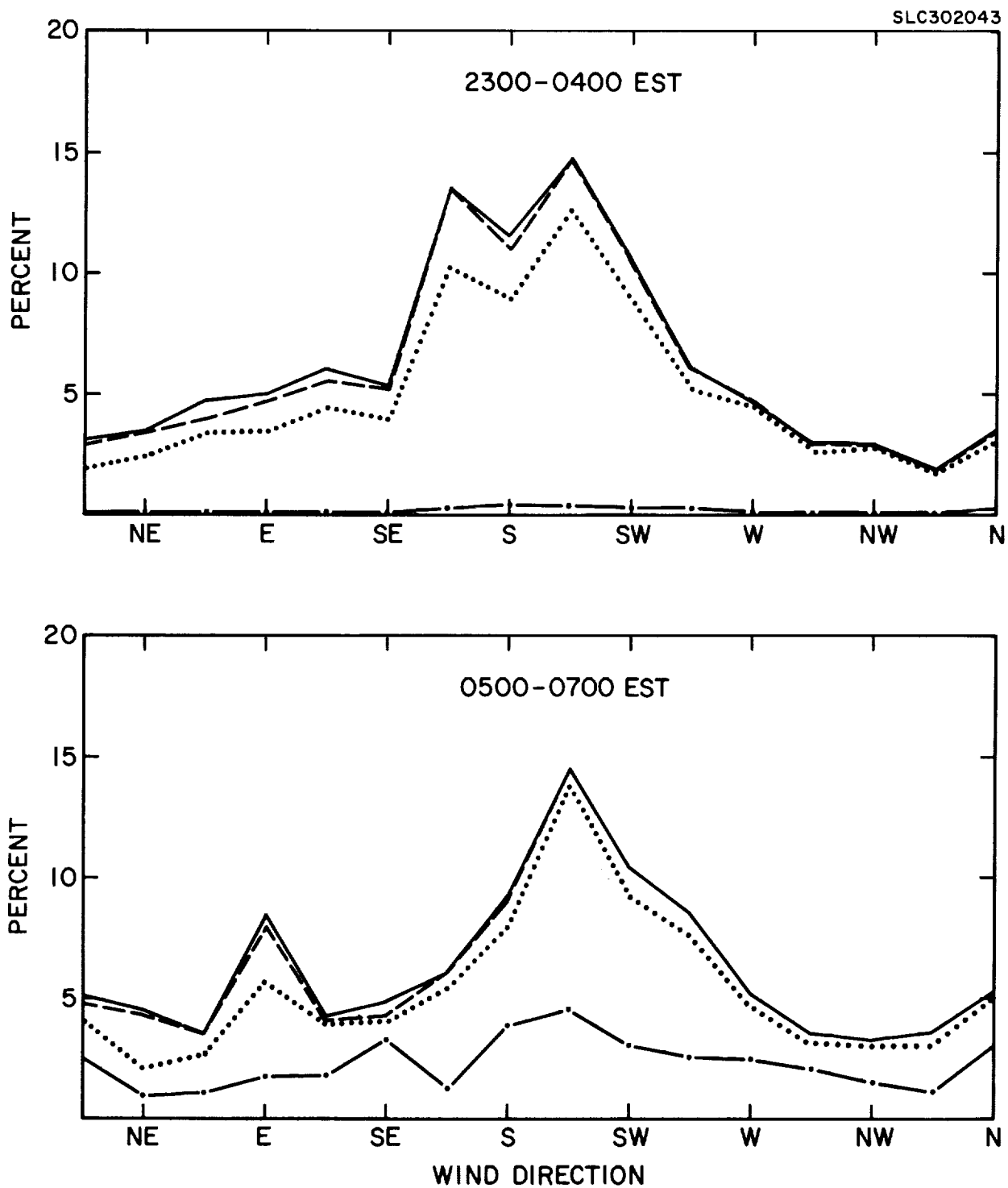


FIGURE 2-22. Cumulative frequency distributions of wind direction by wind speed category for six time periods during summer. Wind categories are: — . — < 2 m/sec; < 4 m/sec; ---- < 7 m/sec; ————— all wind speeds.

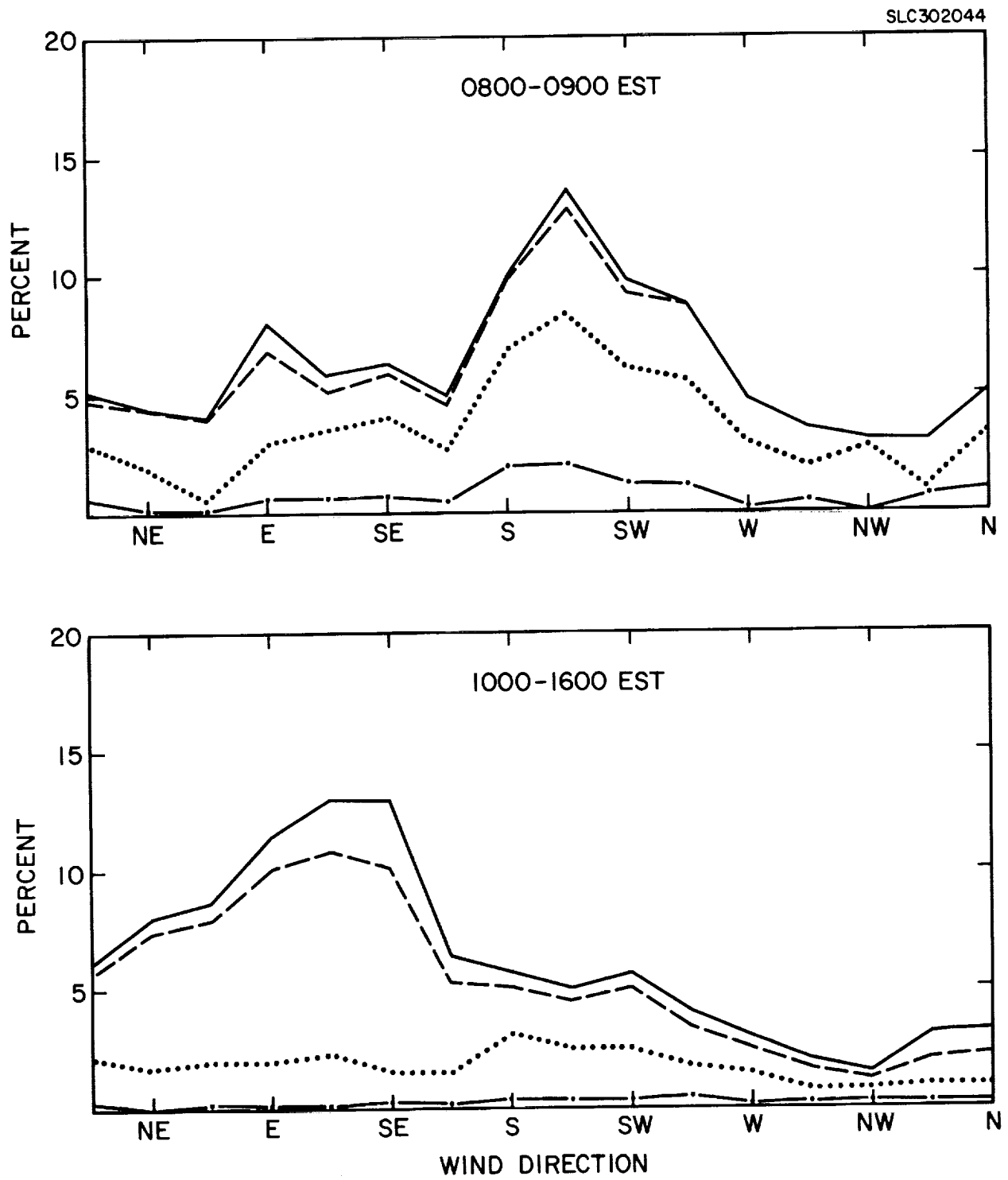


FIGURE 2-22. (Continued)

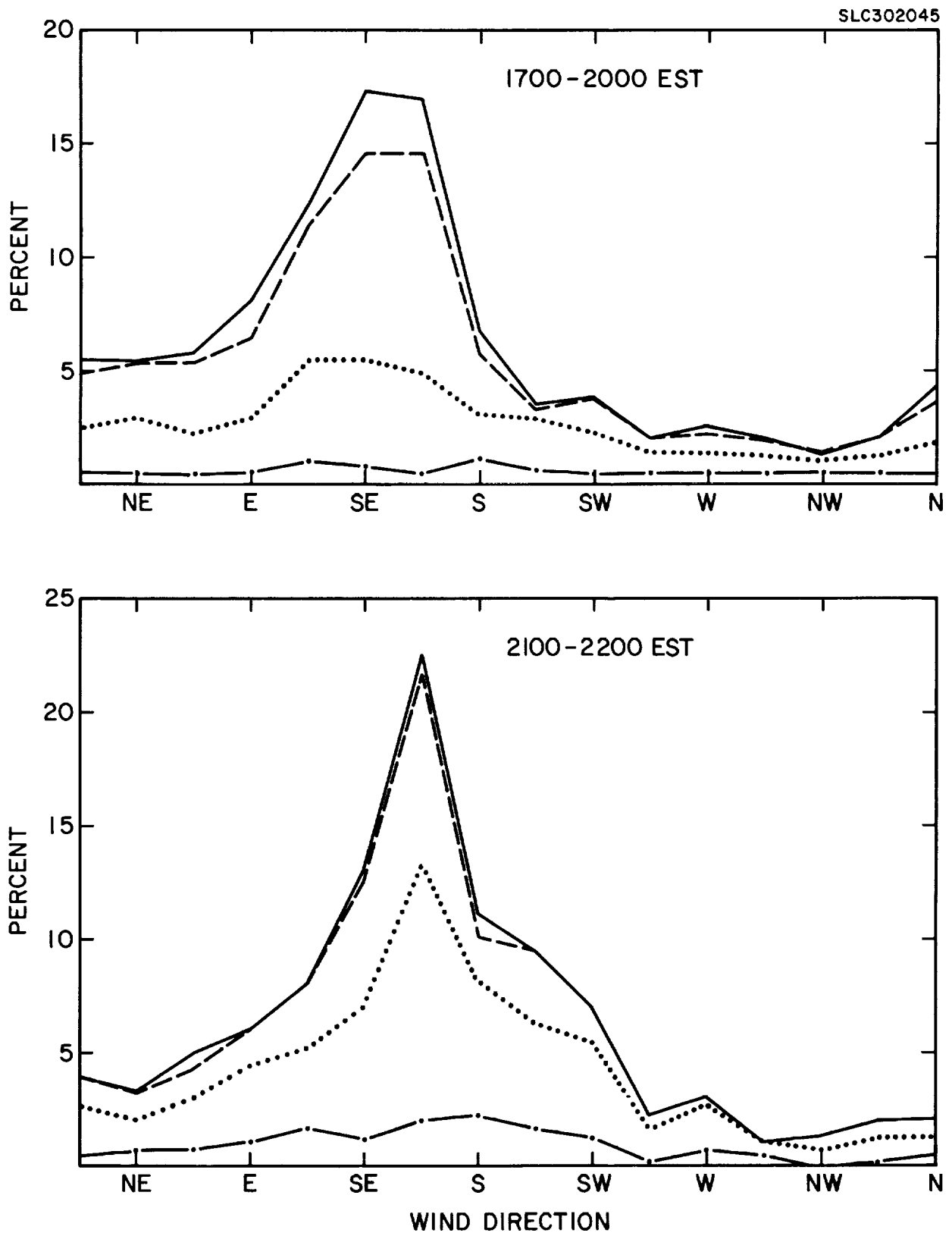


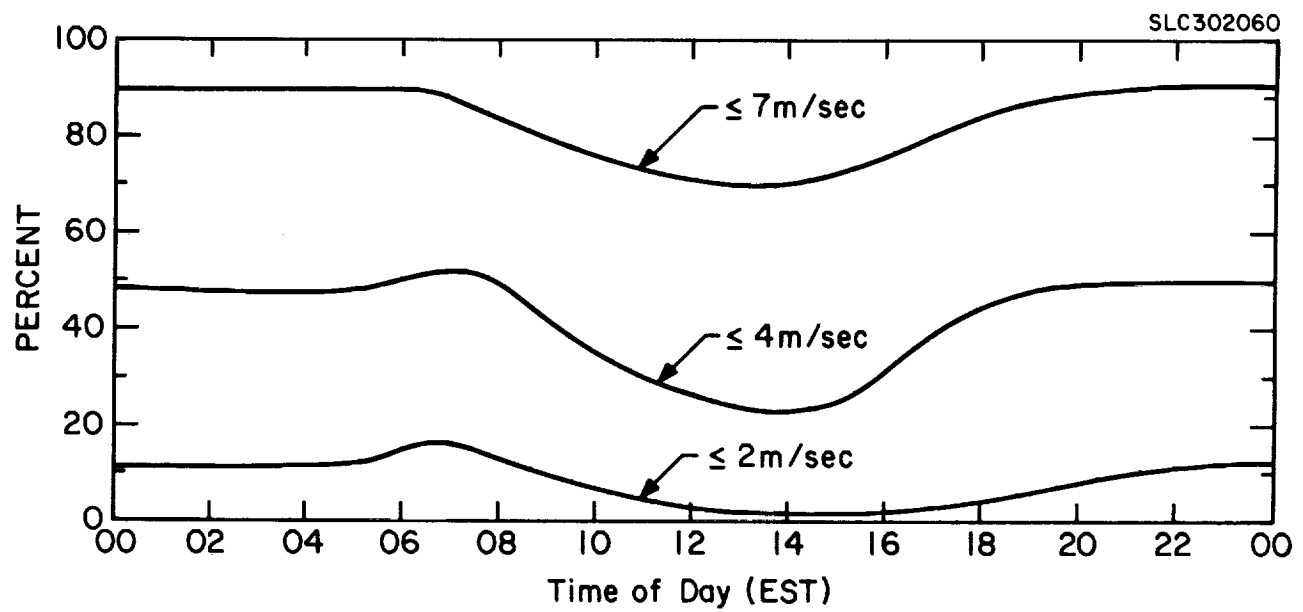
FIGURE 2-22. (Continued)

The diurnal variations in wind speed for the two seasons can also be seen clearly in Figure 2-23 where the 18-meter wind speed frequency distributions are plotted as a function of time of day without regard to wind direction.

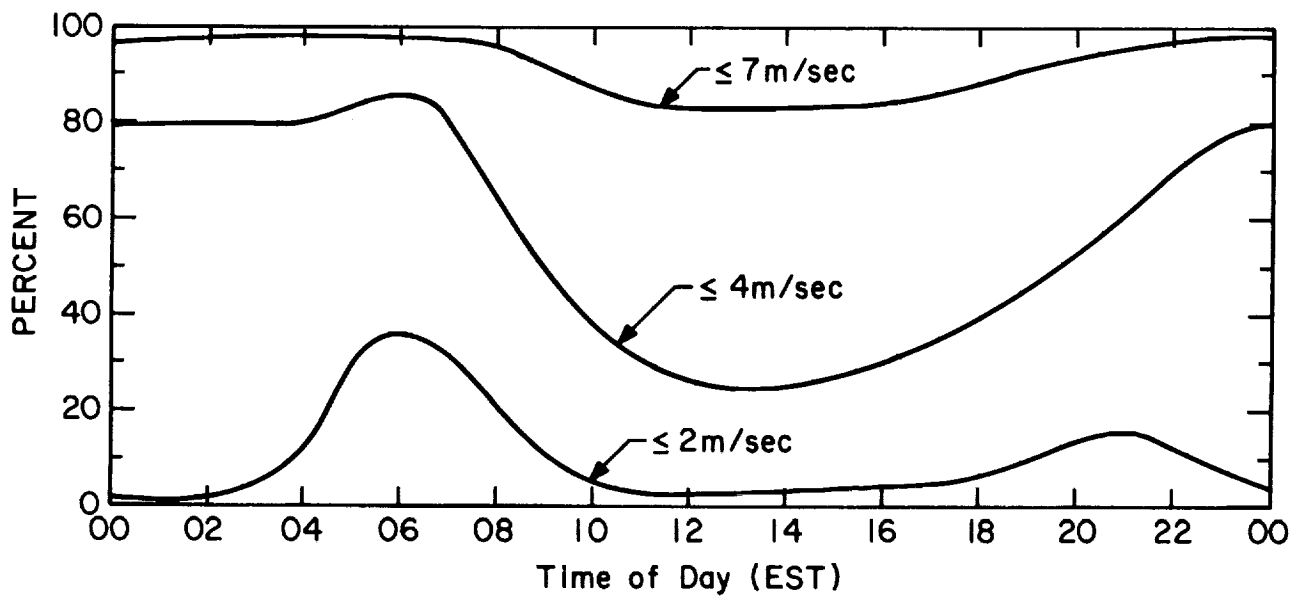
2.2 TETROON FLIGHTS

During the summer seasons of 1966 and 1967, a number of radar-positioned constant-volume balloon (tetroon) flights were made at Kennedy Space Center. The three-dimensional coordinates of the tetroon's position in space and the velocity components, as measured by an FPS-16 radar, were recorded at 2-second intervals for each flight. Twelve of the 25 available tetroon flight records had at least one period of approximately 30 minutes of continuous record where the tetroon was in neither an ascent nor descent stage and where it had a well-defined overland or over-water trajectory. A total of five 30-minute periods for the over-water category and ten 30-minute periods for the overland category were selected for analysis. Three of the releases had two 30-minute periods that were judged acceptable for analysis.

Standard deviations of the vertical velocity fluctuations σ_w were determined using alternate 2-second readings (4-second intervals) for averaging times of 2.5, 5, 10 and 30 minutes. Results of this analysis, given in Table 2-3, indicate there is little difference in the mean σ_w between overland and over-water flights for averaging times of 10 minutes or less. However, for longer averaging times the mean overland σ_w increases in magnitude, while the mean over-water σ_w remains nearly constant. From the small difference between the σ_w estimates for the 2.5-minute and 10-minute averaging times, it appears that nearly all the turbulent energy is contained in frequencies greater than 0.2 cycles per minute. The increase in the overland σ_w between the 10- and 30-minute periods is probably due to large convective circulations having scale lengths of a few kilometers.



a. Winter



b. Summer

FIGURE 2-23. Cumulative frequency distributions of the 18-meter wind speed for two seasons.

TABLE 2-3

ESTIMATES OF σ_w AS A FUNCTION OF AVERAGING TIME FOR SELECTED PORTIONS
OF TETROON FLIGHTS AT THE KENNEDY SPACE CENTER COMPLEX

Release Number	Date	Release Time (EST)	Approximate Starting Time of Sampling Period (EST)	Average Height of Tetroon (m)	Average Wind Speed (m/sec)	Standard Deviation of Vertical Velocity Fluctuations σ_w (m/sec)			
						Averaging Time			
						2.5 min	5 min	10 min	30 min
						Over-water Trajectory			
1515-01	7/27/67	0802	0850	500	8.0	0.35	0.35	0.36	0.36
4453-01	8/8/67	0812	0910	800	3.4	0.37	0.38	0.38	0.38
0941-02	7/14/66	1031	1120	500	5.3	0.90	0.97	0.97	0.98
0941-02	7/14/66	1031	1150	500	5.5	0.63	0.65	0.67	0.74
0886-02	8/8/66	1036	1150	1200	6.2	0.63	0.66	0.64	0.72
Mean					5.7	0.58	0.60	0.60	0.64
Overland Trajectory									
4453-2	9/8/67	1203	1230	400	3.8	0.56	0.61	0.62	0.66
4453-4	9/8/67	1606	1630	350	5.6	0.44	0.51	0.52	0.57
8460-3	8/24/67	1213	1230	200	6.4	0.90	0.98	1.03	1.31
7555-2	8/29/67	1200	1240	800	5.1	1.08	1.19	1.19	1.65
7555-2	8/29/65	1200	1310	1000	3.7	1.85	1.99	2.04	2.03
7555-3	8/29/67	1703	1720	350	5.0	0.22	0.22	0.23	0.36
7555-4	8/29/67	1800	1800	400	5.2	1.03	1.04	1.04	2.02
0254-4	6/23/67	1500	1520	450	2.1	0.27	0.31	0.30	0.34
0254-4	6/23/67	1500	1550	400	2.7	0.25	0.26	0.28	0.25
5459-3	9/23/65	1710	1730	400	6.4	0.80	0.83	0.93	1.29
Mean					4.6	0.74	0.79	0.82	1.05

No detailed relationships between σ_w and altitude or meteorological conditions could be established with this limited data set. In the overland trajectory data, the large values of σ_w calculated for Release No. 7555-2 are associated with the highest flight altitude. The average values of σ_E , obtained from the relationship $\sigma_E = \sigma_w / \bar{u}$, is 6.5 degrees for over-water flights and 10.6 degrees for overland flights.

2.3 LAND- AND SEA-BREEZE CIRCULATIONS AT KSC

A detailed knowledge of local land- and sea-breeze circulations is essential to the development and application of quantitative hazard prediction techniques for use at Kennedy Space Center. These thermally-driven wind circulations dominate the wind and temperature fields from about 30 kilometers offshore to as far as 50 kilometers inland, and up to maximum heights of about 3 kilometers above the surface. Because of the complexity of land- and sea-breeze wind systems and their interactions with large scale wind, temperature, and pressure patterns, many simplifications must be made if the effects of these thermally-driven circulations are to be incorporated in hazard prediction. An example of the influence of land and sea breezes on the wind field near ground level, as revealed by hourly observations made at NASA's 150-meter Meteorological Tower Facility at Kennedy Space Center on 13 and 14 July 1967, is shown in Figure 2-24. A land breeze with southwesterly wind directions is well established by 2300 EST and maximum speeds are observed shortly after midnight. The winds remain westerly until late morning. A sudden transition from the land breeze to a sea breeze is evident at 1100 EST when the wind directions become southeasterly. As expected, the wind speeds increase throughout the afternoon and the wind direction gradually veers because of the Coriolis effect. At sunset (1900 EST), the wind direction is nearly parallel to the coastline. After 1900 EST, the land-breeze circulation becomes established with southwesterly winds. By 2300 EST, the wind speed and direction profiles are nearly identical with those observed on the

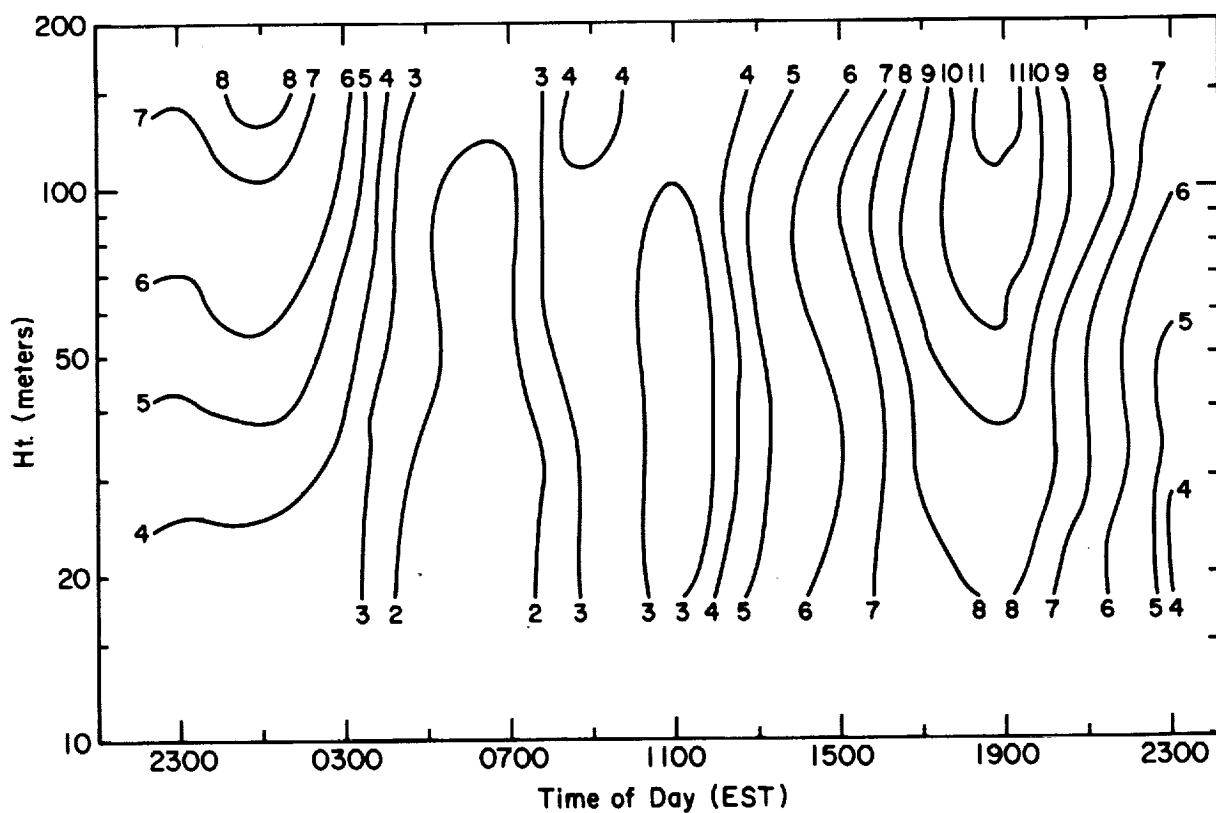
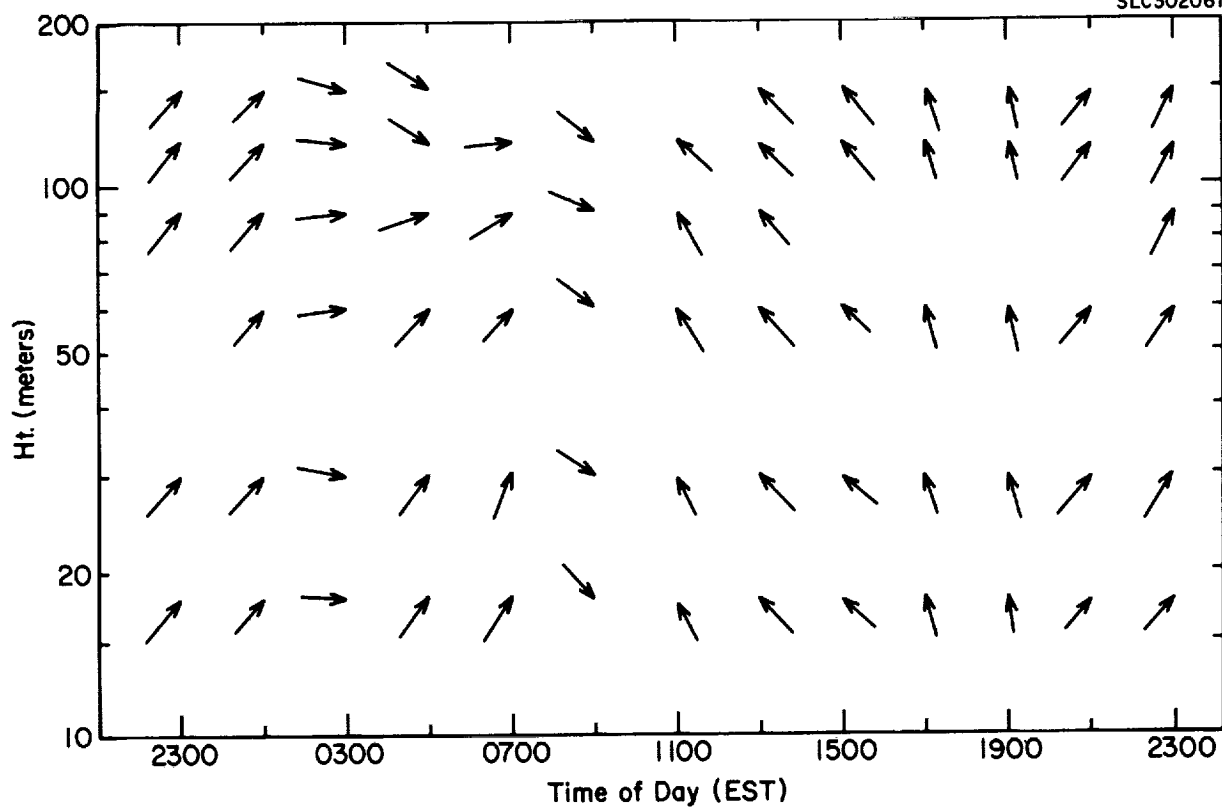


FIGURE 2-24. Time variations in vertical profiles of wind direction (top) and speed (bottom) for 13 and 14 July 1967, from observations made on the 150-meter Meteorological Tower at Kennedy Space Center.

previous evening. Details of the transition from land breeze to sea breeze, (commonly called a sea-breeze front) at Cape Kennedy, are described by Hill (1967).

2.3.1 Case Studies of Land- and Sea-Breeze Circulations from Tower and Jimsphere Data

A number of days were selected from the summer seasons of 1966 and 1967 for a detailed study of the structure of land- and sea-breeze circulations at Cape Kennedy, using observations from the NASA 150-meter Meteorological Tower Facility. The selection criteria included the requirement that synoptic conditions be favorable for the development of a land or sea breeze. Jimsphere data also were required to be available to provide wind speed and direction profiles to an altitude of at least 5000 meters. There were relatively few sets of Jimsphere data available in which the buildup and/or decay of a land or sea breeze was clearly evident.

Figures 2-25 and 2-26 show the time variations in the vertical profiles of wind speed and wind direction, respectively, for a sea-breeze situation that occurred on 21 July 1967. The sky was nearly overcast during the entire day so the wind speeds are lower than would be expected on a clear day. As shown in the figures, the surface winds are from the northeast in the late morning and veer to the southeast as the day progresses. Wind directions are easterly between the surface and 1500 meters with the maximum speed occurring in the layer from 400 to 800 meters after 1108 EST. The organized easterly flow due to sea breeze extends up to about one kilometer. However, the overall depth of the layer influenced by the sea-breeze circulation appears to be about 3 kilometers. Above this height both the speed and direction agree with those of the large-scale circulation patterns. The development of a land-breeze circulation is illustrated in Figures 2-27 and 2-28, which show the vertical profiles of wind speed and wind direction, respectively, for 4 and 5 July 1966. At 1940 EST

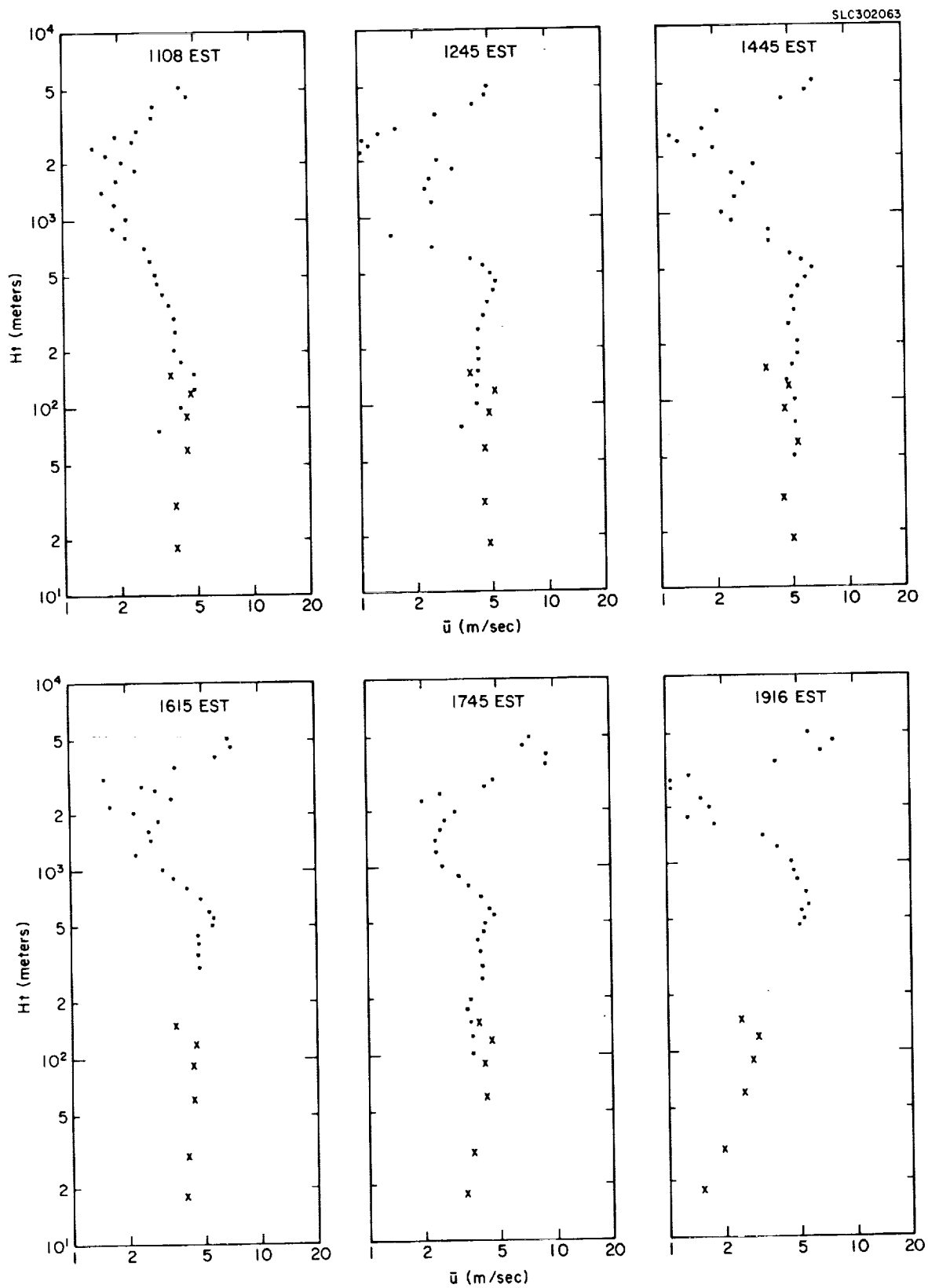


FIGURE 2-25. Time variations in vertical profiles of wind speed for 21 July 1967. Symbol x denotes 150-meter Meteorological Tower data while the filled circles refer to Jimsphere measurements.

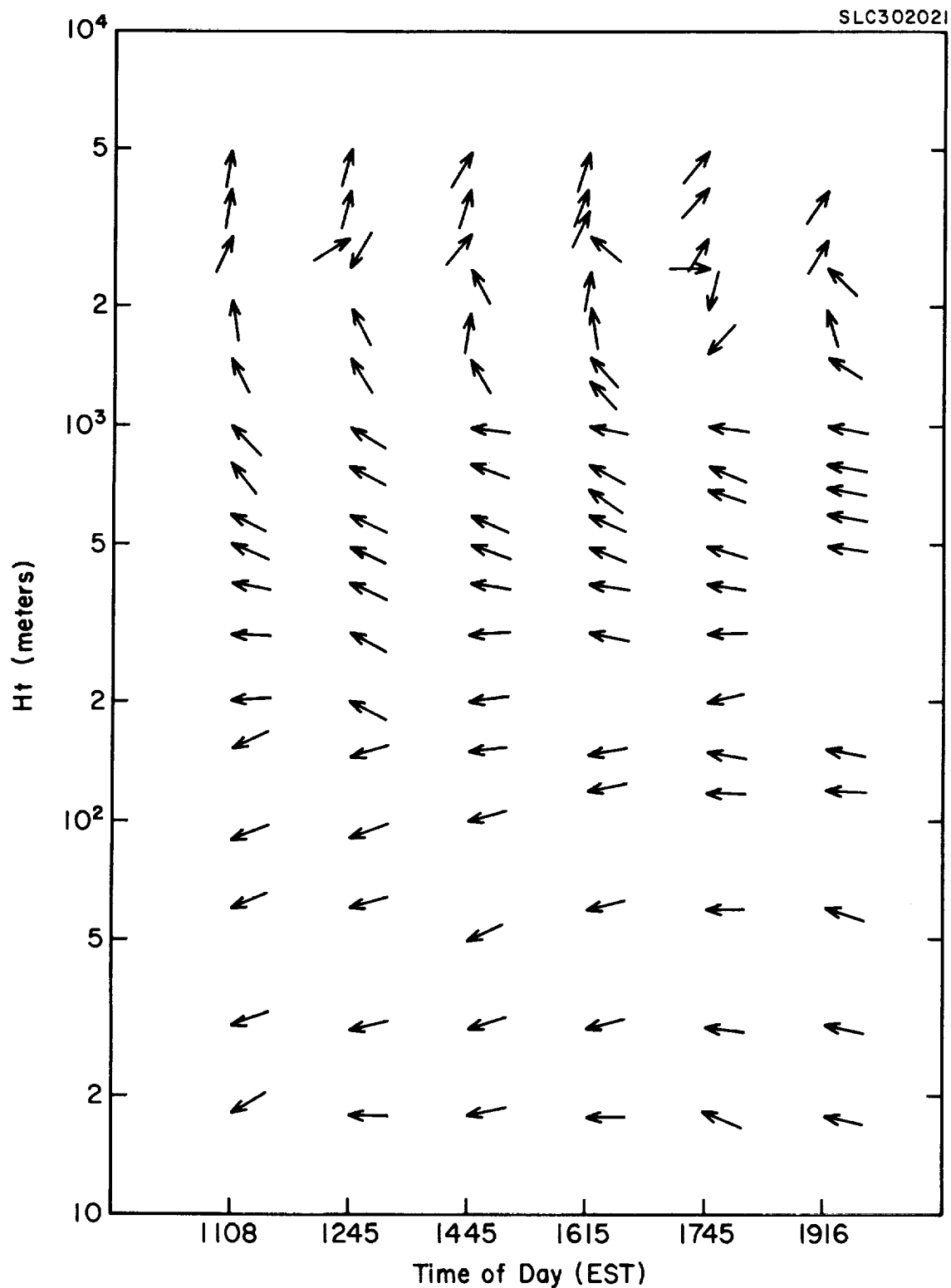


FIGURE 2-26. Time variations in vertical profiles of azimuth wind direction for 21 July 1967. Wind directions at 150 meters and below refer to Tower measurements while those above 150 meters refer to Jimsphere data.

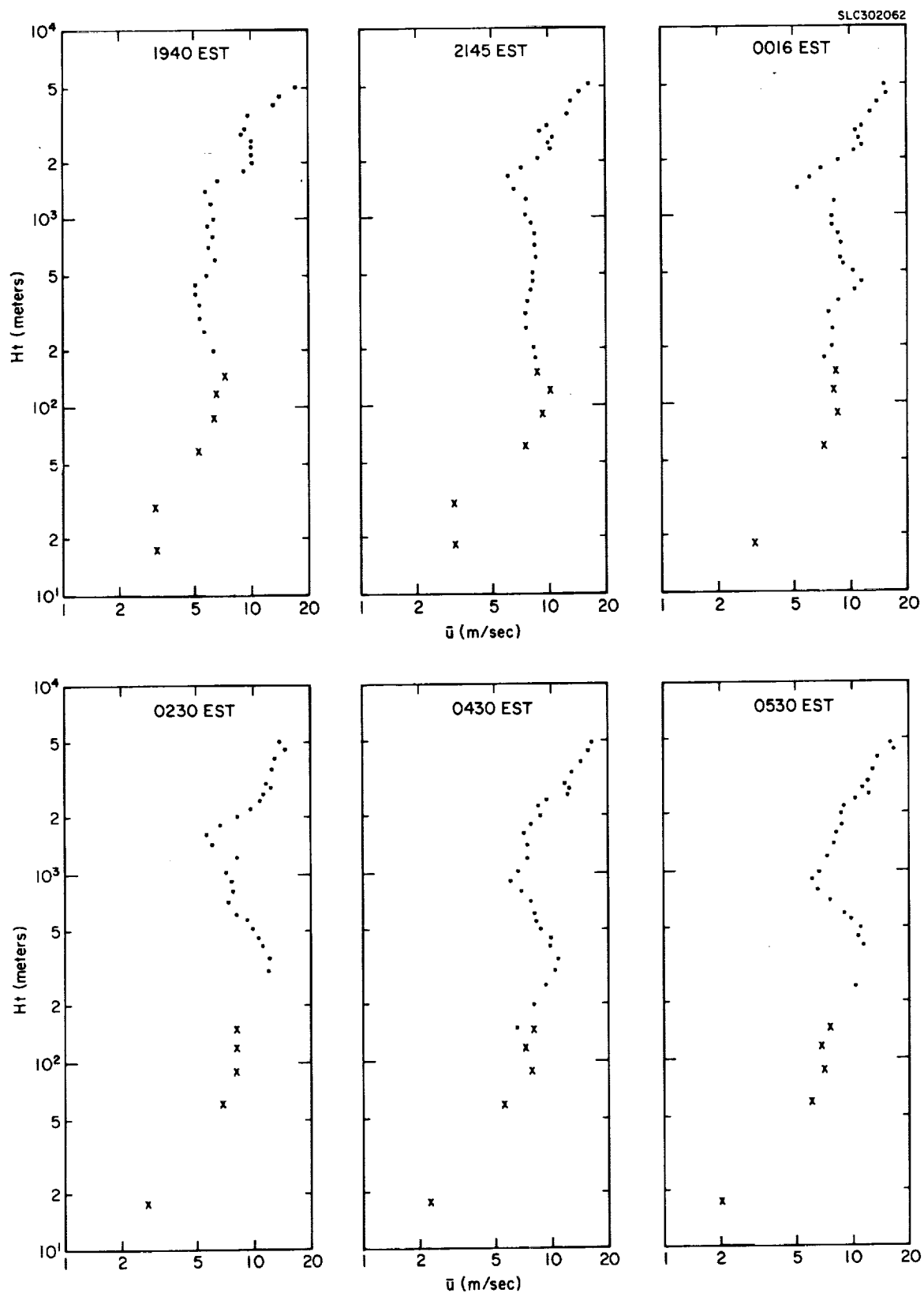


FIGURE 2-27. Time variations in vertical profiles of wind speed for 4 and 5 July 1966. Symbol x denotes 150-meter Meteorological Tower data while filled circles refer to Jimsphere measurements.

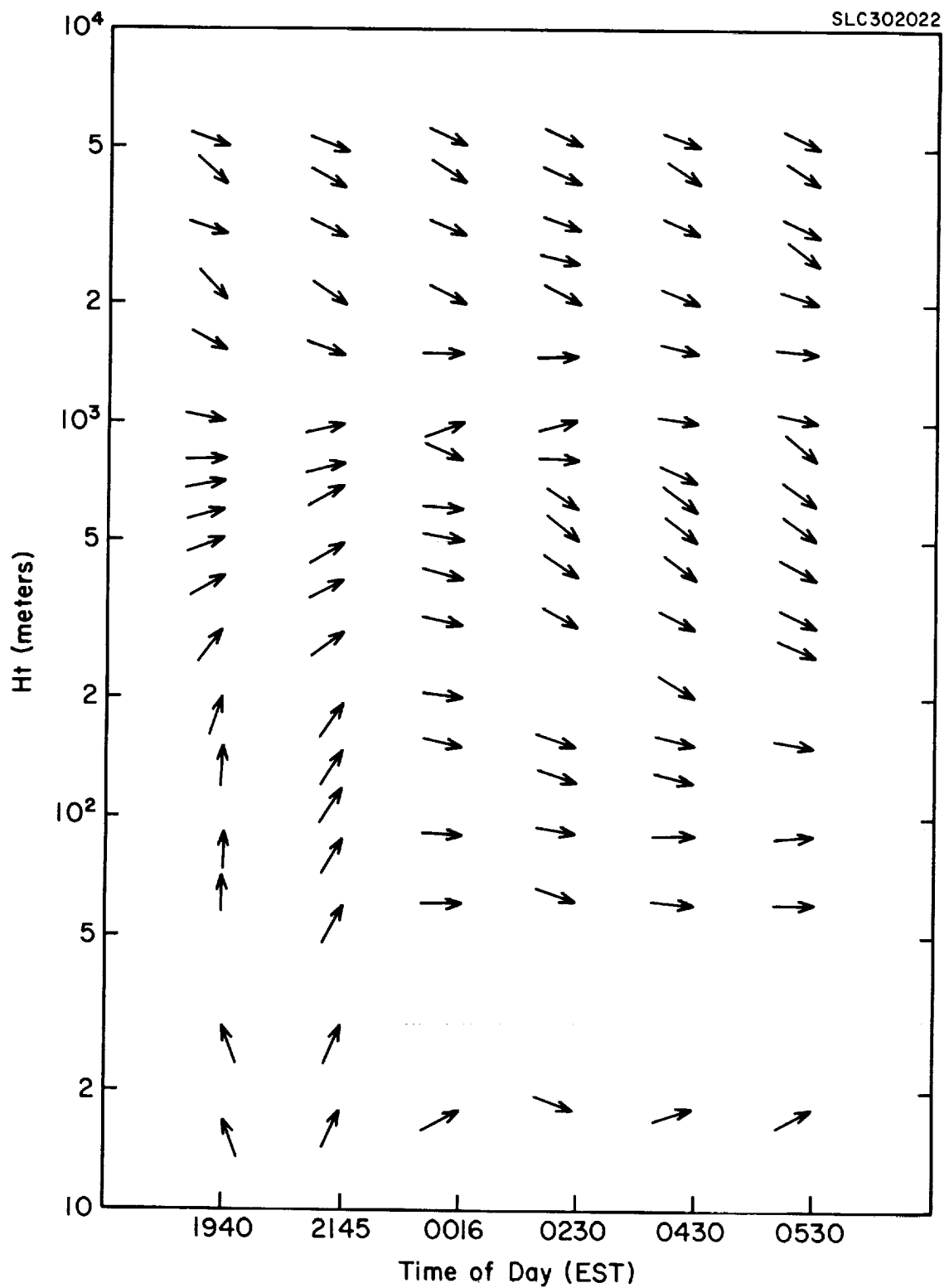


FIGURE 2-28. Time variations in vertical profiles of azimuth wind direction for 4 and 5 July 1966. Wind directions up to 150 meters refer to Tower measurements while those above 150 meters refer to Jimsphere data.

on 4 July, the sea-breeze circulation extends from ground level to a height of about 800 meters. As the night progresses, the wind directions at the lower level veer from southerly to westerly and the height of the low level wind speed maximum increases with time from about 150 meters at 1940 EST to 400 meters at 0530 EST. The depth of the land-breeze circulation, indicated by the wind profiles, is approximately 1 kilometer.

2.3.2 Average Vertical Profiles of Wind Direction and Wind Speed for the Land- and Sea-Breeze Circulations at KSC

Vertical profiles of wind direction and wind speed from the case studies mentioned in Section 2.3.1, and from other measurements made in the summers of 1966 and 1967 in which Jimsphere data were available only for the periods 0600-0800 EST and 1800-2000 EST, were combined to obtain averaged profiles for interim use in hazard estimation at Kennedy Space Center. The average profiles extend from the lowest measurement height (18 meters) on the 150-meter NASA Meteorological Tower to a height of about 1.5 kilometers. The average directions above this height were judged to have little significance. In general, no well-defined return circulations were found in the individual soundings for the land- and sea-breeze regimes at KSC.

Figure 2-29 shows the average vertical profiles of wind direction and wind speed for the land-breeze circulation at KSC. These profiles were obtained by combining the profiles from five cases in which the gradient wind direction was southwesterly and the gradient wind speeds were about 5 meters per second. As might be expected, it is difficult to find examples of well-defined land-breeze circulations at KSC when the easterly Trade Winds are controlling the gradient flow. Under these conditions, the nighttime land-breeze component tends to weaken the on-shore easterly winds near the surface to produce a south-easterly flow or a light, variable wind regime in the surface layer. The wind speed profile in Figure 2-29 shows a maximum of about 8 meters per second at

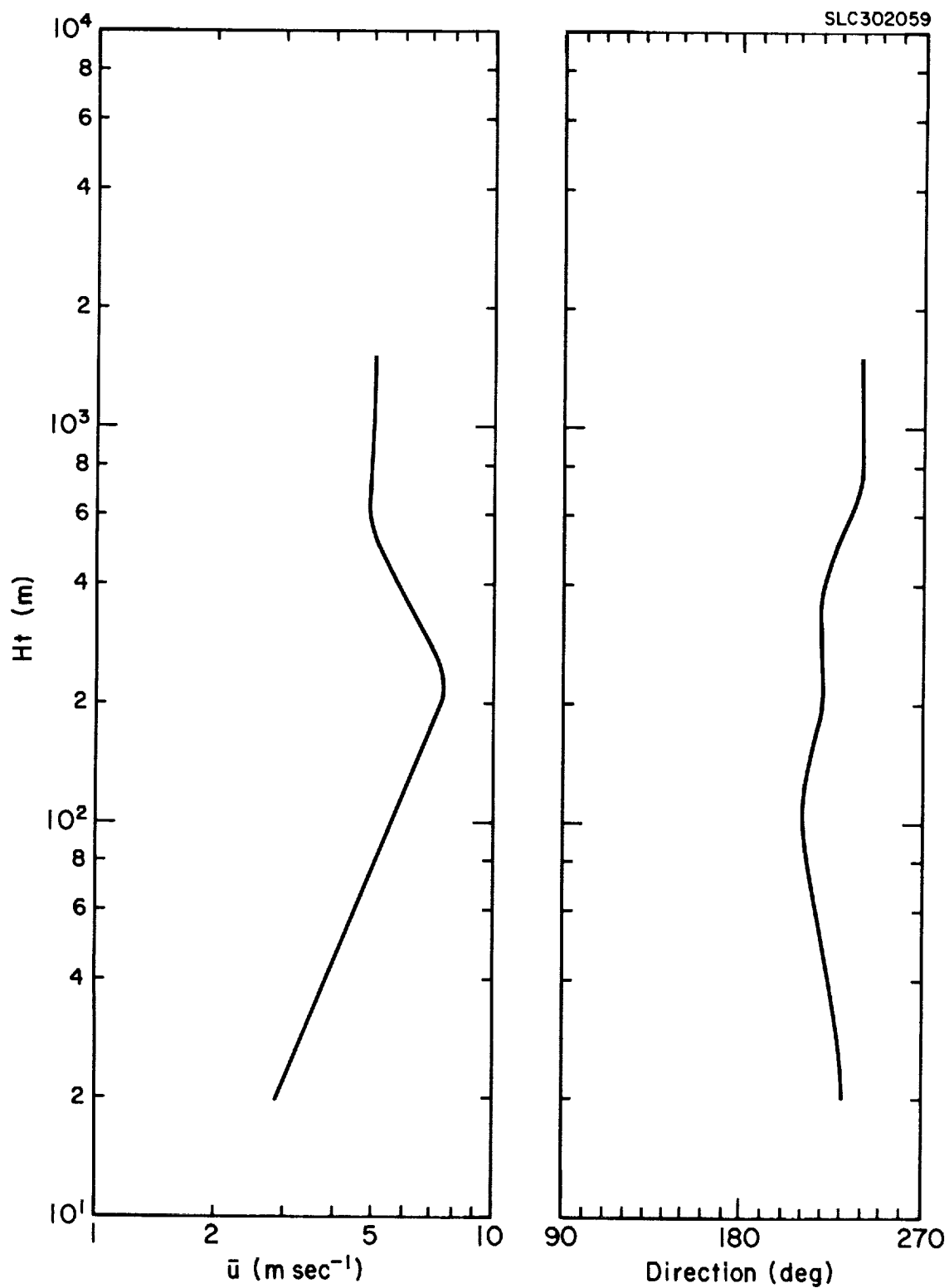


FIGURE 2-29. Vertical profiles of wind speed and wind direction for the land-breeze circulation at KSC. Curves are averages of five sets of concurrent Jimsphere and 150-meter Meteorological Tower measurements.

a height of approximately 250 meters. The wind direction profile reveals a 20-degree backing of the direction between 18 and 100 meters; a fairly constant direction in the layer from 100 to 400 meters that contains the wind speed maximum; a 10- to 20-degree veering of the wind direction from 400 to 700 meters; and a constant wind direction above 800 meters. From the shape of the two profiles in Figure 2-29, it appears that the mean depth of the land breeze is about 700 meters.

Vertical profiles of wind speed and wind direction for the sea-breeze circulation, obtained by averaging eight sets of profile data, are shown in Figure 2-30. The maximum depth of the on-shore flow is 600 to 800 meters and there is some evidence for the presence of a weak return flow in the layer above 800 meters.

It is clear that much additional work is required to achieve a satisfactory documentation of the structure of the land- and sea-breeze circulations at KSC. Although more information on this structure can undoubtedly be gained from further studies of existing measurements, a comprehensive observational program will probably be necessary before the spatial and temporal variations in KSC land- and sea-breeze circulations can be adequately modeled for hazard prediction purposes. Significant features of these circulations that are at present not documented include:

- The landward and seaward dimensions of the primary circulations and counter flows
- The intensity and depth of the primary and counter flow circulations
- The extent to which pollutants that are injected in the land- or sea-breeze circulation tend to be confined to

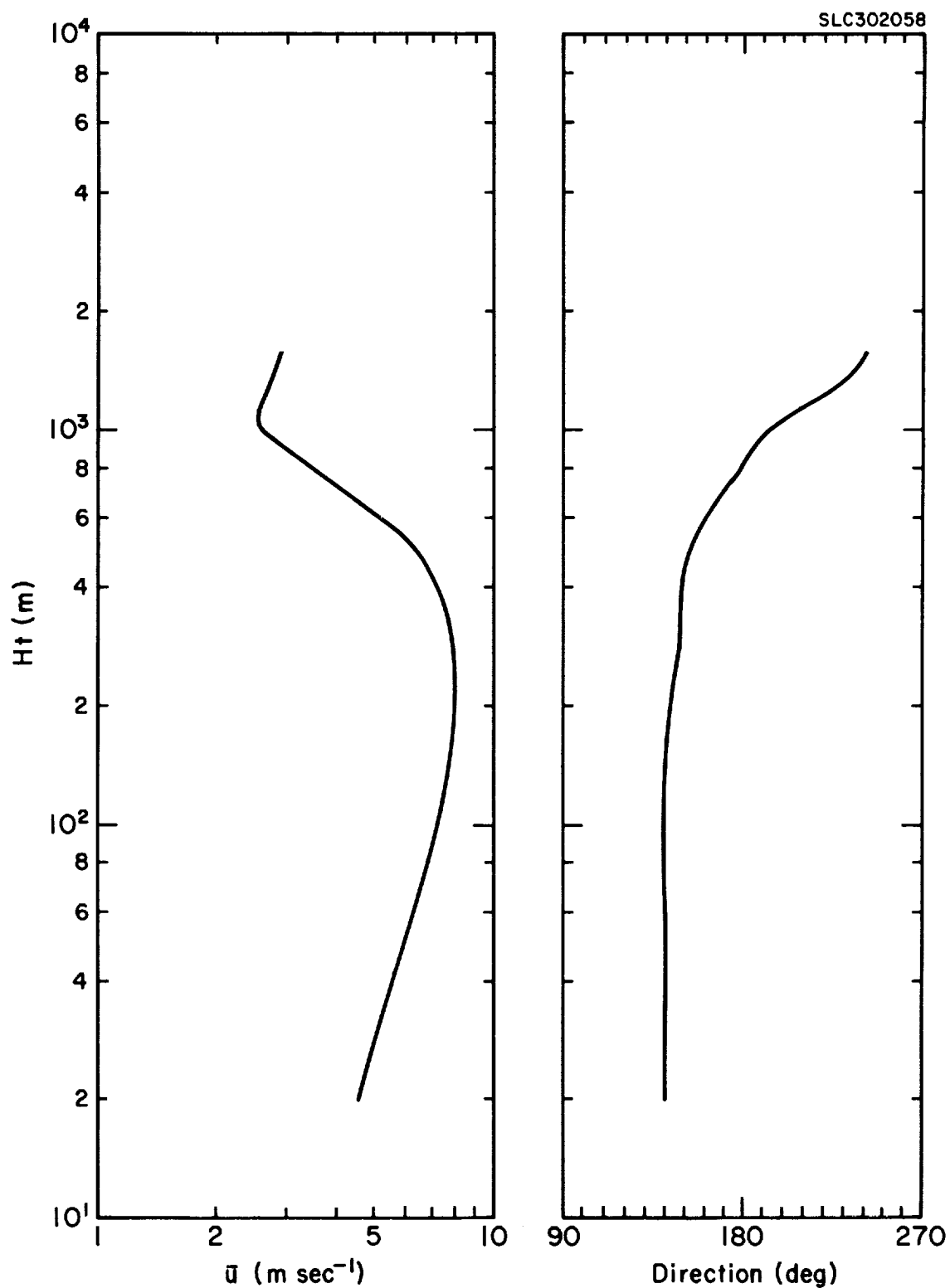


FIGURE 2-30. Vertical profiles of wind speed and wind direction for the sea-breeze circulation at KSC. Curves are averages of eight sets of concurrent Jimsphere and 150-meter Meteorological Tower observations.

the air volume directly involved in the circulation.

In other words, are these circulations essentially closed systems or is there a significant mass transfer across the system boundaries

- The relationship between the structure of the land- and sea-breeze circulations and the gross synoptic pattern

2.3.3 Hsu's (1969) Synthesized Model of the Texas Coast Land- and Sea-Breeze Systems

Scientists at the University of Texas have recently carried out a comprehensive semi-empirical study of the land- and sea-breeze circulations along the Texas coast (Hsu, 1967; 1969; McPherson, 1968; and Feit, 1969). The results of this study are incorporated in Hsu's synthesized model shown in Figure 2-31. Until more information is available on the land- and sea-breeze circulations at Kennedy Space Center, it is not possible to state the extent to which the details of this Texas coast model apply to KSC. However, the spatial dimensions and intensities of the solenoidal circulations shown in the figure, as well as their time dependence, provide a very interesting and valuable insight to the principal features of these wind systems. Judging from the remarks in Section 2.3.2 above, one discrepancy between the KSC systems and the ones shown for the Texas coast is likely to be in the intensity of the counter flows. The landward and seaward extensions of the circulations in Figure 2-31 are of considerable interest. The fully developed land- and sea-breeze systems each extend about 40 kilometers in both the inland and seaward directions from the shoreline. The indicated depth of the primary circulations varies from about 0.6 to 1.0 kilometers, with the corresponding counterflows occurring in superposed layers of approximately the same vertical extent.

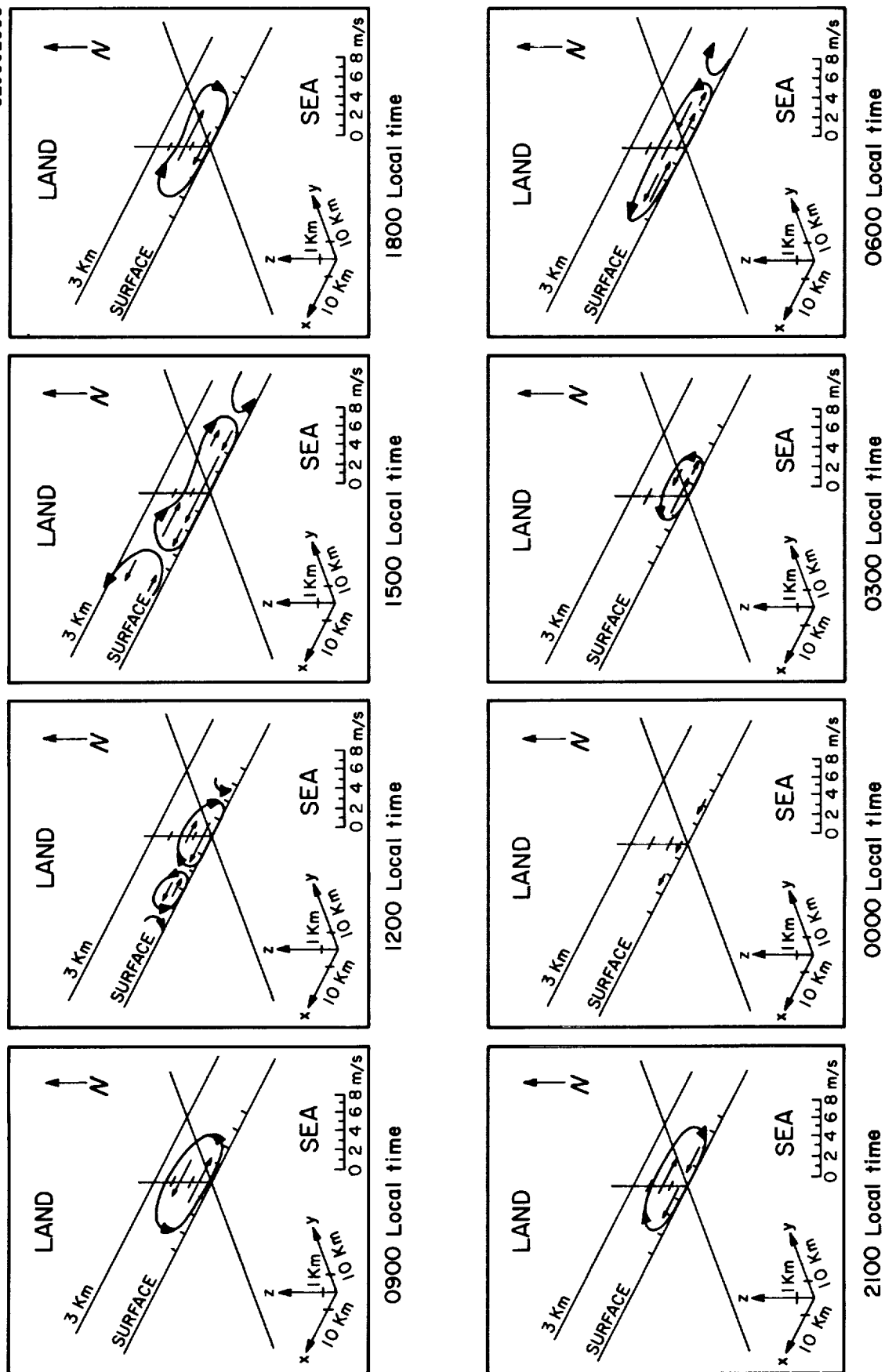


FIGURE 2-31. Hsu's (1969) synthesized model of land- and sea-breeze systems on the Texas coast.

SECTION 3

METEOROLOGICAL MODEL INPUTS FOR SELECTED KSC WEATHER REGIMES

The meteorological inputs required for the multi-layer diffusion model recommended for use at Cape Kennedy have been identified in Section 1.3. In principle, these quantities are determined from a detailed knowledge of the structure of the wind, temperature, humidity and turbulence fields within a large reference air volume. This reference volume has a maximum vertical dimension of 5 kilometers, and extends radially from the point of release of toxic materials to maximum horizontal distances of the order of 100 kilometers. In practice, the assignment of layer boundaries and the selection of gross meteorological model inputs must be made from a very limited number of radiosonde soundings, supplemented by Jimsphere data when available. Because direct measurements of turbulence are not routinely made, on the scale of the reference volume, the assignment of model turbulence parameters must be based on limited observations and on existing empirical and theoretical knowledge of turbulent structure. Suggested procedures for the specifying meteorological model inputs are illustrated below, using Cape Kennedy rawinsonde data, semi-empirical relationships for the behavior of turbulence parameters with height, and results of the analysis of 2 years' climatological data from the NASA 150-meter Meteorological Tower Facility (Section 2.1). The problem of forecasting changes in the wind field during the downwind transport phase is not considered in these examples.

At the start of the contract, it was assumed that an analogue approach would be useful in establishing meteorological model inputs for Cape Kennedy. This approach called for the development of a general classification system consisting of a small number of synoptic weather patterns, characteristic of the

major gross weather regimes at Cape Kennedy, subdivided on the basis of trajectory, wind speed, and stability. Representative vertical profiles of wind and temperature were then to be assigned to the various subclasses for use in diffusion calculations. Accordingly, synoptic maps covering the 1966-1967 period were examined and a number of typical weather regimes at Cape Kennedy were delineated. However, examination of the radiosonde data showed very large variations in the vertical profiles of wind speed, wind direction, temperature and dew point for individual cases within any one regime. Even when two soundings exhibited the same major features, such as temperature inversions or layers with strong wind shear, the heights at which these phenomena occurred and their magnitudes were rarely the same. Because of these very large variations in vertical profiles, within typical synoptic regimes, the analogue approach was abandoned in favor of a direct specification of meteorological model inputs through deep layers of the atmosphere from observed or forecast profiles. To illustrate this procedure, tables of meteorological inputs were constructed from soundings made on eight days during the 1966-1967 period that are representative of typical synoptic patterns at Cape Kennedy.

3.1 SELECTION OF LAYERS AND THE ASSIGNMENT OF GROSS METEOROLOGICAL INPUT PARAMETERS

In principle, the maximum depth of the atmosphere to be considered in diffusion model calculations extends from the surface to the maximum height reached by the top of the cloud of toxic material as it travels downwind. Because the source configurations at Kennedy Space Center include the combustion trail from normal launches as well as vehicle destruct situations, the depth of the atmosphere that must be considered extends from the surface to an arbitrary height of 5 kilometers. In applying the multi-layer diffusion model concept, the 5-kilometer depth is subdivided into layers within which the wind, temperature, and humidity show a regular variation with height. Layer

boundaries are thus placed at heights where discontinuities are observed or expected to occur in the vertical profiles of these quantities. As pointed out in Section 1.2, the multi-layer model hypothesis states that adjacent layers are decoupled as far as turbulent mixing is concerned and, except for gravitational settling and removal of material by precipitation, it is assumed that no significant flux of material occurs across layer boundaries.

In the eight examples described below in Section 3.3, layers are assigned to the region from the surface to a height of 5 kilometers (16,400 feet) to conform with input requirements under Contract No. NAS8-21453. The first step in the layer assignment process is to define the upper boundary of the surface layer. This is done from an inspection of available low-level wind, temperature, and humidity information which, at Cape Kennedy, includes Jimsphere, tower and radiosonde data. When a ground-based inversion exists, the top of the surface layer is assumed to coincide with the top of the inversion. The next step is to examine the vertical profiles for well-defined discontinuities above the surface layer. The wind-speed and wind-direction profiles are used in conjunction with the temperature and dew-point profiles to locate the boundaries of thermally-stable layers. Finally, the wind profiles are inspected for evidence of strong shear, and additional layers are identified as required. Minor discontinuities in the profiles are disregarded since their inclusion has little effect on the estimates of ground-level concentration. Also, comparison of vertical profiles shows that minor discontinuities can seldom be identified for more than a few hours or over long distances.

The assignment of values of wind speed, wind direction and potential temperature at a reference height within the surface layer and at the top and bottom of all other layers completes the specification of the gross meteorological input parameters for the multi-layer diffusion model.

3.2 ASSIGNMENT OF TURBULENCE PARAMETERS

To meet the meteorological input requirements for the generalized diffusion model outlined in Section 1.2, the turbulence parameters σ_A and σ_E must be specified at each layer boundary. As an interim procedure for general use at the Kennedy Space Center, it is suggested that σ_A and σ_E at a reference height of 18 meters be obtained from Figures 2-13 and 2-18, respectively, in Section 2.1. The independent variables used to predict σ_A and σ_E in these figures are the 18-meter wind speed and the temperature difference between 3 meters and 60 meters, as measured on the 150-meter Tower or estimated. It will usually be sufficient to estimate the requisite temperature difference from the forecast weather conditions and the time of day. Under strong solar heating, temperature differences of -1 or -2 degrees Celsius are typical. Zero temperature differences are expected near the morning and afternoon transition times. Under moderately stable and extremely stable conditions, estimates of σ_A and σ_E obtained from Figures 2-13 and 2-18 are relatively insensitive to the absolute magnitude of the temperature difference.

Figure 3-1 has been prepared as a guide in estimating the time of occurrence throughout the year of the two diurnal transition periods. The dashed curves are based on data presented by Scoggins and Alexander (1964) and show the time of day each month when the temperature difference between 1.8 and 62 meters at Air Force Station 700 on Cape Kennedy indicated lapse conditions 50 percent of the time. The transition to lapse conditions in the morning occurs about 1.5 hours after sunrise throughout the year. In the evening, the transition from lapse to inversion coincides closely with the time of sunset, except during the months of June, August and September. The occurrence of the transition period at about 1.5 hours after sunset during the summer season probably reflects the persistence of the daytime sea-breeze circulation into the late afternoon and early evening. The data point for July appears to be an anomaly.

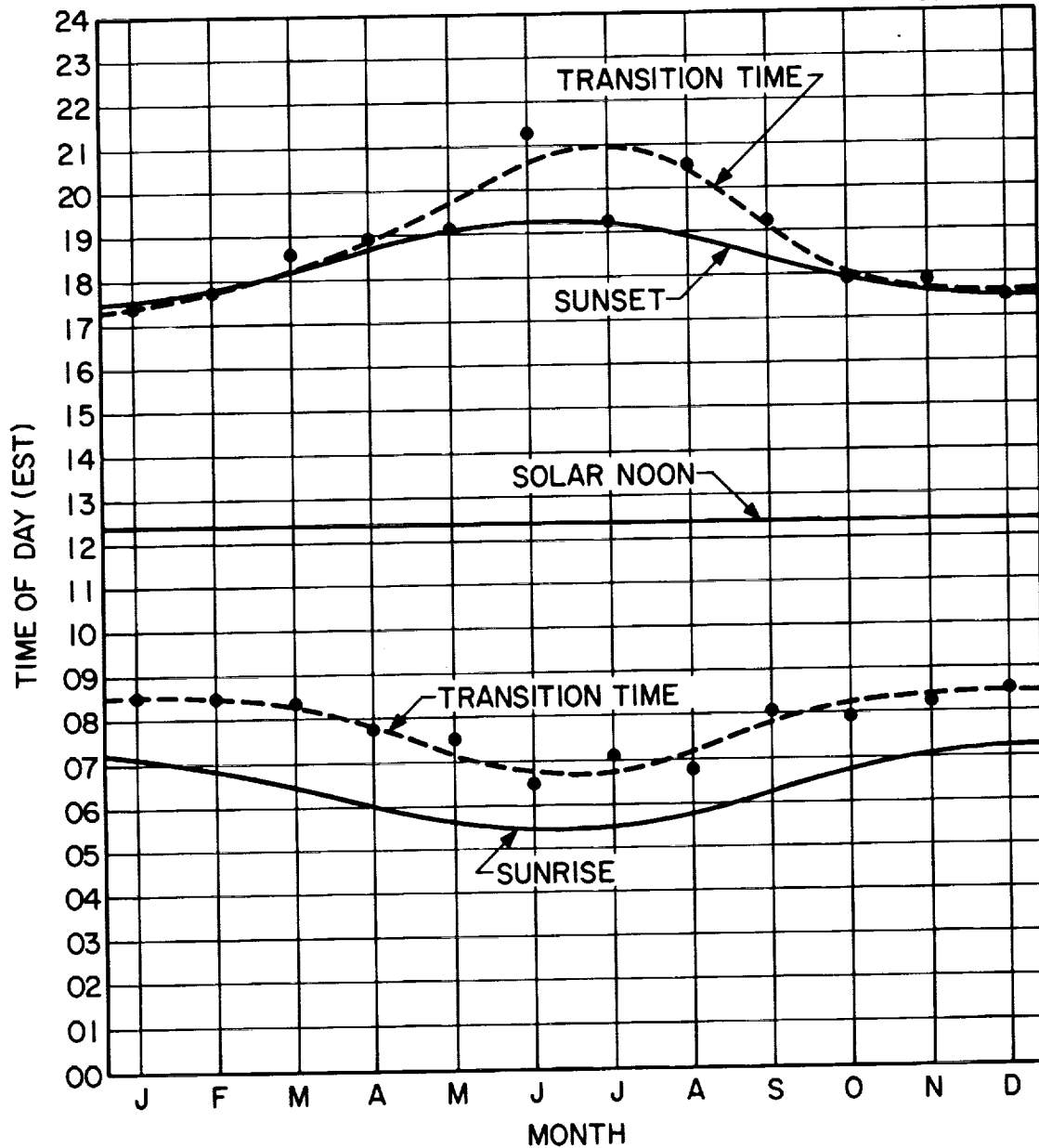


FIGURE 3-1. Seasonal variations in the time of transition from lapse to inversion (above) and from inversion to lapse (below) with respect to sunset and sunrise.

Above the surface layer, mechanical and convective turbulent energy is assumed negligible and the controlling meteorological factors are the mean flow and the wind shear within each layer. If turbulent mixing occurs in the layers above the surface layer, in the absence of well-defined convection, it must be associated with very low turbulent intensities and relatively small scale motions. It follows that the values for σ_A and σ_E assigned to the boundaries of quiescent layers above the surface layer should be very small or even zero (see Pasquill, 1967). A general summary of the behavior of σ_A and σ_E from near ground level to heights of 400 to 1000 feet is given in Slade (1968). Near the surface, 10-minute values of σ_A increase from 2 or 3 degrees during very stable conditions to more than 25 degrees during periods of light winds and strong convection. In general, σ_A decreases slowly with height under all conditions. From an analysis of tower measurements made at White Sands Missile Range, Swanson and Cramer (1965) showed that σ_A decreases with height according to z^{-p} where p is the power-law exponent for the vertical profile of mean wind speed. Near the surface, σ_E increases from 1 or 2 degrees under very stable, light wind conditions to a maximum of 15 degrees under very unstable, light wind conditions. During neutral and stable conditions, σ_E decreases slowly with increasing height; during unstable conditions, σ_E increases with height.

The following guidelines are offered for use in assigning σ_A and σ_E values to the layer boundaries:

- Assign σ_A and σ_E values at a reference height of 18 meters on the basis of the observed or predicted 18-meter wind speed and stability conditions and Figures 2-13 and 2-18.

- Under stable or near-neutral conditions, assume that both σ_A and σ_E are proportional to height raised to the $-p$ power (z^{-p}) throughout the surface layer:

$$\sigma_A \{z\} = \sigma_A \{18m\} \left(\frac{z}{18} \right)^{-p} ; \quad \sigma_E \{z\} = \sigma_E \{18m\} \left(\frac{z}{18} \right)^{-p}$$

- Under unstable conditions, assume that σ_A varies as z^{-p} and that σ_E varies as $z^{0.3-p}$ throughout the surface layer:

$$\sigma_A \{z\} = \sigma_A \{18m\} \left(\frac{z}{18} \right)^{-p} ; \quad \sigma_E \{z\} = \sigma_E \{18m\} \left(\frac{z}{18} \right)^{0.3-p}$$

- Assign minimal values to σ_A and σ_E at the boundaries of all upper layers judged to be decoupled from the surface layer. (In the examples which follow, minimal values are indicated by zero.)

3.3 METEOROLOGICAL MODEL INPUTS FOR SELECTED WINTER REGIMES

During winter, the circulation between the surface and 5 kilometers at Cape Kennedy is dominated by the prevailing westerlies and the passage of frontal systems from the northwest. However, westerly flow at low levels is frequently replaced by easterly flow on the south side of high pressure cells which have moved off the east coast of the United States. The depth of the layer of easterly winds depends on the strength and vertical development of the anti-cyclone, but may exceed 5 kilometers. The vertical temperature profile at Cape Kennedy often shows a marked upper-level inversion or an isothermal layer several thousand feet in depth. Under light wind conditions, a nighttime inversion typically develops between the surface and a height of about 1000 feet. An average of five or six cold fronts pass during each winter month,

frequently preceded by a squall line of showers and thunder showers. Warm front passages are usually associated with wave development and occur, on the average, about twice a month. A thick, multi-layered cloud deck generally develops in the over-running tropical air in advance of the warm front and produces widespread precipitation.

The four winter regimes from which the illustrative examples have been selected are:

- Southwesterly flow in advance of a cold front
- Westerly flow to the rear of a cold front
- Deep easterly flow associated with a large anti-cyclone off the east coast of the United States
- Shallow easterly flow associated with an anti-cyclone off the southeast coast of the United States

3.3.1 Southwesterly Flow in Advance of a Cold Front -2315 GMT, 27 November 1966

Figures 3-2, 3-3 and 3-4 show the synoptic-scale circulation pattern and the vertical structure above Cape Kennedy during the approach of a major, rapidly-moving cold front. Figures 3-2 and 3-3 show the surface and 700-millibar maps, respectively, when the cold front was approximately 300 miles to the northwest of Cape Kennedy. Temperature and dewpoint values at the significant levels of the 2315 GMT Cape Kennedy sounding are plotted on a section of a USAF Modified Skew T, Log P Diagram at the left in Figure 3-4. Wind speed and direction are plotted at 1000-foot intervals at the right in Figure 3-4. The dashed horizontal lines indicate the division of the lowest 5 kilometers into five layers for multi-layer model calculations. Layer 1 comprises

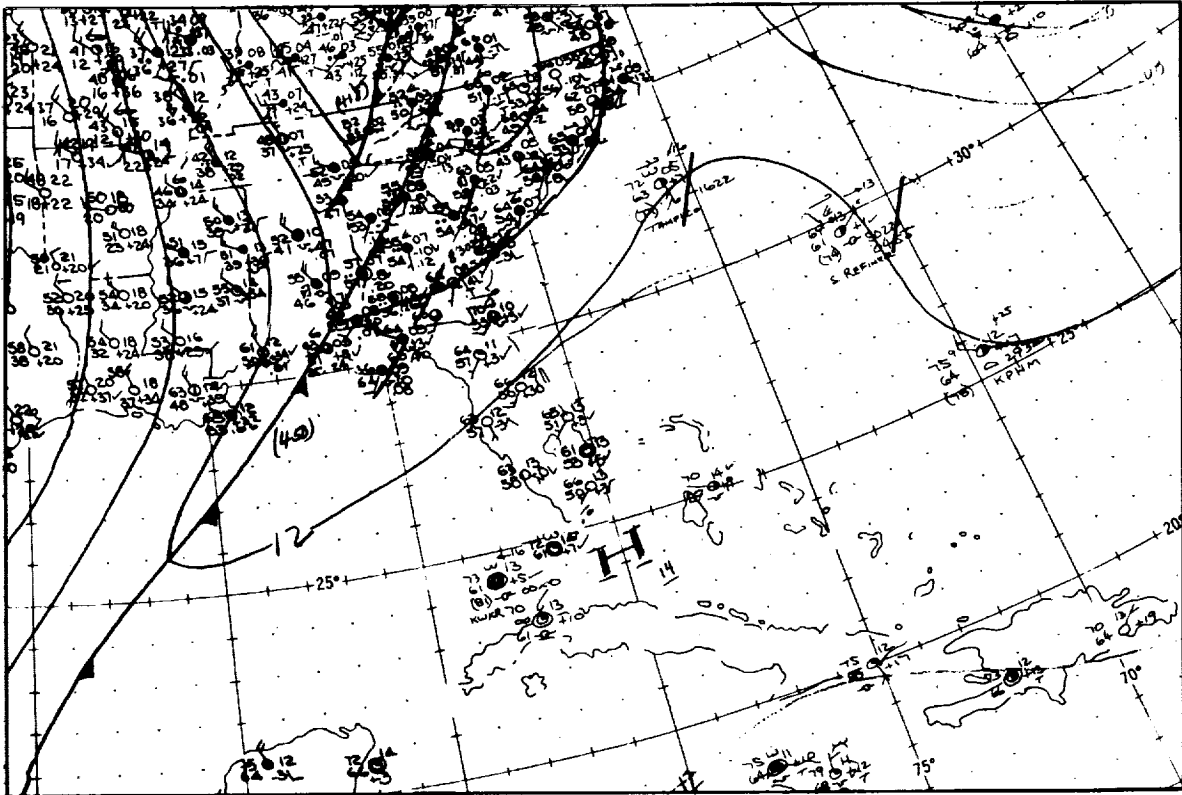


FIGURE 3-2. Surface map for 0000 GMT, 28 November 1966.

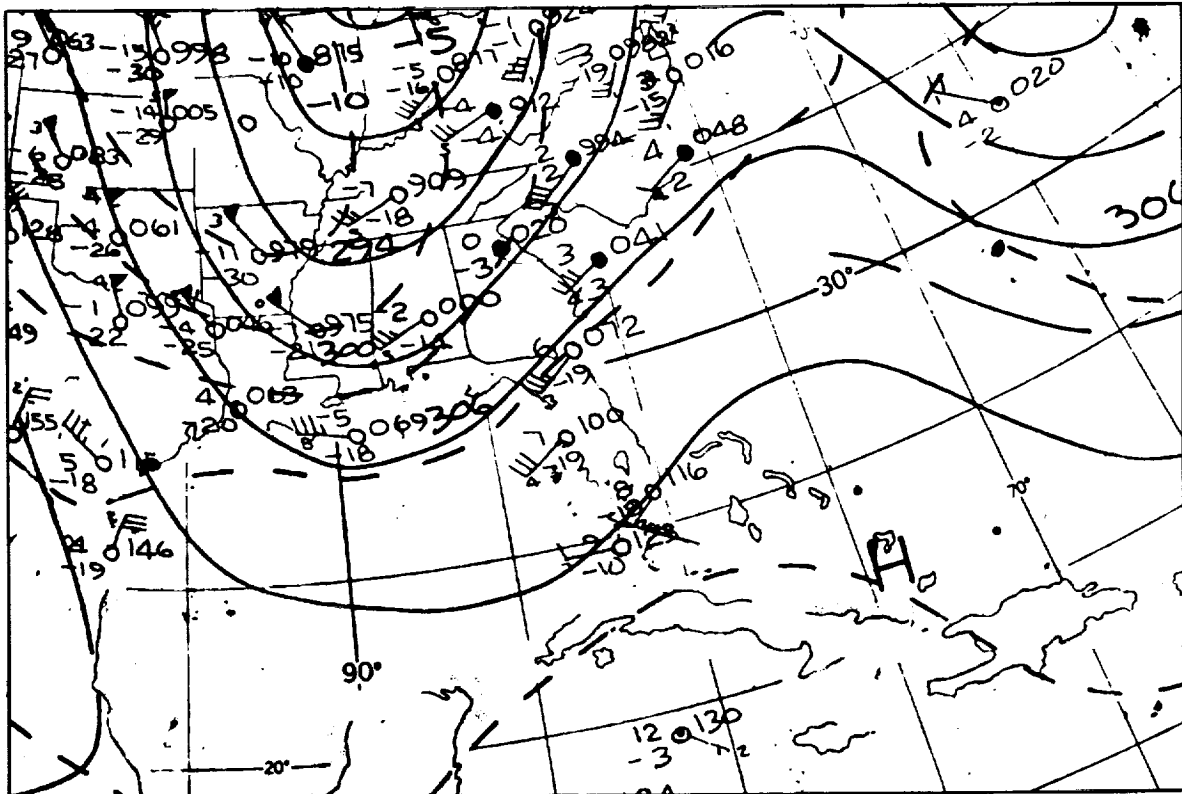


FIGURE 3-3. 700-mb map for 0000 GMT, 28 November 1966.

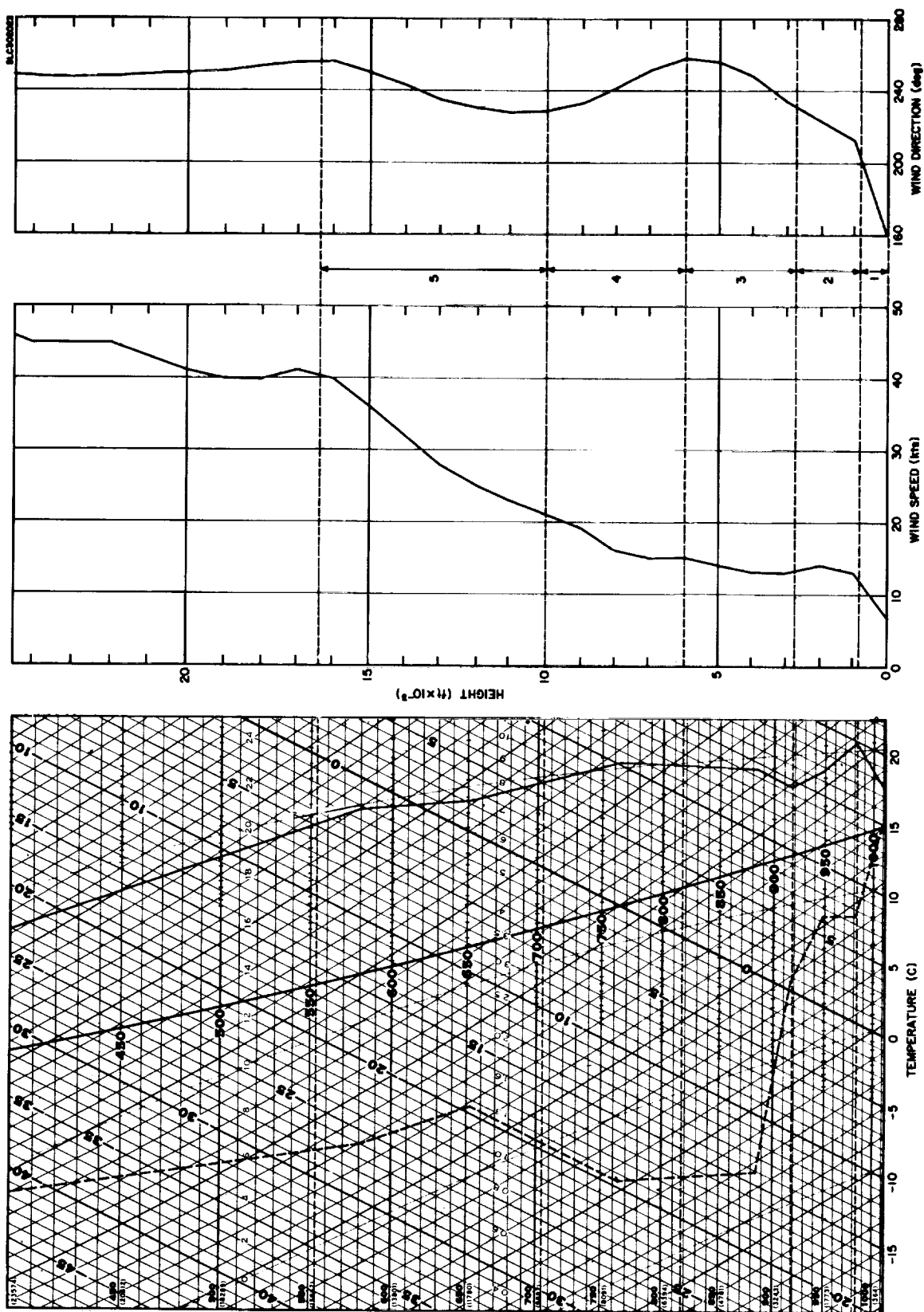


FIGURE 3-4. Vertical profiles for 27 November 1966, 2315 GMT. Solid line on Skew T, Log P diagram is air temperature; dashed line is dew point temperature. Assignment of layers for diffusion model is indicated between wind speed and wind direction profiles.

the surface inversion, and extends to about 900 feet. Layer 2 is approximately dry adiabatic and extends to about 2800 feet. Layer 3 is an isothermal layer within which the dewpoint decreases rapidly. The top of Layer 3 is at 6000 feet where the wind direction begins to back with height. The lapse rate between 6000 and 16,400 feet is approximately moist adiabatic and the wind speed increases steadily with height. However, this height interval has been divided into two layers on the basis of the wind direction shear. Table 3-1 lists meteorological inputs to the diffusion model at the surface reference height and at the five layer boundaries obtained from the profiles in Figure 3-4. The values of σ_A and σ_E given in Table 3-1 were determined by the procedures outlined in Section 3.2. Within the surface inversion, $p = 0.14$ and σ_A and σ_E are assumed to vary as $z^{-0.14}$. The temperature and wind speed profiles indicate a lapse rate close to the dry adiabatic in Layer 2 and $p = 0.06$. According to the guidelines in Section 3.2, if Layer 2 is unstable, σ_A and σ_E may be assumed to vary, respectively, as $z^{-0.06}$ and $z^{0.24}$. However, Layer 2, which is the upper part of the daytime mixing layer, is becoming decoupled from the surface by the developing ground-level inversion and it would probably be equally valid either to let σ_E vary as z^{-p} , or to assign minimal values to both σ_A and σ_E at the 2800-foot boundary.

3.3.2 Westerly Flow to the Rear of a Cold Front - 2315 GMT, 28 November 1966

By 0000 GMT on 29 November 1966, the cold front shown approaching Cape Kennedy in Figure 3-2 had moved to a position about 300 miles to the east of Cape Kennedy. Figures 3-5 and 3-6 show the surface and 700-millibar maps at this time. Figure 3-7 shows the vertical profiles of temperature, dewpoint, wind speed and wind direction at 2315 GMT, 28 November 1966. Winds are westerly at all levels between the surface and 16,400 feet. There is a temperature inversion of 9.4 C between about 5,700 and 8,200 feet. Below the

TABLE 3-1

METEOROLOGICAL MODEL INPUTS FOR 2315 GMT, 27 NOVEMBER 1966

Layer No.	Height (ft)	Wind Speed (knot)	Wind Direction (deg)	Potential Temperature (C)	σ_A (deg)	σ_E (deg)
1	59	8	160	17	8	4.5
2	870	12	206	22	6	3
3	2,800	13	231	22	5	4
4	6,000	15	258	29	0	0
5	10,000	21	229	36	0	0
	16,400	40	256	45	0	0

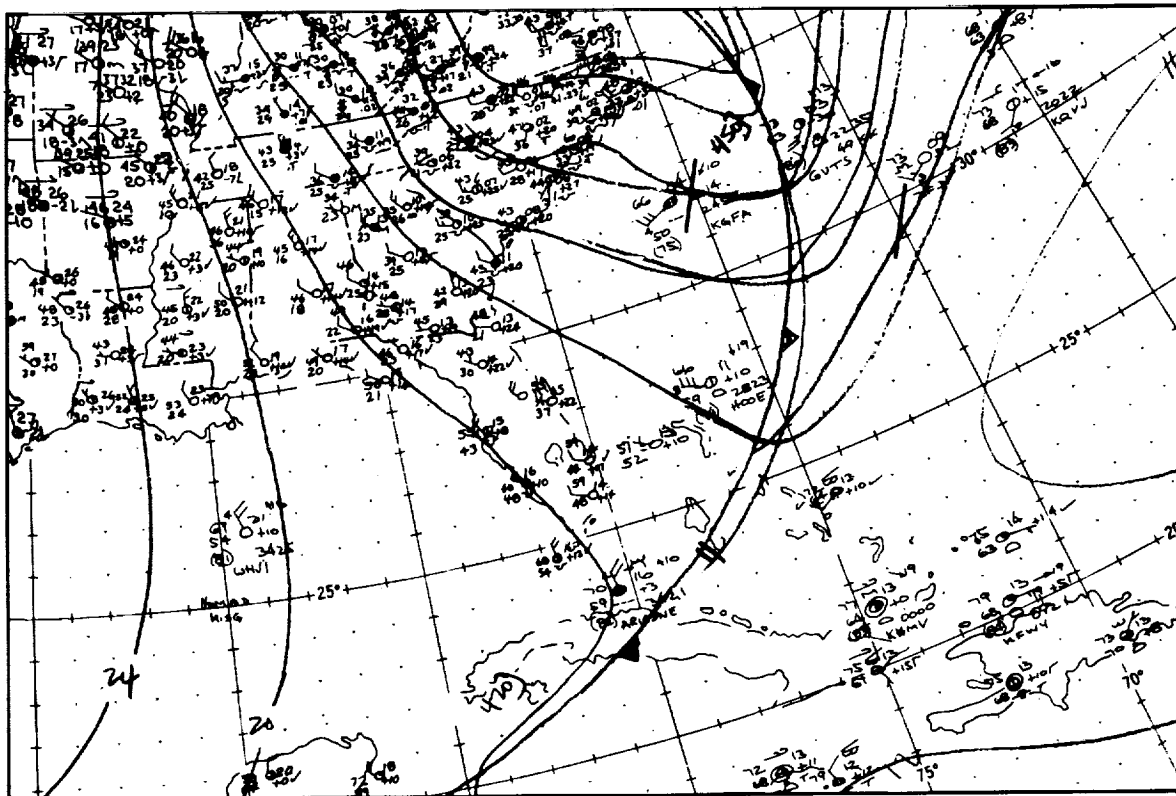


FIGURE 3-5. Surface map for 0000 GMT, 29 November 1966.

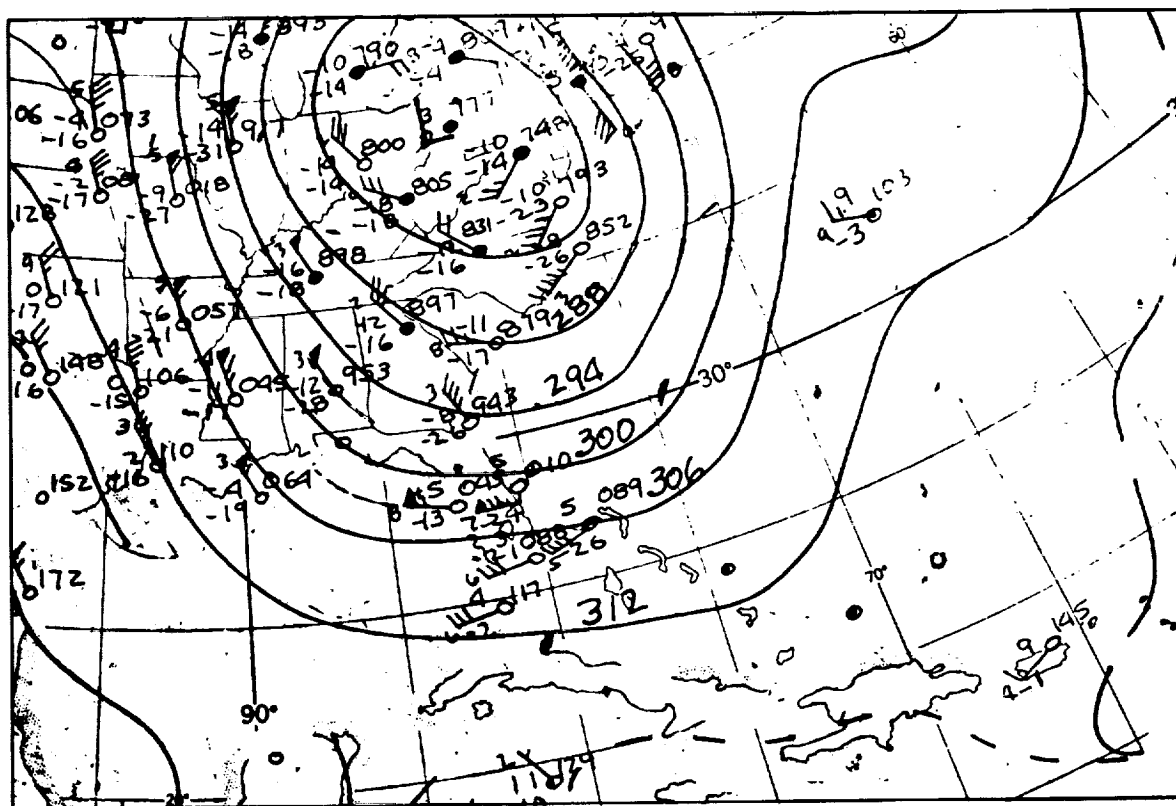


FIGURE 3-6. 700-mb map for 0000 GMT, 29 November 1966.

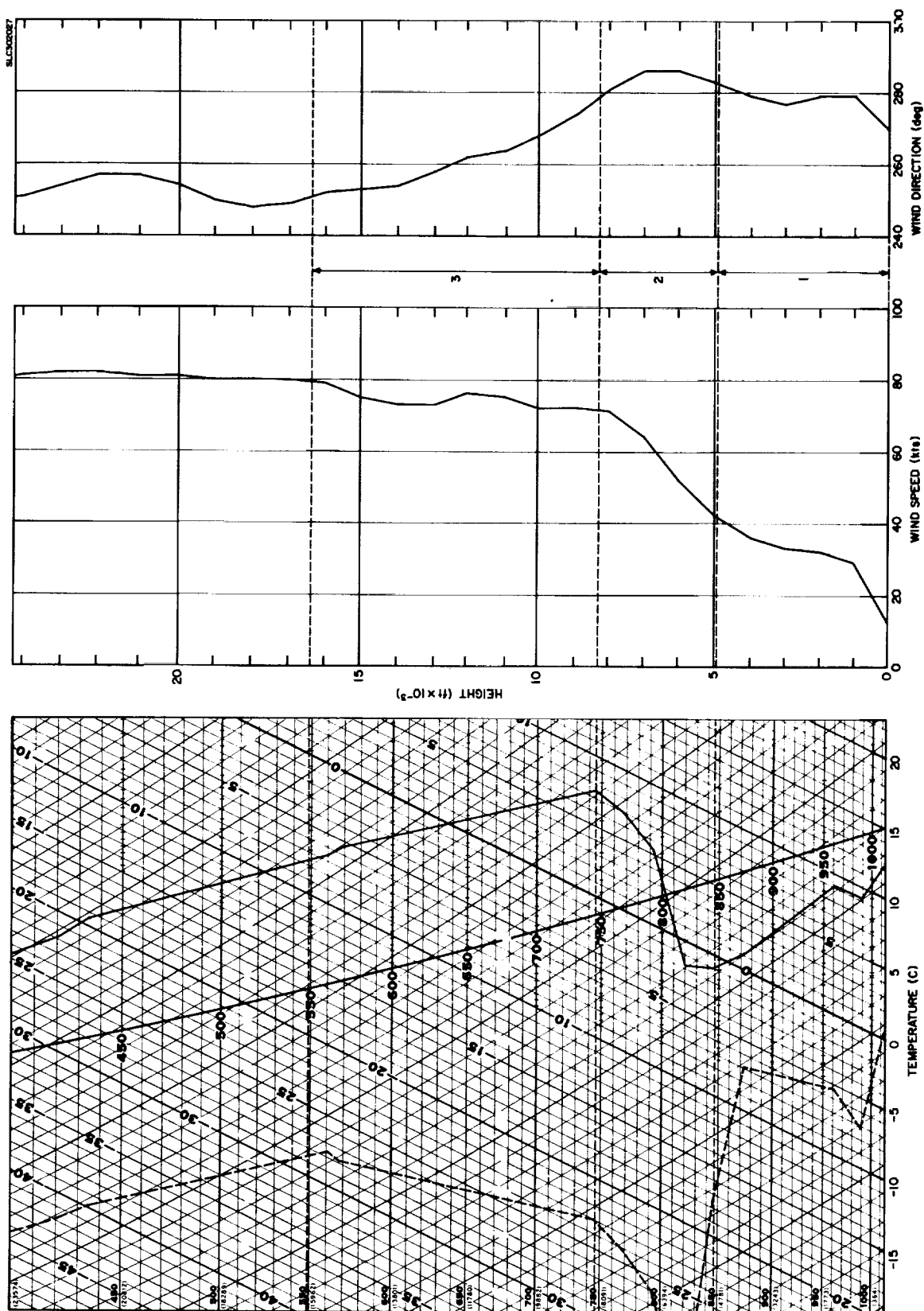


FIGURE 3-7. Vertical profiles for 28 November 1966, 2315 GMT. Solid line on Skew T, Log P diagram is air temperature; dashed line is dew point temperature. Assignment of layers for diffusion model is indicated between wind speed and wind direction profiles.

inversion, the lapse rate is approximately dry adiabatic. Winds increase from 12 knots at the surface to 52 knots at the base of the inversion; from the top of the inversion to 16,400 feet, the wind speed varies from 72 to 79 knots. The vertical structure suggests the division of the lowest 16,400 feet into three layers. With strong winds and unstable conditions prevailing generally behind the cold front, it is unlikely that the superadiabatic-isothermal layers shown in Figure 3-7 between the surface and 960 millibars are real. Layer 1 has therefore been extended from the surface to the base of the inversion. The height selected for the top of Layer 1, 4800 feet, represents a compromise position between a slightly lower height suggested by the dewpoint profile and a slightly higher one suggested by the temperature profile. The division between Layers 2 and 3 is at the top of the inversion at 8200 feet.

The meteorological inputs for the multi-layer diffusion model are given in Table 3-2. Because of the strong winds and dry-adiabatic lapse rate, Layer 1 is considered near-neutral and σ_A and σ_E are assumed to vary as z^{-p} , or $z^{-0.21}$.

3.3.3 Deep Easterly Flow Associated with a Large Anticyclone off the East Coast of the United States - 0255 GMT, 10 February 1966

At 0000 GMT on 10 February 1966, a large high pressure cell off the east coast of the United States controlled the circulation between the surface and 16,400 feet at Cape Kennedy. Figures 3-8 and 3-9 show the surface and 700 millibar maps for this time. The vertical profiles, plotted in Figure 3-10, show a ground-level inversion extending to 1000 feet and an upper-level inversion of 5 C between 6,500 and 8,400 feet. Wind directions are east-southeast between the surface and 16,400 feet. The wind speed decreases from 29 knots at the top of the surface inversion to 2 knots at 16,400 feet.

TABLE 3-2

METEOROLOGICAL MODEL INPUTS FOR 2315 GMT, 28 NOVEMBER 1966

Layer No.	Height (ft)	Wind Speed (knot)	Wind Direction (deg)	Potential Temperature (C)	σ_A (deg)	σ_E (deg)
1	59	16	270	11	9	5
	4,800	42	282	12	3	2
2	8,200	71	279	32	0	0
	16,400	79	251	43	0	0

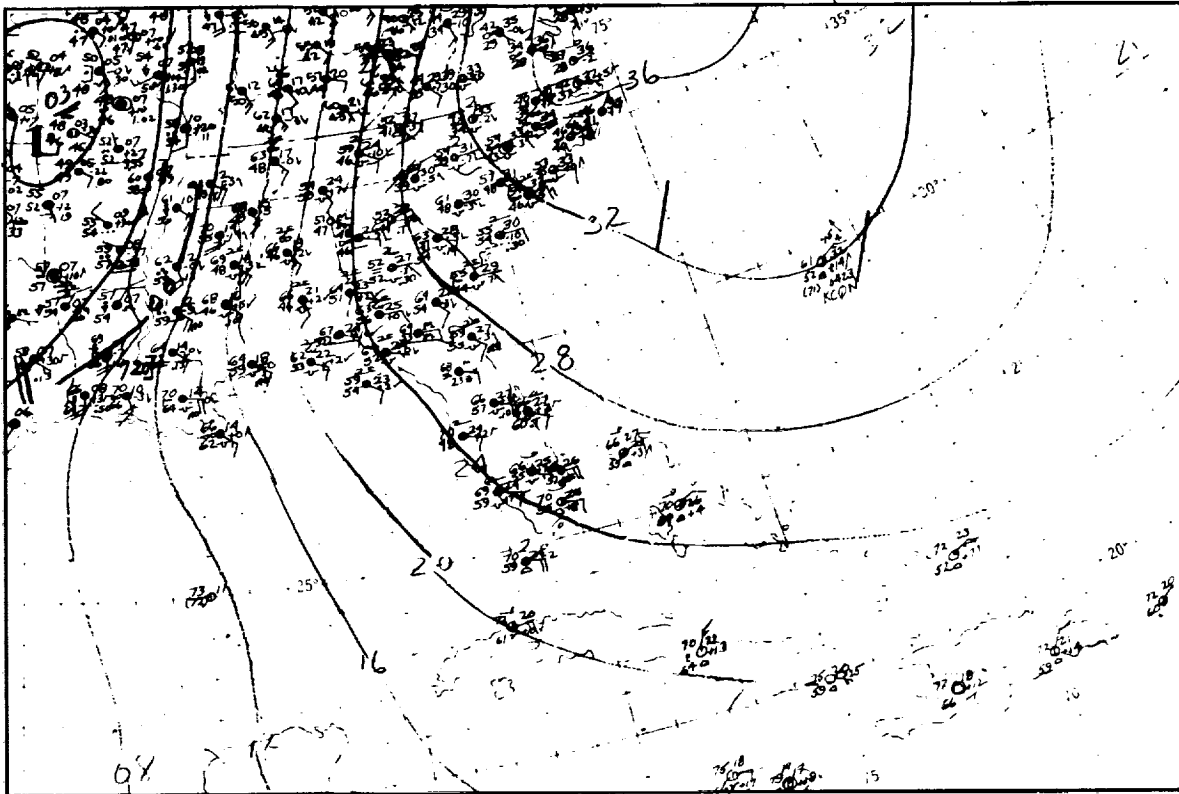


FIGURE 3-8. Surface map for 0000 GMT, 10 February 1966.

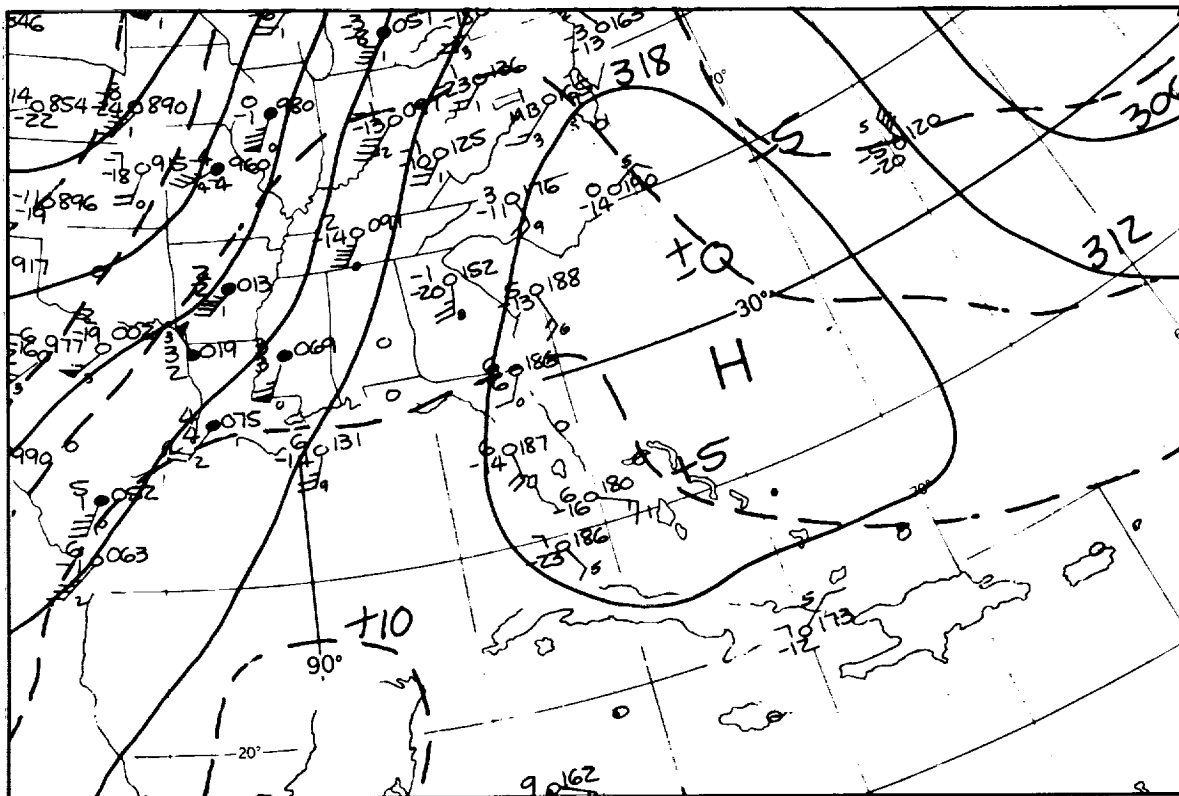


FIGURE 3-9. 700-mb map for 0000 GMT, 10 February 1966.

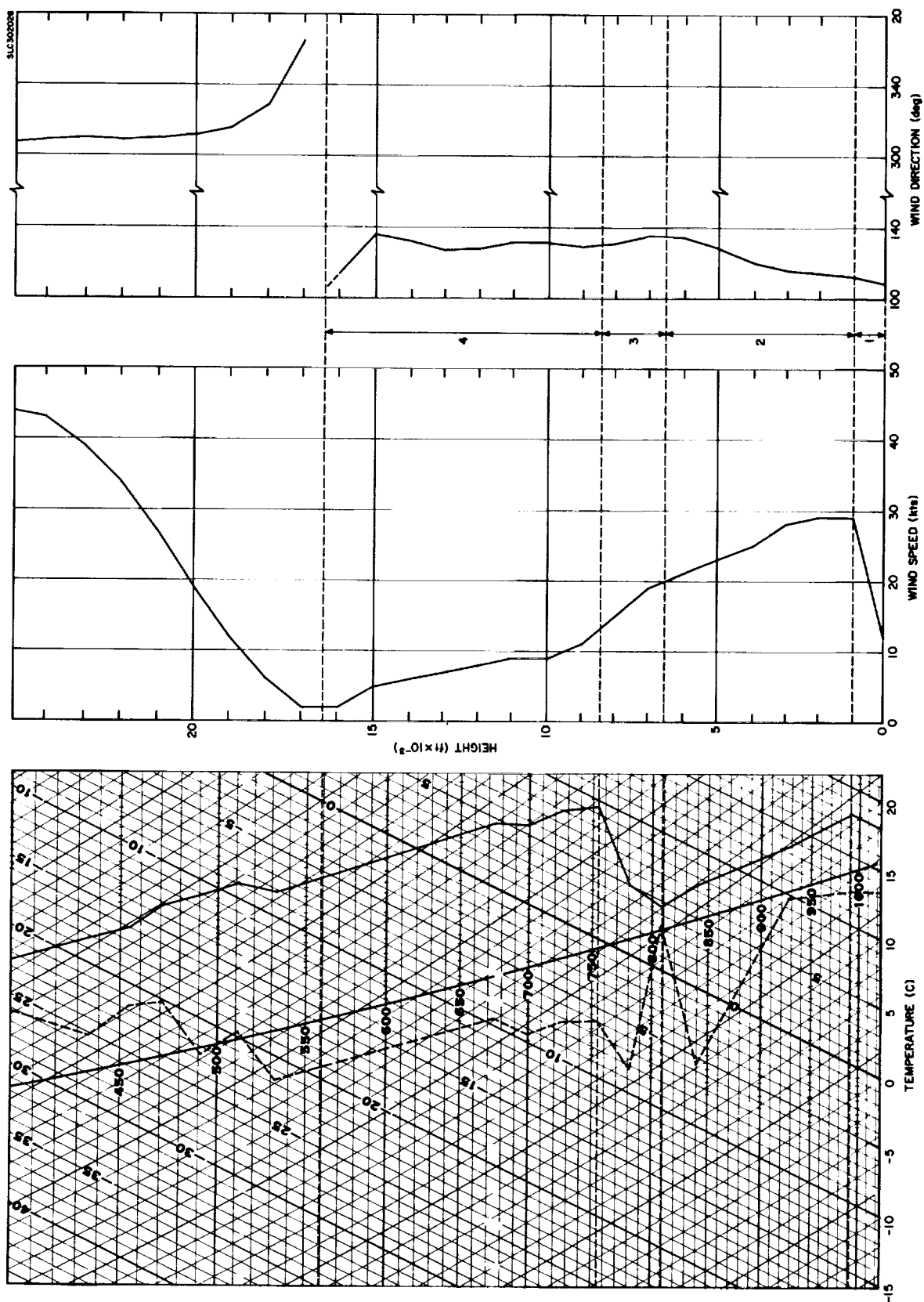


FIGURE 3-10. Vertical profiles for 10 February 1966, 0255 GMT. Solid line on Skew T, Log P diagram is air temperature; dashed line is dew point temperature. Assignment of layers for diffusion model is indicated between wind speed and wind direction profiles.

The subdivision by layers is shown in Figure 3-10. Layer 1 contains the surface inversion and extends to 1000 feet. Layer 2 extends from 1000 feet to the base of the upper-level inversion at 6,500 feet. Layer 3 contains the upper-level inversion, and Layer 4 extends from the top of the upper-level inversion to 16,400 feet.

The meteorological inputs are shown in Table 3-3. In the surface inversion layer, $p = 0.21$, and σ_A and σ_E are both assumed to vary as $z^{-0.21}$.

3.3.4 Shallow Easterly Flow Associated with an Anticyclone off the Southeast Coast of the United States - 1115 GMT, 8 December 1966

At 1200 GMT on 8 December 1966, a 1024-millibar high pressure cell was centered about 400 miles off the Georgia-Carolina coast and a cold front was moving eastward through Missouri. The surface and 700-millibar maps for this time are shown in Figures 3-11 and 3-12, respectively. The temperature profile in Figure 3-13 shows a surface inversion of about 3 C and an inversion of about 2 C between 7,200 and 9,000 feet. Winds are southeasterly below the upper-level inversion, and southwesterly above the inversion. Layer 1 extends from the surface to the top of the surface inversion at 800 feet. Layer 2 extends from the top of the surface inversion to the base of the upper-level inversion. The wind speed in Layer 2 decreases from a maximum of 17 knots at 2,000 feet to 7 knots at 7,200 feet. Layer 3 begins at 7,200 feet, includes the upper-level inversion, and extends to 11,000 feet where the wind direction begins to back with height, after veering strongly with height in Layer 3. Layer 4 extends from 11,000 feet to 16,400 feet and has a uniform lapse rate and light, southwesterly winds.

TABLE 3-3

METEOROLOGICAL MODEL INPUTS FOR 0255 GMT, 10 FEBRUARY 1966

Layer No.	Height (ft)	Wind Speed (knot)	Wind Direction (deg)	Potential Temperature (C)	σ_A (deg)	σ_E (deg)
1	59	16	109	16	9	5
	1,000	29	112	19	5	3
2	6,500	20	135	22	0	0
	8,400	13	130	33	0	0
3	16,400	2	104	43	0	0

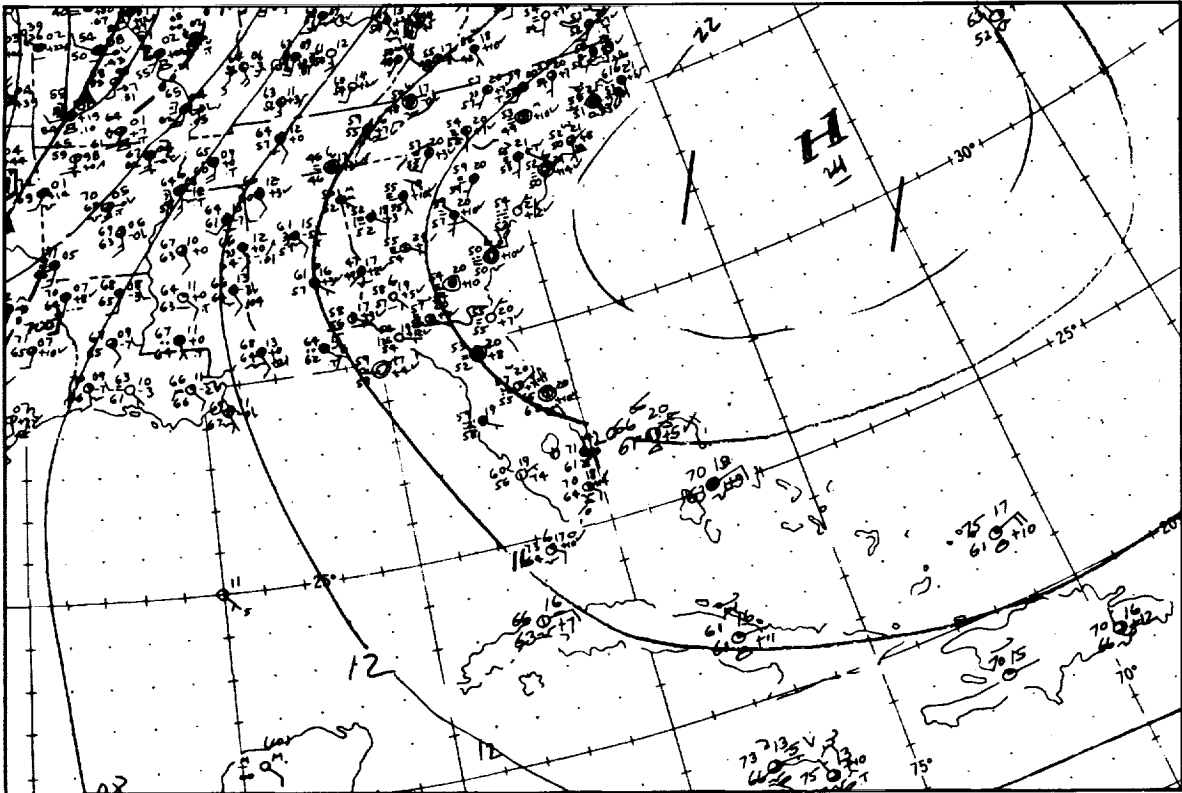


FIGURE 3-11. Surface map for 1200 GMT, 8 December 1966.

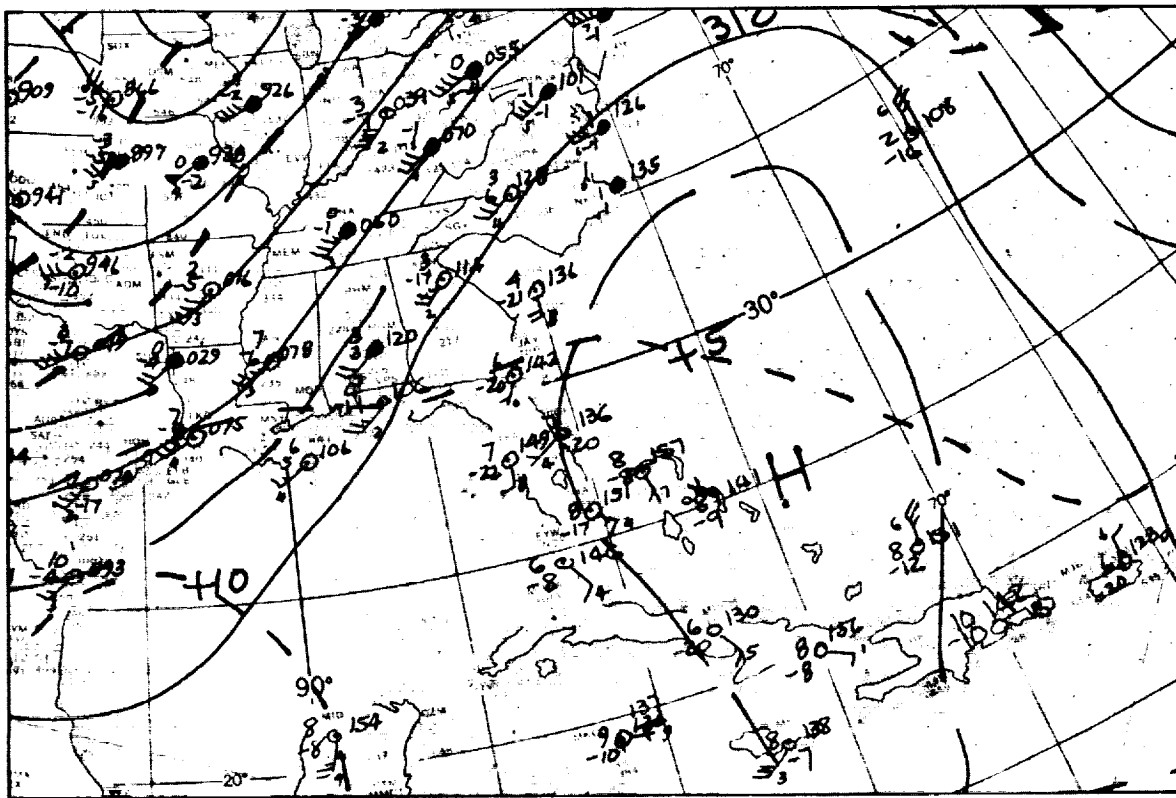


FIGURE 3-12. 700-mb map for 1200 GMT, 8 December 1966.

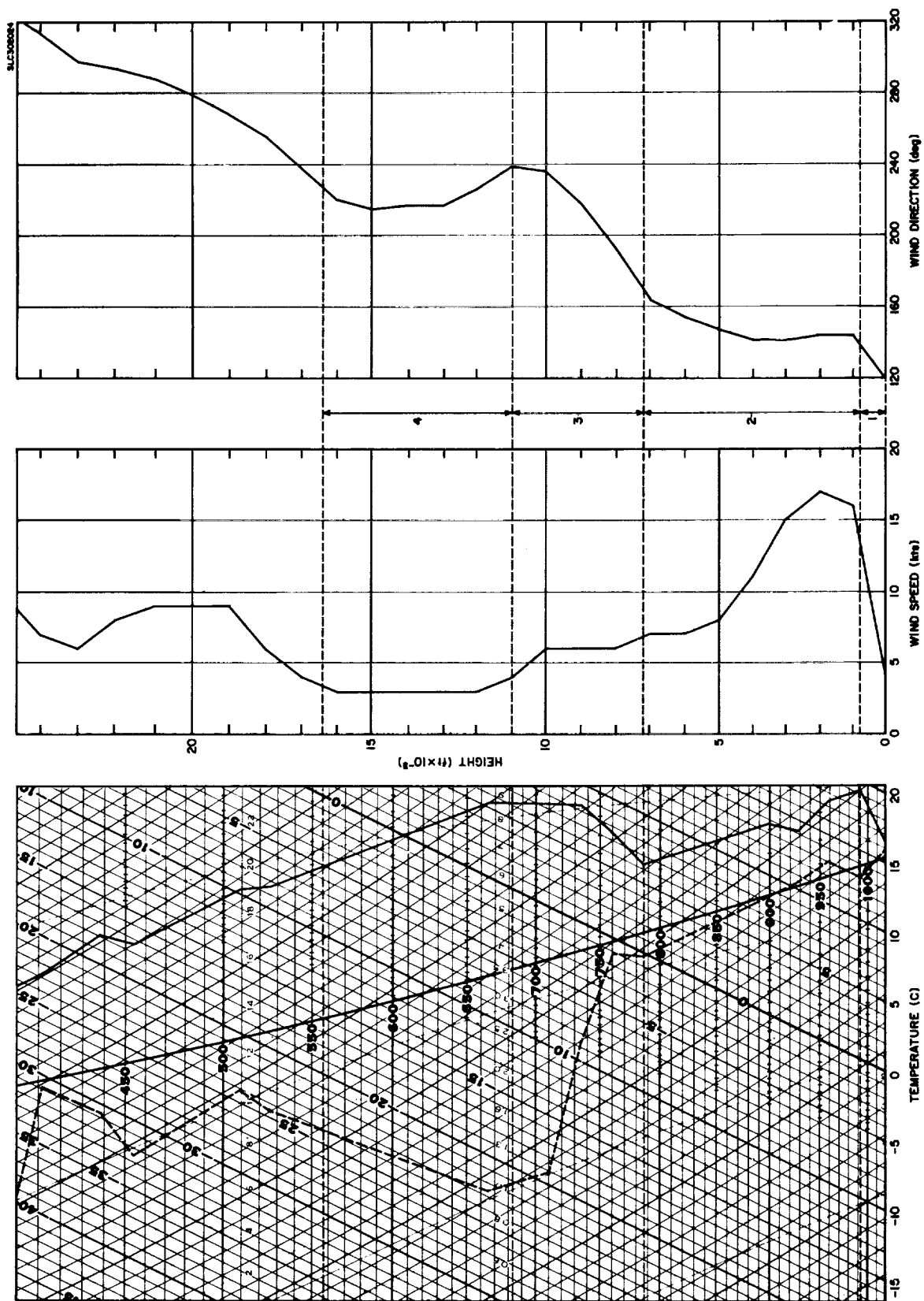


FIGURE 3-13. Vertical profiles for 8 December 1966, 1115 GMT. Solid line on Skew T, Log P diagram is air temperature; dashed line is dew point temperature. Assignment of layers for diffusion model is indicated between wind speed and wind direction profiles.

The meteorological inputs for this example are shown in Table 3-4 within the surface layer, $p = 0.30$ and σ_A and σ_E are assumed to vary as $z^{-0.30}$.

3.4 METEOROLOGICAL MODEL INPUTS FOR SELECTED SUMMER REGIMES

During summer, the general circulation between the surface and 5 kilometers at Cape Kennedy is controlled to a large extent by the position and strength of the Bermuda High. At lower levels, the westward extension of this semi-permanent anticyclone provides a nearly constant flow of warm moist air over central Florida, and afternoon showers and thunderstorms occur quite regularly. This flow of maritime tropical air is interrupted about once a month in mid-summer by the passage of a cold front. Typically, the cold front stalls in southern Florida and returns as a warm front. At the higher levels, westerly winds are common. A principal feature of deep easterly flow in the summertime is the occurrence of easterly waves and tropical cyclones within the region.

The four summer regimes from which the illustrative examples have been selected are:

- Southwesterly flow in advance of a cold front
- Northeasterly flow to the rear of a cold front
- Extension of the Bermuda High into the Gulf of Mexico
- Circulation controlled by a tropical cyclone

TABLE 3-4

METEOROLOGICAL MODEL INPUTS FOR 1115 GMT, 8 DECEMBER 1966

Layer No.	Height (ft)	Wind Speed (knot)	Wind Direction (deg)	Potential Temperature (C)	σ_A (deg)	σ_E (deg)
1	59	6	119	15	6	3
2	800	13	139	20	3	1
3	7,200	7	170	26	0	0
4	11,000	4	239	39	0	0
	16,400	3	227	44	0	0

3.4.1 Southwesterly Flow in Advance of a Cold Front - 0515 GMT, 16 May 1966

A cold front moved off the mainland on 15 May 1966 and at 0600 GMT on 16 May extended in a northeast-southwest direction across northern Florida. Figure 3-14 shows the surface map for 0600 GMT and Figure 3-15 shows the 700-millibar map for six hours earlier. The vertical profiles for 0515 GMT on 16 May 1967 are plotted in Figure 3-16. The temperature profile shows two layers that are approximately isothermal: one layer extends from the ground to 2700 feet, and the second layer extends from about 7600 to 8600 feet. The wind speed profile shows the speed increasing to 900 feet, decreasing slightly from 900 to 5000 feet, increasing again from 5,000 to 9,000 feet, and remaining nearly constant from 9,000 to 16,400 feet. With the exception of a layer between 6,000 and 9,000 feet within which the wind direction is invariant with height, the wind backs steadily from 293 degrees at the top of the surface layer to 191 degrees at 14,000 feet. Between 14,000 and 16,400 feet the wind veers slightly. The division of the lowest 16,400 feet into the six layers shown in Figure 3-16 has been done rather arbitrarily on the basis of these relatively small changes in profile characteristics. Nearly similar ground-level concentrations would be expected from the multi-layer diffusion model if the layer breakdown were made solely from the wind direction profile. In this case, five layers would be used with boundaries at 900, 6,000, 9,000, 14,000 and 16,400 feet. The meteorological inputs for the layers indicated in Figure 3-16 are shown in Table 3-5. In the surface layer, $p = 0.24$ and σ_A and σ_E are both assumed to vary as $z^{-0.24}$.

3.4.2 Northeasterly Flow to the Rear of a Cold Front - 2320 GMT, 22 July 1966

Figures 3-17 and 3-18 show the surface and 700-millibar maps respectively for a typical post cold-front situation during the summer. Northeasterly flow prevails throughout the lowest 16,400 feet, and broken stratiform

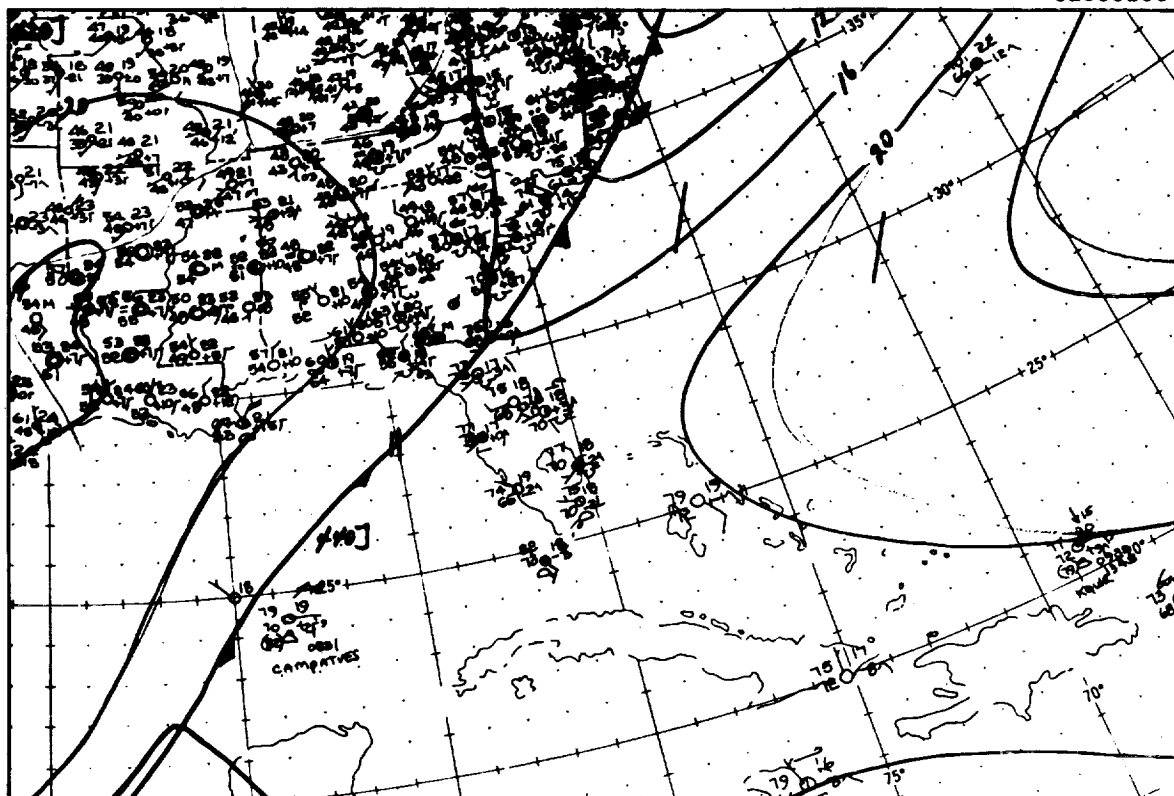


FIGURE 3-14. Surface map for 0600 GMT, 16 May 1967.

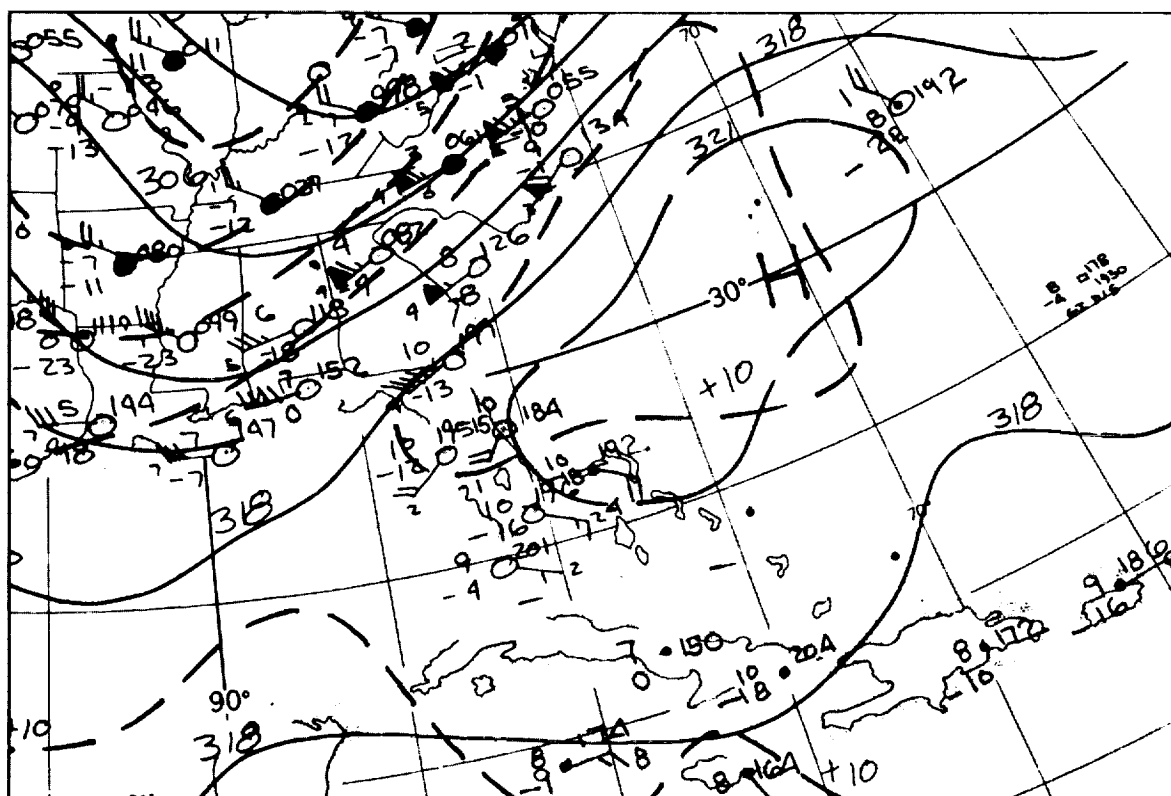


FIGURE 3-15. 700-mb map for 0000 GMT, 16 May 1967.

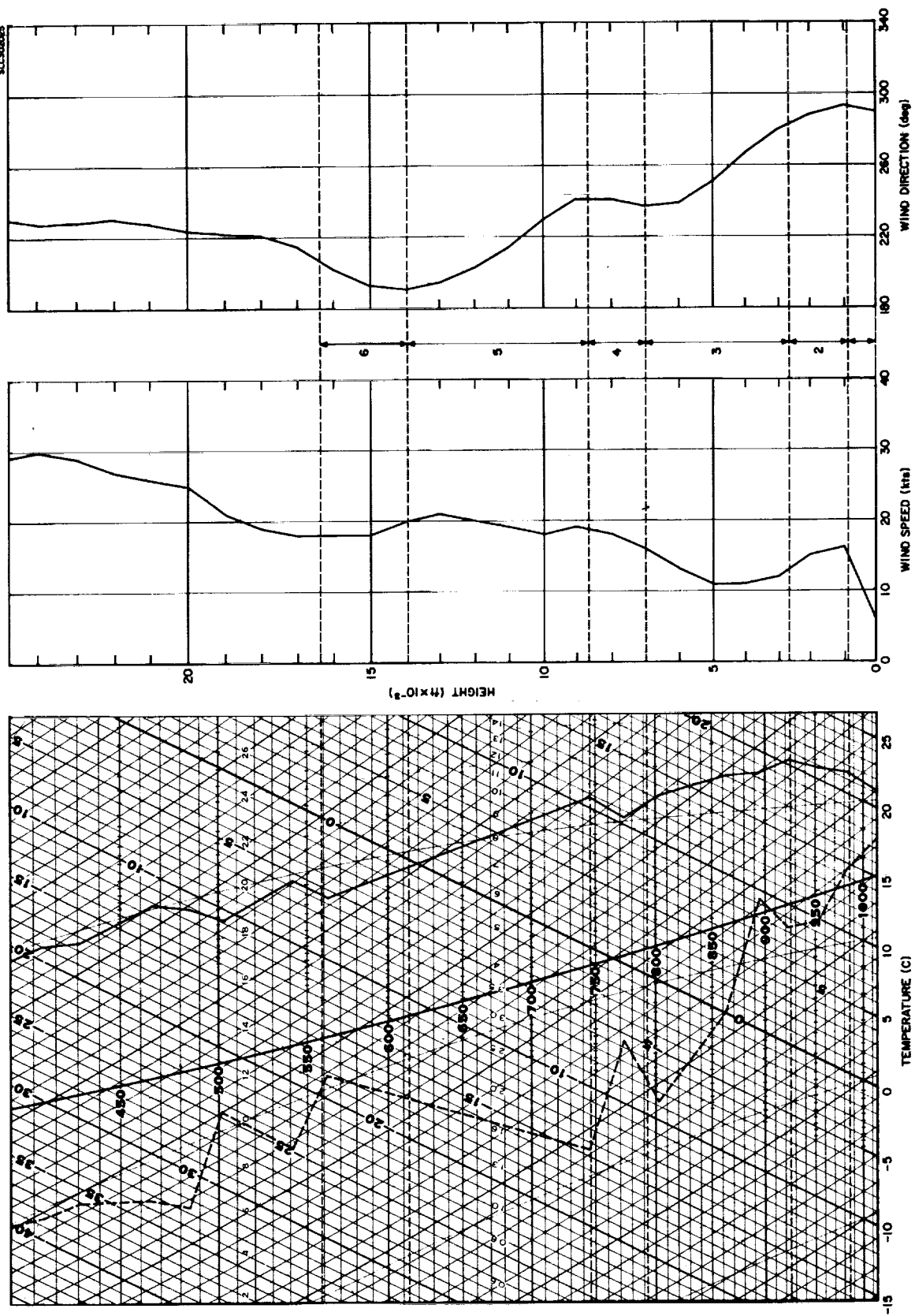


FIGURE 3-16. Vertical profiles for 16 May 1967, 0515 GMT. Solid line on Skew T, Log P diagram is air temperature; dashed line is dew point temperature. Assignment of layers for diffusion model is indicated between wind speed and wind direction profiles.

TABLE 3-5

METEOROLOGICAL MODEL INPUTS FOR 0515 GMT, 16 MAY 1967

Layer No.	Height (ft)	Wind Speed (knot)	Wind Direction (deg)	Potential Temperature (C)	σ_A (deg)	σ_E (deg)
1	59	8	290	20	7	3.5
	900	16	293	23	4	2
2	2,700	13	282	27	0	0
	7,000	16	237	32	0	0
3	8,600	19	241	26	0	0
	14,000	20	191	41	0	0
4	16,400	18	207	43	0	0

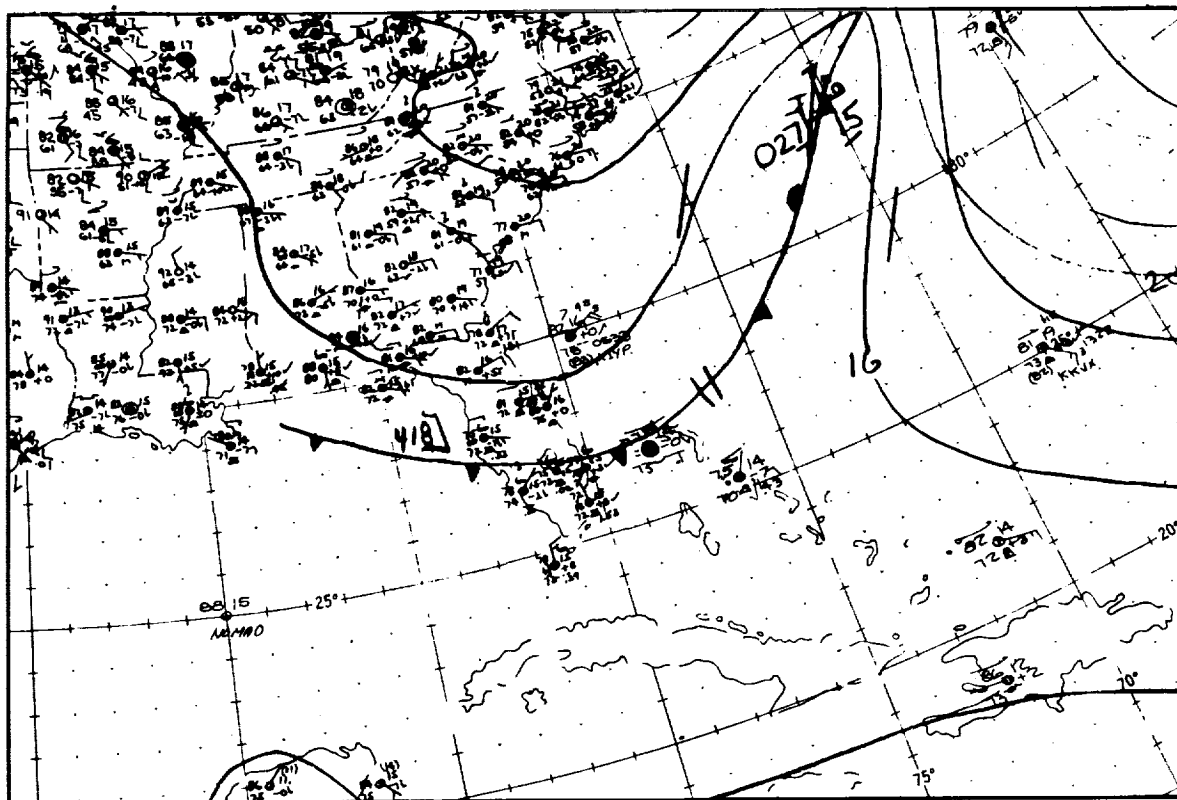


FIGURE 3-17. Surface map for 0000 GMT, 23 July 1966.

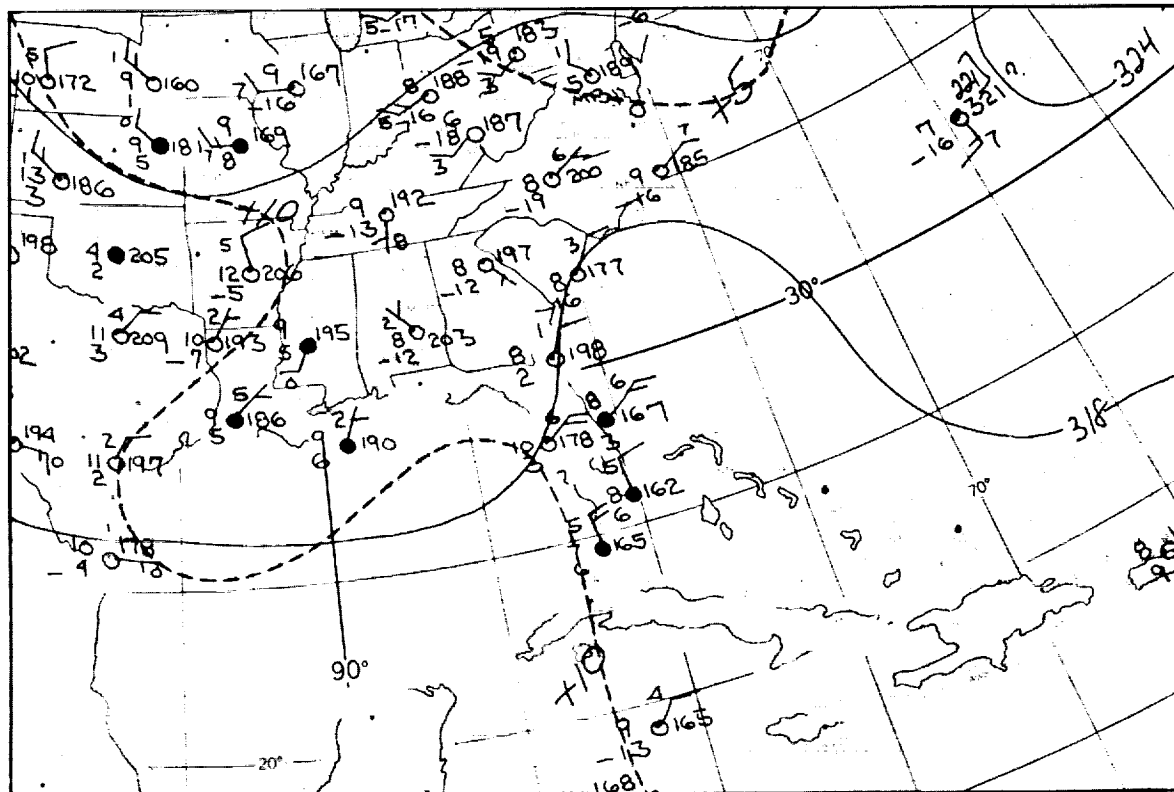


FIGURE 3-18. 700-mb map for 0000 GMT, 23 July 1966.

clouds have formed in the modifying polar air mass. Figure 3-19 shows the associated vertical profiles of temperature, wind speed and wind direction for Cape Kennedy at 2320 GMT on 22 July 1966. The temperature profile shows an approximately dry adiabatic lapse rate from the surface to about 2500 feet, and a layer from 2500 to 6700 feet in which the lapse rate is slightly less than the moist adiabatic. The remaining discontinuities in the temperature profile are minor. The wind profiles exhibit no pronounced shear above the surface layer. Again, the division of the lowest 16,400 feet into layers is somewhat arbitrary. In Figure 3-19 the surface layer extends to 2500 feet and is the principal shear layer. The top boundary of Layer 2 has been indicated as 6700 feet where the lapse rate becomes greater than the moist adiabatic. The layer from 6700 to 16,400 feet has not been subdivided, although layer boundaries might be added at 10,000 and 14,000 feet on the basis of wind shear.

The meteorological inputs are shown in Table 3-6. In the unstable surface layer, $p = 0.22$ and σ_A and σ_E are assumed to vary as $z^{-0.22}$ and $z^{0.08}$, respectively.

3.4.3 Extension of the Bermuda High into the Gulf of Mexico

On 12 May 1967, the Bermuda High extended westward to the Gulf of Mexico and a weak surface pressure gradient existed over Florida. Figure 3-20 shows the surface map for 0600 GMT and Figure 3-21 shows the 700-millibar map for 0000 GMT on this date. The lowest 16,400 feet have been divided into the five layers shown in Figure 3-22 for use in the multi-layer diffusion model. Layer 1 extends to the top of the weak ground-level inversion at 850 feet. Layer 2 extends from 850 feet to the base of the subsidence inversion at 3500 feet. Layer 3 contains the subsidence inversion and extends from 3500 to 5300 feet. The height interval from 5300 to 16,400 feet has been divided at 10,000 feet into Layers 4 and 5 on the basis of the wind speed profile. The wind

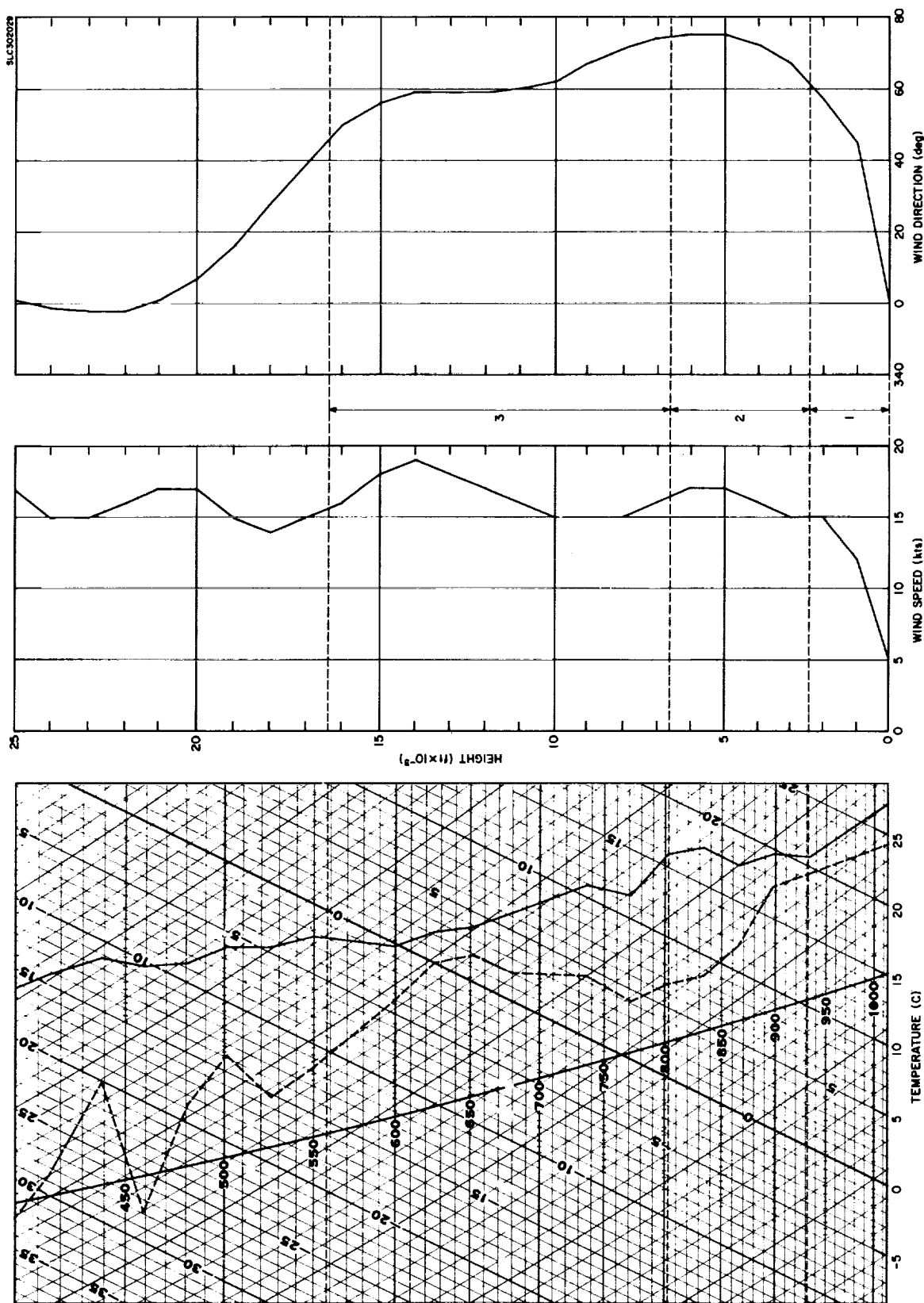


FIGURE 3-19. Vertical profiles for 22 July 1966, 2320 GMT. Solid line on Skew T, Log P diagram is air temperature; dashed line is dew point temperature. Assignment of layers for diffusion model is indicated between wind speed and wind direction profiles.

TABLE 3-6

METEOROLOGICAL MODEL INPUTS FOR 2320 GMT, 22 JULY 1966

Layer No.	Height (ft)	Wind Speed (knot)	Wind Direction (deg)	Potential Temperature (C)	σ_A (deg)	σ_E (deg)
1	59	7	0	26	10	6
	2,500	15	62	27	5	8
2	6,700	16	74	35	0	0
	16,400	16	45	47	0	0

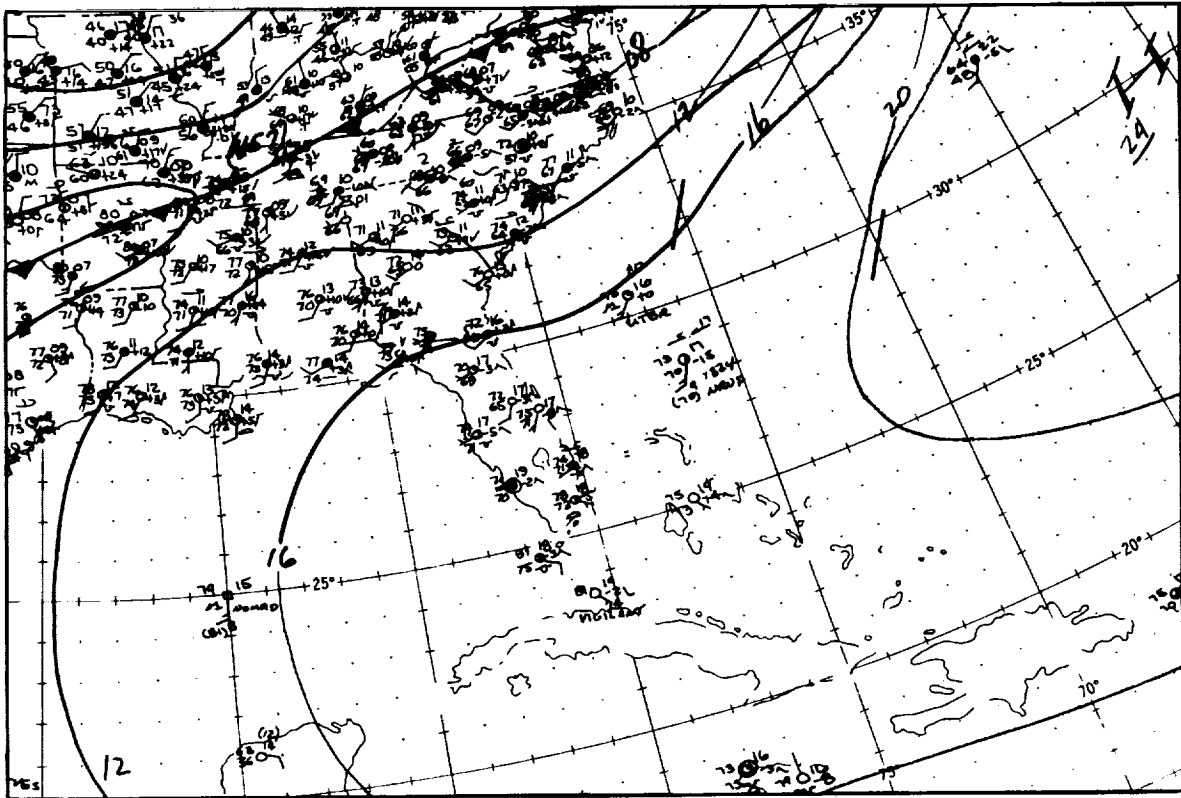


FIGURE 3-20. Surface map for 0600 GMT, 12 May 1967.

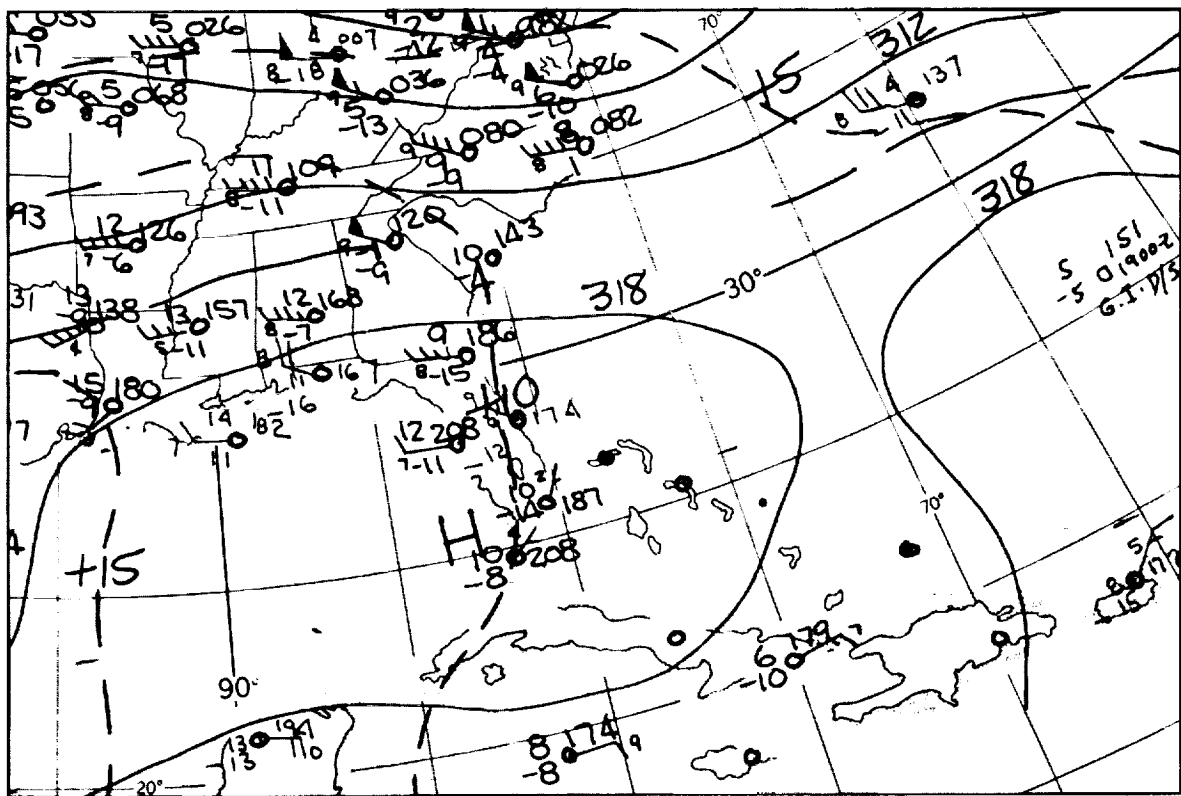


FIGURE 3-21. 700-mb map for 0000 GMT, 12 May 1967.

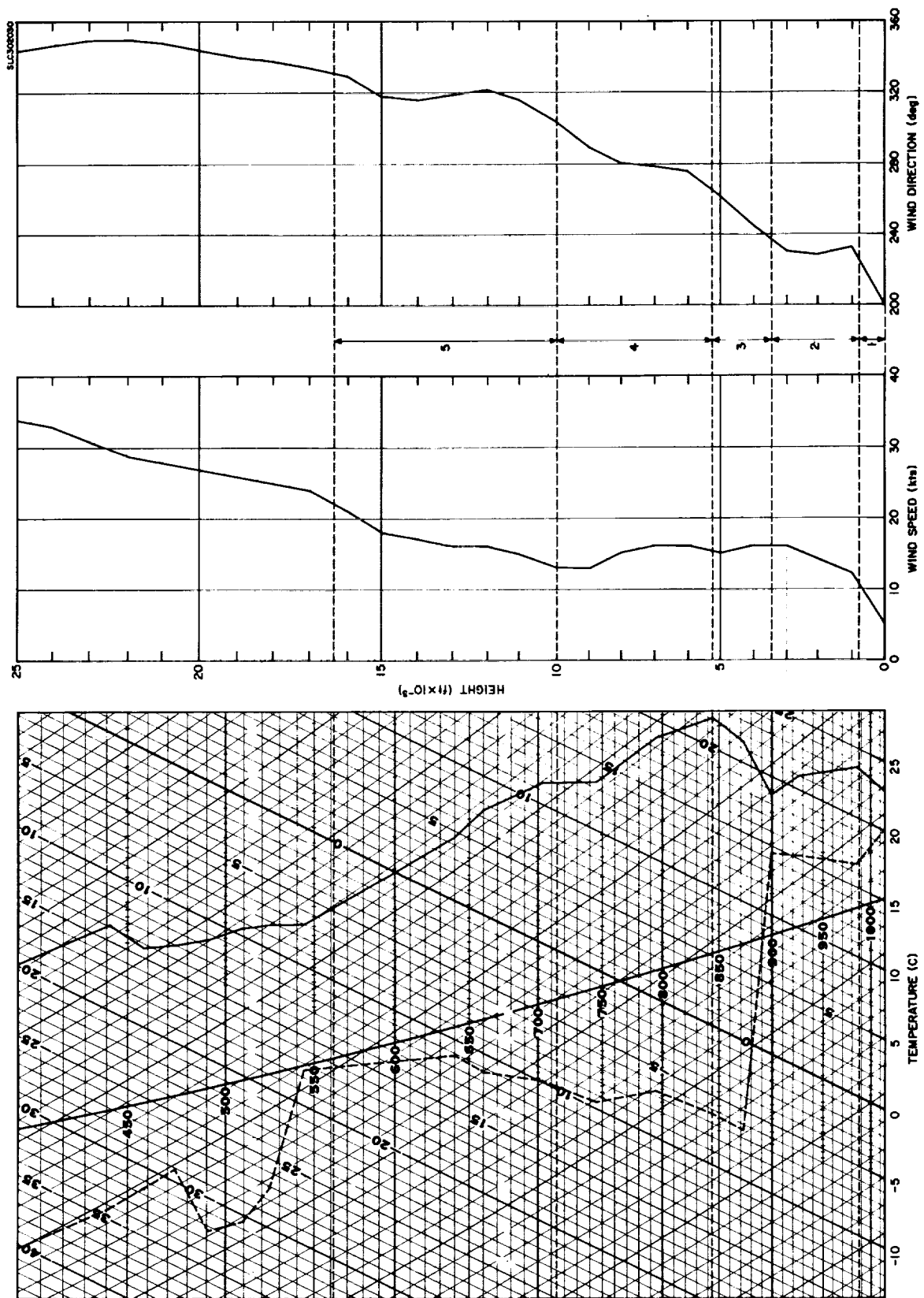


FIGURE 3-22. Vertical profiles for 12 May 1967, 0515 GMT. Solid line on Skew T, Log P diagram is air temperature; dashed line is dew point temperature. Assignment of layers for diffusion model is indicated between wind speed and wind direction profiles.

speed decreases with height slightly between 5300 and 10,000 feet, and increases between 10,000 and 16,400 feet.

The meteorological inputs for this example are listed in Table 3-7. Both σ_A and σ_E are assumed to vary as z^{-p} in Layers 1 and 2. The p values for Layers 1 and 2 are 0.20 and 0.27, respectively.

3.4.4 Circulation Controlled by a Tropical Cyclone - 1148 GMT, 1 July 1966

At 1200 GMT on 1 July 1966 a tropical depression was moving up the west coast of Florida and the center was located west of Cape Kennedy. The weather over the Florida peninsula consisted principally of broken or overcast clouds and scattered showers. No rain was occurring at Cape Kennedy. Figures 3-23 and 3-24 show the surface and 700-millibar maps, respectively, for 1200 GMT. The vertical profiles at 1148 GMT at Cape Kennedy are plotted in Figure 3-25. Figure 3-25 divides the lower 16,400 feet into three layers for use in the diffusion model. Layer 1 extends from the surface to 1000 feet. The boundary at 1000 feet divides the surface layer of strong wind speed shear from Layer 2 within which the wind speed is nearly invariant with height. The top of Layer 2 at 10,700 feet coincides with the bottom of an isothermal layer where the dewpoint begins to decrease rapidly with height. The top of Layer 2 also is the top of the layer within which the wind backs with height. Layer 3 extends from 10,700 to 16,400 feet. The variation of wind direction within this layer is about 5 degrees and the wind speed increases with height from 20 to 28 knots.

The meteorological inputs at the boundaries of the layers are listed in Table 3-8. Within Layer 1, which is near-neutral in stratification, $p = 0.22$, and σ_A and σ_E are assumed to vary as $z^{-0.22}$.

TABLE 3-7

METEOROLOGICAL MODEL INPUTS FOR 0515 GMT, 12 MAY 1967

Layer No.	Height (ft)	Wind Speed (knot)	Wind Direction (deg)	Potential Temperature (C)	σ_A (deg)	σ_E (deg)
1	59	6	200	22	6	3
2	850	11	230	25	4	2
3	3,500	16	237	28	3	1
4	5,300	15	263	37	0	0
5	10,000	13	303	41	0	0
	16,400	22	328	44	0	0

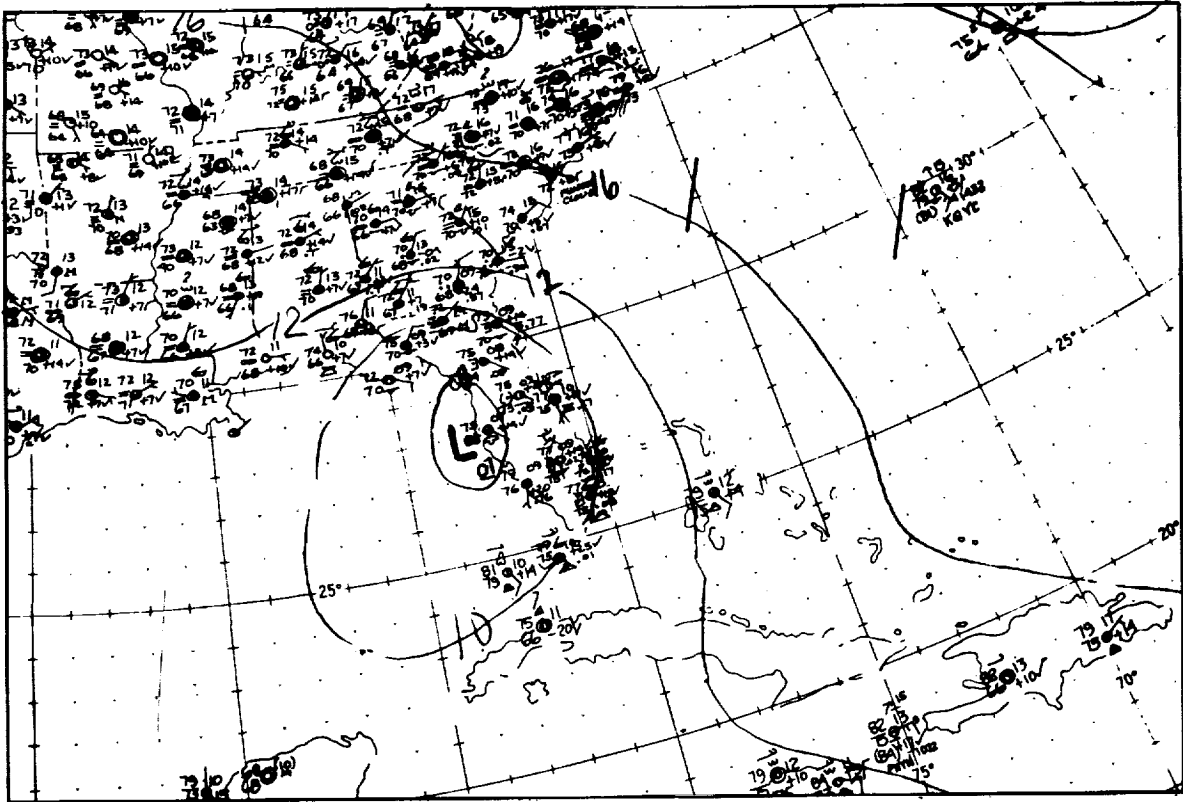


FIGURE 3-23. Surface map for 1200 GMT, 1 July 1966.

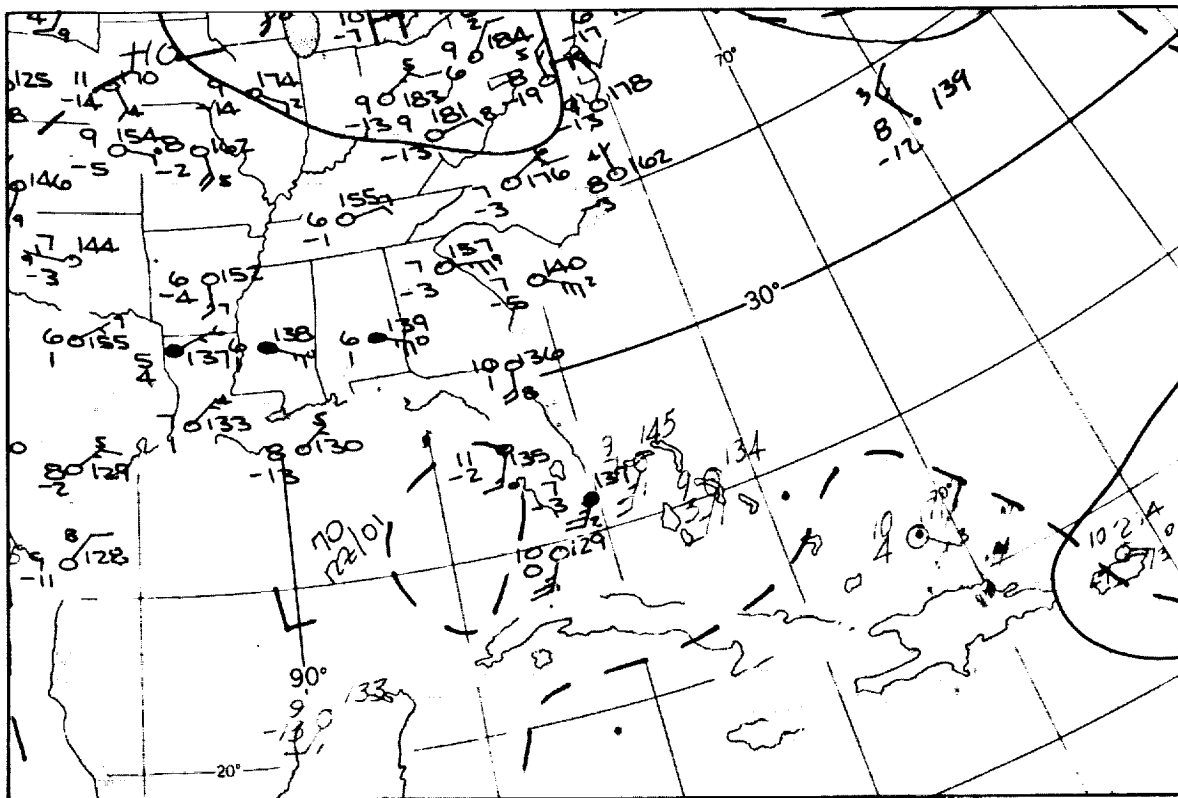


FIGURE 3-24. 700-mb map for 1200 GMT, 1 July 1966.

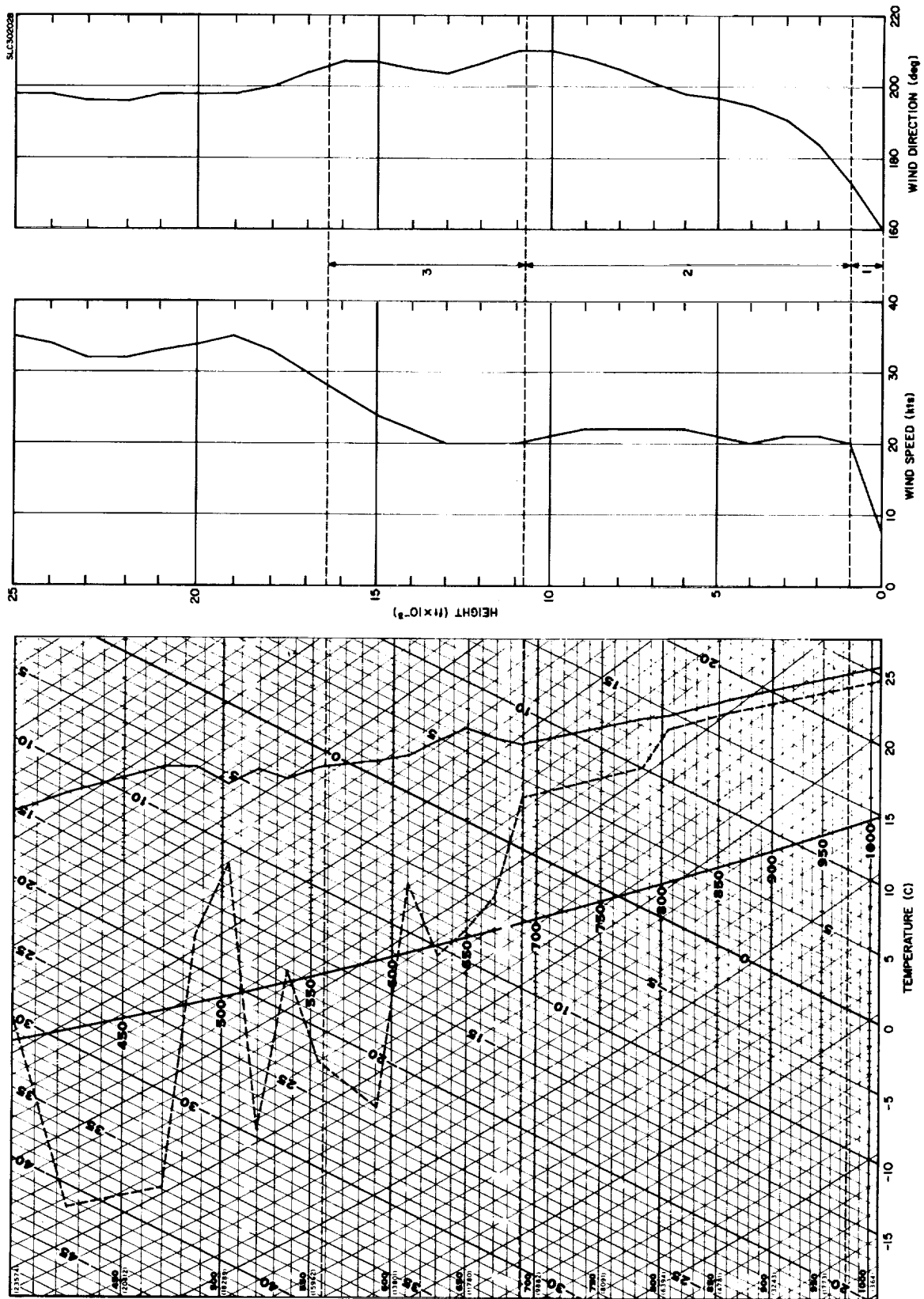


FIGURE 3-25. Vertical profiles for 1 July 1966, 1148 GMT. Solid line on Skew T, Log P diagram is air temperature; dashed line is dew point temperature. Assignment of layers for diffusion model is indicated between wind speed and wind direction profiles.

TABLE 3-8

METEOROLOGICAL MODEL INPUTS FOR 1148 GMT, 1 JULY 1966

Layer No.	Height (ft)	Wind Speed (knot)	Wind Direction (deg)	Potential Temperature (C)	σ_A (deg)	σ_E (deg)
1	59	10	160	25	9	5
	1,000	20	173	26	5	3
2	10,700	20	210	39	0	0
	16,400	28	206	49	0	0

3.5 EXTENSION TO OTHER LAUNCH SITES

The diffusion models recommended for use at Cape Kennedy are general in form and are not restricted to this site. Further, the basic procedures suggested for structuring the atmosphere for application of the multi-layer diffusion model are also independent of the site. However, mesoscale circulations, which may control the transport of airborne material within the surface layer, are typically closely related to the surface features of a particular area. Also, the vertical profiles of wind speed and turbulence parameters near the surface, as well as the low-level reference values of the turbulence parameters, are dependent upon the roughness and thermal properties of the underlying surface. The meteorological inputs developed in Section 2.1 for use in modeling diffusion from low-level releases refer specifically to Cape Kennedy. They should not be applied to other launch sites without first making a careful study of the surface features of these sites and the local wind circulation patterns. The near-neutral value of σ_A is a useful indicator of site roughness, and, in the absence of extensive local measurements, the use of Figures 2-10, 2-13, 2-17 and 2-18 is acceptable for the estimation of p , σ_A , q and σ_E at sites where σ_A under near-neutral conditions is approximately 9 degrees at a height of about 18 meters.

Within Kennedy Space Center and its immediate environs, the terrain is quite flat and the principal causes for local irregularities in flow characteristics are differences in vegetative cover, the presence of buildings and other structures, and the water-land boundaries. The curves for the estimation of σ_A , σ_E , p and q presented in Section 2.1 were developed from data collected during both winter and summer seasons, all times of day, and all wind directions, and are generally applicable throughout Kennedy Space Center. However, diffusion from small sources in the immediate vicinity of structures will be controlled in the initial stages by the flow created by these obstacles. Although some adjustment

to the average curves for the prediction of the meteorological inputs may be made for differences in upwind vegetation from the polar coordinate charts of Section 2.1 and a knowledge of the site at the Meteorological Tower Facility, this refinement would seldom be justified because of the large space and time variations inherent in turbulent structure.

SECTION 4

CONCLUSIONS AND RECOMMENDATIONS

This report has outlined in detail a method for calculating toxic fuel hazards arising from operations at Kennedy Space Center, listed the various types of meteorological information required for these calculations, and described interim procedures for obtaining specific meteorological inputs for a computerized multi-layer diffusion model, based on an intensive analysis of previous meteorological measurements made at KSC.

As pointed out in Section 1 of the report, the requirements for meteorological information in connection with toxic fuel hazard estimation at KSC may extend throughout a reference volume having vertical dimensions of several kilometers and horizontal dimensions of the order of 100 kilometers. However, the meteorological information which is routinely available within this volume is chiefly limited to a few surface and tower observations over land, and the radiosonde and Jimsphere soundings made at Cape Kennedy. Sections 2 and 3 of the report have illustrated the use of these limited data for the specification of meteorological inputs to the diffusion models. It is clear, however, that the present density of observations is inadequate to describe the time and space variations in atmospheric structure which affect transport and diffusion within the reference volume for all scale requirements. A better understanding of these variations can undoubtedly be achieved as a result of a continuing analysis of data collected with the present observational network. Suitable data are available from:

- Jimsphere soundings
- Radiosonde soundings

- NASA's 150-meter Tower Facility
- Hourly surface observations
- Weather radar reports

To obtain the requisite data for further study of time and space variations, it is recommended that a field program be undertaken which would take full advantage of current observational techniques. These techniques include the use of:

- An instrumented aircraft
- Jimsphere soundings (with temperature probe)
- Radiosonde soundings
- Tetroons
- Weather radar
- Surface and tower observations

It is particularly important that the program be designed to study the dimensions and strength of the land- and sea-breeze circulations and counter flows, and the changes in stability and wind structure which occur as air moves from water to land and from land to water.

There is also an absence of source information in a convenient and readily available form for the wide variety of release modes and toxic products to be considered. The source information required consists of the amount and rate of toxic material released and its chemical and physical properties, and the dimensions, and position in space of the cloud after reaching equilibrium. It is recommended that a continuing program be maintained to observe stabilization

heights, source dimensions and cloud characteristics during operations at KSC.

The program should include the use of:

- lidar
- photographic techniques
- visual observations

The work carried out under this contract and the development of computer programs and plotting routines under Contract NAS8-21453 represents a major step toward the prediction of toxic hazards at Kennedy Space Center for planning and operational purposes. It is recognized, however, that the development of prediction procedures must be an evolutionary iterative process, and that any statistical validation of the procedures will require a very large number of detailed observations.

REFERENCES

- Alexander, M., D. W. Camp, C. K. Hill, and J. W. Kaufman, 1967: Wind and gust characteristics in the lower 150 m of the atmosphere at KSC, Florida, in Research Achievements Review, Vol. 11, No. 10, NASA TM X-53706, NASA-MSFC, Huntsville, Alabama.
- Blackadar, A. K., J. A. Dutton, H. A. Panofsky, and A. Chaplin, 1969: Investigation of the turbulent wind field below 150 M altitude at the Eastern Test Range, NASA CR-1410, Contract No. NAS8-21140, Penn. St. U., University Park, Pa.
- Church, H. W., 1969: Cloud rise from high-explosives detonations, Research Report No. SC-RR-68-903, Sandia Laboratories, Albuquerque, N. Mex., 24 pp.
- Cramer, H. E., G. M. DeSanto, R. K. Dumbauld, P. Morgenstern, R. N. Swanson, 1964: Meteorological prediction techniques and data system, Final Report, Contract No. DA-42-007-CML-552, U. S. Army Dugway Proving Ground, Dugway, Utah.
- Cramer, H. E., H. L. Hamilton, and G. M. DeSanto, 1965: Atmospheric transport of rocket motor combustion by-products, Final Report, Contract No. N123 (61756)34657(PMR), Pacific Missile Range, Point Mugu, Calif., Vols. I & II.
- Cramer, H. E., F. A. Record, and J. E. Tillman, 1966: Round Hill turbulence measurements, M.I.T. Tech. Rpt. Vol. I-V, ECOM-65-G10 under Contract DA-AMC-28-043-65-G10, U. S. Army Electronics Command, Fort Huachuca, Arizona.
- Cramer, H. E., R. K. Dumbauld, B. R. Greene, and R. N. Swanson, 1967: Determination of hazard prediction procedures, GCA Tech. Rpt. No. 67-8-G, Final Report under Contract No. DA-42-007-AMC-359(R), U. S. Army Dugway Proving Ground, Dugway, Utah.
- Cramer, H. E. and R. K. Dumbauld, 1968: Experimental designs for dosage prediction in CB field tests, GCA Tech. Rpt. No. 68-17-G, Final Report under Contract No. DA-42-007-AMC-276(R), U. S. Army Dugway Proving Ground, Dugway, Utah.
- DeMarrais, G. A., 1959: Wind speed profiles at Brookhaven National Laboratory, J. Met., 16, 181-190.
- Dumbauld, R. K., J. R. Bjorklund, H. E. Cramer, and F. A. Record, 1970: Toxic fuel diffusion handbook, GCA Tech. Rpt. No. TR-69-16N, Contract No. NAS8-21453, GCA Corporation, Bedford, Mass.

- Endlich, R. M., R. C. Singleton, K. A. Drexhage and R. L. Marcuss, 1969: Studies of vertical wind profiles at Cape Kennedy, Florida, NASA CR-61263, Contract No. NAS8-21148, Stanford Research Institute, Menlo Park, California.
- Feit, D. M., 1969: Analysis of the Texas Coast land breeze, Report No. 18, Atmospheric Science Group, College of Eng., U. of Texas, Austin, Texas.
- Fichtl, G. H., 1968: An analysis of the roughness length associated with the NASA 150-meter Meteorological Tower, NASA TM-X-53690, NASA-MSFC, Huntsville, Ala.
- Fichtl, G. H. and G. E. McVehil, 1969: Longitudinal and Lateral Spectra of Turbulence in the Atmospheric Boundary Layer. Unpublished manuscript.
- Hill, K., 1967: Study of the land and sea breeze regimes at Cape Kennedy, Florida, from May 23 through September 1966, Branch Memorandum R-AERO-YE-29-67, NASA-MSFC, Huntsville, Ala.
- Hilst, G. R., 1967: Environmental hazards study, NASA CR-61163, Contract No. NAS8-11450, Travelers Research Center, Inc., Hartford, Conn.
- Hsu, S. A., 1967: Mesoscale surface temperature characteristics of the Texas Coast sea breeze, Report No. 6, Atmospheric Science Group, College of Eng., U. of Texas, Austin, Texas.
- Hsu, S. A., 1969: Mesoscale structure of the Texas Coast sea breeze, Report No. 16, Atmospheric Science Group, College of Eng., U. of Texas, Austin, Texas.
- Kaufman, J. W. and L. F. Keene, 1968: NASA's 150-meter Meteorological Tower located at the Kennedy Space Center, Florida. NASA TM X-53699 NASA-MSFC, Huntsville, Ala.
- McPherson, R. D., 1968: A three-dimension numerical study of the Texas Coast sea breeze, Report No. 15, Atmospheric Science Group, College of Eng., U. of Texas, Austin, Texas.
- McVehil, G. E. and H. G. Camnitz, 1969: Ground wind characteristics at Kennedy Space Center, CAL No. VC-2488-P-1, Final Report, Contract No. NA58-21178, Cornell Aeronautical Laboratory, Buffalo, N. Y.

- Morton, B. R., G. I. Taylor and J. S. Turner, 1956: Turbulent gravitational convection from maintained and instantaneous sources, Proc. Roy. Soc. (London), Ser. A, 234:1-23.
- Pasquill, F., 1962: Some observed properties of medium scale diffusion in the atmosphere, Quart. J. Roy. Met. Soc., 88(375), 70-79.
- Pasquill, F., 1962: Atmospheric Diffusion, D. Van Nostrand Company, Ltd., London.
- Pasquill, F., 1967: The vertical component of atmospheric turbulence at heights up to 1200 meters, Atmos. Environ., 1, 444-450.
- Scoggins, J. R. and M. B. Alexander, 1964: Stability conditions of the lower atmosphere and their implications regarding diffusion at Cape Kennedy, Florida, NASA TM X-53132, NASA-MSFC, Huntsville, Ala.
- Sellers, W. D., 1965: Physical Climatology, The University of Chicago Press, Chicago, Ill.
- Slade, D. H. (Editor), 1968: Meteorology and Atomic Energy, 1968, prepared by Air Resources Laboratories, ESSA, for U. S. Atomic Energy Commission.
- Susko, M., J. W. Kaufman, and K. Hill, 1968: Rise rate and growth of static test vehicle engine exhaust clouds, NASA TMX-53782, Aero-Astrodynamic Research Review No. 7, George C. Marshall Space Flight Center, NASA, Marshall Space Flight Center, Alabama.
- Swanson, R. N. and H. E. Cramer, 1965: A study of lateral and longitudinal intensities of turbulence, J. Appl. Met., 4, 409-417.
- Tyldesley, J. B. and C. E. Wallington, 1965: The effect of wind shear and vertical diffusion on horizontal dispersion, Quart J. Roy. Met. Soc., Vol. 91, pp. 158-174.